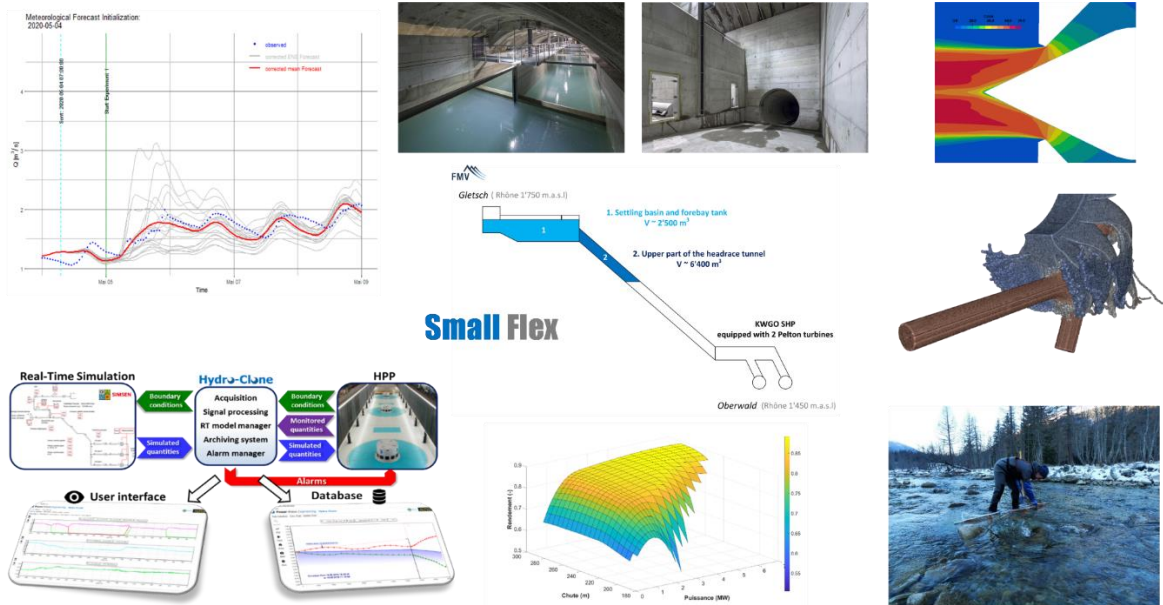




Final report dated 31 January 2021.

# SmallFLEX

## Demonstrator for flexible small hydropower plant



Source: ©SmallFLEX 2021



Hes·so

EPFL



eawag  
aquatic research



**Date:** 31 January 2021

**Location:** Sion

**Publisher:**

Swiss Federal Office of Energy SFOE  
Energy Research and Cleantech  
CH-3003 Bern  
[www.bfe.admin.ch](http://www.bfe.admin.ch)

**Co-financing:**

FMV  
Rue de la Dixence 9, 1950 Sion  
[www.fmv.ch](http://www.fmv.ch)

**Subsidy recipients:**

HES SO Valais, Route du Rawyl 47, 1950 Sion, [www.hevs.ch/hydro](http://www.hevs.ch/hydro)  
EPFL LMH et LCH, CH-15 Lausanne, [www.epfl.ch](http://www.epfl.ch)  
WSL, Eidg. Forschungsanstalt WSL, Zürcherstrasse 111, CH-8903 Birmensdorf, [www.wsl.ch](http://www.wsl.ch)  
Eawag, Seestrasse 79, CH-6047 Kastanienbaum, [www.eawag.ch](http://www.eawag.ch)  
PVE, Rue des Jordils 40, CH-1025 St-Sulpice, <https://www.powervision-eng.ch/>  
FMV, Rue de la Dixence 9, CP 506, CH-1951 Sion, [www.fmv.ch](http://www.fmv.ch)

**Authors:**

J. Decaix, C. Münch-Alligné, HES SO Valais, [cecile.muench@hevs.ch](mailto:cecile.muench@hevs.ch)  
J. Zordan, P. Manso, G. De Cesare, EPFL LCH [pedro.manso@epfl.ch](mailto:pedro.manso@epfl.ch)  
S. Alimirzazadeh, F. Avellan, EPFL LMH, [francois.avellan@epfl.ch](mailto:francois.avellan@epfl.ch)  
M. Schmid, C. Weber, C. Aksamit, D. Vanzo, Eawag, [martin.schmid@eawag.ch](mailto:martin.schmid@eawag.ch)  
K. Bogner, M. Stähli, WSL, [konrad.bogner@wsl.ch](mailto:konrad.bogner@wsl.ch)  
M. Dreyer, C. Nicolet, PVE, [christophe.nicolet@powervision-eng.ch](mailto:christophe.nicolet@powervision-eng.ch)  
S. Crettenand, FMV, [steve.crettenand@fmv.ch](mailto:steve.crettenand@fmv.ch)

**SFOE project coordinators:**

Klaus Jorde, [klaus.jorde@kiconsult.net](mailto:klaus.jorde@kiconsult.net)  
Men Wirz, [men.wirz@bfe.admin.ch](mailto:men.wirz@bfe.admin.ch)

**SFOE contract number:** SI/501636-01

**The authors bear the entire responsibility for the content of this report and for the conclusions drawn therefrom.**



## Zusammenfassung

Das multidisziplinäre Projekt "SmallFLEX: Demonstrator der Flexibilität von Kleinwasserkraft" zielt darauf ab, das Potenzial von Kleinwasserkraftwerken zur Bereitstellung von Spitzenenergie und Systemdienstleistungen unter Berücksichtigung der Umweltauswirkungen zu untersuchen. Der ausgewählte Demonstrationsstandort ist das von den Forces Motrices Valaisannes (FMV) betriebene Kleinlaufwasserkraftwerk Gletsch Oberwald (KWGO). Ziel ist es, einen flexiblen Betrieb der Anlage zu ermöglichen und so zusätzliche Einnahmen für die Eigentümer zu generieren. Durch numerische Simulationen und Feldversuche wurden die Kapazität der Infrastruktur, und der Maschinen, sowie auch andere Anpassungsmassnahmen zur Ermöglichung einer flexiblen Produktion untersucht und gleichzeitig die Auswirkungen dieses flexiblen Betriebs auf Umwelt, Stromproduktion und Einnahmen betrachtet. Mit einem nutzbaren Speichervolumen von 6'200 m<sup>3</sup>, welches den Entsander, die Druckkammer und den oberen Teils des Druckrohrs umfasst, kann die Anlage einerseits im Winter ihre Produktion verdoppeln und gleichzeitig die Anzahl Abschaltungen und Starts stark reduzieren. Ausserdem können das ganze Jahr über Primärdienste von  $\pm 1,5$  MW durch Integration in einen Pool virtueller Kraftwerke angeboten werden. Um die Umweltauswirkungen des flexiblen Betriebs auf die unterliegenden Gewässerabschnitte möglichst gering zu halten, werden die Leistungsspitzen so geregelt, dass die künstlich erzeugten Abflussspitzen das 1,5-fache des Basisabflusses nicht überschreiten. Im Winter wird der Abfluss aufgrund der geringeren Anzahl von Abschaltungen und Neustarts sogar geglättet. Die entwickelte Methodik könnte nun auf andere Laufwasserkraftwerke mit ähnlichen Eigenschaften angewendet werden.

## Résumé

Le projet multidisciplinaire « SmallFLEX : Démonstrateur de la flexibilité de la petite hydraulique » vise à étudier la capacité des petites centrales hydroélectriques à fournir de l'énergie de pointe et des services systèmes tout en respectant l'environnement. Le site de démonstration sélectionné est la petite centrale au fil de l'eau de Gletsch Oberwald (KWGO), mise à disposition par les FMV. L'objectif est de proposer un fonctionnement flexibilisé de la centrale et générer ainsi des revenus supplémentaires pour les propriétaires de l'aménagement. Grâce à des simulations numériques et des essais sur site, la capacité de l'infrastructure, des équipements et d'autres mesures d'adaptation permettant de produire de manière flexible a été évaluée tout en mesurant l'impact de ce nouveau fonctionnement sur l'environnement, la production et les revenus. Avec un stockage utilisable en toute sécurité de 6'200 m<sup>3</sup> intégrant le volume du dessableur, de la chambre de mise en charge et la partie supérieure de la conduite forcée, la centrale pourra d'une part durant l'hiver doubler sa production tout en diminuant drastiquement le nombre d'arrêt-démarrage, et d'autre part durant toute l'année proposer des services primaires de  $\pm 1.5$  MW en s'intégrant à un pool de centrales virtuelles. Pour minimiser les effets sur l'écologie de la rivière en aval, les pics de puissances sont réglés afin de limiter les débits d'écluse à 1.5 fois le débit plancher. En hiver, le débit sera même lissé du fait de la réduction du nombre d'arrêt-démarrage. La méthodologie développée pourrait maintenant s'appliquer à d'autres centrales au fil de l'eau présentant des caractéristiques similaires.

## Summary

The multidisciplinary project "SmallFLEX: Demonstrator for flexible Small Hydropower Plant" aims to investigate the capacity of small hydropower plants to provide peak energy and system ancillary services while respecting the environment. The selected demonstration site is the small run-of-river power plant



of Gletsch Oberwald (KWGO), owned by FMV. The objective is to offer flexible operation of the plant and thus generate additional income for the owners. Through numerical simulations and field tests, the capacity of the infrastructure, equipment, and other adaptation measures to allow flexible production was assessed while measuring the impact of this new operation on the environment, production, and income. With a safe usable storage of 6'200 m<sup>3</sup> integrating the volume of the desander and forebay chambers as well as the upper part of the headrace tunnel, the plant will be able, on the one hand, during the winter to double its production while drastically reducing the number of start-and-stop, and secondly throughout the year to offer primary services of  $\pm 1.5$  MW by integrating KWGO into a pool of virtual power plants. To minimize the environmental impacts of the flexible power production on the downstream river stretches, the power peaks are limited such the peak discharge does not exceed the baseflow by a factor of more than 1.5. In winter, the discharge will even be smoothed by reducing the number of start-and-stop. The methodology developed could be then applied to other run-of-river power plants with similar characteristics.

## Main findings

- Through a multi-disciplinary approach, a complete study from the inflow forecast to the hydropeaking effect on the alluvial area via a numerical modelling and field tests of the KWGO power plant has been carried out.
- A smart storage of 6'200 m<sup>3</sup> been identified and assessed for the small run-of-river KWGO power plant.
- Primary services of  $\pm 1.5$  MW can be proposed by the small run-of-river KWGO power plant.
- An economic analysis using the identified smart storage has evidenced the possibility to double winter production, to reduce the number of start-and-stop and to propose ancillary services by integrating the KWGO hydropower plant into a virtual pool.



# Contents

<b>Zusammenfassung.....</b>	<b>3</b>
<b>Résumé.....</b>	<b>3</b>
<b>Summary .....</b>	<b>3</b>
<b>Main findings .....</b>	<b>4</b>
<b>Contents .....</b>	<b>5</b>
<b>Abbreviations.....</b>	<b>7</b>
<b>1 Introduction.....</b>	<b>8</b>
1.1 Background information and current situation .....	8
1.2 Context of the project .....	9
1.3 Objectives .....	11
<b>2 Description of facility .....</b>	<b>16</b>
<b>3 Procedures and methodology.....</b>	<b>17</b>
3.1 Task 1: Investigation of the storage potential .....	17
3.2 Task 2: Hydraulic machines flexibility.....	18
3.3 Task 3: Real-time hydrological forecasts .....	20
3.4 Task 4: Short term hydropeaking effects on ecosystems .....	23
3.5 Task 5: On-site tests.....	25
3.6 Task 6: Business model of a flexible small hydropower plant.....	29
<b>4 Results and discussion .....</b>	<b>32</b>
4.1 Task 1: Investigation of the storage potential .....	32
4.2 Task 2: Hydraulic machines flexibility.....	34
4.3 Task 3: Real-time hydrological forecasts .....	50
4.4 Task 4: Short term hydropeaking effects on ecosystems .....	58
4.5 Task 5: On-site tests.....	65
4.6 Task 6: Business model of a flexible small hydropower plant.....	67
<b>5 Conclusions .....</b>	<b>69</b>
5.1 Task 1: Investigation of the storage potential .....	69
5.2 Task 2: Hydraulic machines flexibility.....	69
5.3 Task 3: Real-time hydrological forecasts .....	70
5.4 Task 4: Short term hydropeaking effects on ecosystems .....	71
5.5 Task 5: On-site tests.....	71
5.6 Task 6: Business model of a flexible small hydropower plant.....	72
<b>6 Outlook and next steps .....</b>	<b>73</b>
<b>7 National and international cooperation.....</b>	<b>73</b>
<b>8 Publications .....</b>	<b>74</b>



9	References .....	75
---	------------------	----



## Abbreviations

List of used abbreviations (if applicable)

CFD	Computational Fluids Dynamics
COSMO	Consortium for Small-scale Modelling
FIT	Feed-in tariff system
FVPM	Finite Volume Particle Method
GPU	Graphical Power Unit
HPP	Hydraulic Power Plant
INCA	Integrated Nowcasting through Comprehensive Analysis
PFC	Primary Frequency Control
PREVAH	Precipitation Runoff Evapotranspiration Hydrotope Model
RPC	Rétribution de l'injection à Prix Coûtant
SHP	Small Hydro Plant
SPH	Smoothed-Particle Hydrodynamics
TSE	Time-Step Energy software



# 1 Introduction

## 1.1 Background information and current situation

The 2050 Swiss Energy Strategy is based on a massive development of renewable energy sources. Due to the intermittent nature of these energy sources, mainly composed by wind and solar energies, their integration is a challenging task as far as the power network stability is concerned. In this context, Swiss hydropower plants are expected to play an important role to improve the stability of the power network due to their production flexibility, fast response time and extended operating range. Consequently, the demand for ancillary services, such as primary, secondary, and tertiary control capabilities considerably increased during the last decade, in Switzerland and in Europe. Small Hydro Plants (SHP) which already represent 10% of the hydroelectricity production in Switzerland, are also eligible to provide ancillary services and thus may contribute to support the power network stability. However, the provision of ancillary services requires minimum storage capacity that run-of-the-river SHP do not have. If the project is successful at demonstrating the capability of SHP to provide ancillary services using available infrastructure space for storage (e.g., headwork caverns, headrace tunnel) without detrimental impact for the hydropower plant installations and the environment, this will represent a new potential of revenues for SHP.

SHP are significantly developing in the whole Europe, and thus the know-how and expertise gained in this project in the field of hydraulic, mechanical, and electrical engineering, will represent a strong asset based on a real case study, for the application of similar solutions in Switzerland and abroad. As the present project is a demonstrator, it is expected that the methodologies developed under the proposed project are applicable to other projects after the project conclusion, i.e., at horizon 2021.

Providing storage to mountain intakes is not a brand-new idea (e.g., the headrace tunnel-reservoir of the modified SHP Aboyeu in 1979) but has not been a topic of a systematic research and knowledge transfer to practice, and especially not in the context of a liberalised energy market and with capacity (or regulation) markets. The commissioning of the Stanzertal SHP in Austria with a modified headrace profile allowing for alternated operation in pressurized and free-surface flow is a recent example on how the engineering practice is looking for technical solutions to adapt the design to new operating conditions and/or functionalities. The headrace tunnel profile was purposely provided in different slopes and with intermediate air vents to allow its use as an underground storage during winter. The availability of a surge tank at the transition between the headrace tunnel-reservoir and the steel-lined pressurized shaft allows maintaining the turbine regulation system governed by an upstream water level with limited head variations. Advances over the last decade in terms of air entrainment and detrainment in pressurized waterways also pave the way for innovative waterway design, exploring conditions previously considered as unacceptable due to the risk of upstream or downstream air blowouts.

One of the most interesting features of the case study, which makes its very adequate for research work, is the availability of a single sloped headrace tunnel, resulting from the design compromise between tunnel length, tunnel overburden, excavation methodology and tunnel lining. The partial dewatering of such system on its upstream end forces a major change in turbine governing, in the stability of nozzle jet flows and in the transient behaviour of both the hydraulic system and the electromechanical equipment (turbine-generator unit and ancillary systems). Lessons taken from this case study will instruct guidelines for replication in a large universe of high-head SHPs in Switzerland and abroad. The outcome of the project will benefit in the first place the industrial partners of the project and the authorities (e.g., SFOE). Similar SHP owners in Switzerland and abroad, as well as engineering companies, turbine suppliers and manufacturers of other ancillary systems (e.g., SCADA, hydro-mechanical) will have limited access to the research output (to be object of an agreement).

The major environmental impact of adding flexibility to SHP power production by using available infrastructure as storage volume is the resulting hydropeaking in the river downstream of the water release. The adverse impacts of hydropeaking on stream ecology have been demonstrated in numerous previous field and laboratory studies. Consequently, the Swiss Waters Protection Act requires the implementation of civil engineering measures to prevent or eliminate hydropeaking if it causes serious





harm to the indigenous flora and fauna as well as their habitats. However, since hydropeaking is mainly caused by storage power plants rather than run-of-the-river SHPs, no previous studies exist on the effects of hydropeaking from run-of-the-river SHPs on downstream river reaches. Conclusions from studies on large storage plants are not necessarily transferable to SHPs, due to the different timing, frequency and magnitude of the expected hydropeaks.

If the proposed project demonstrates the ability of SHP to provide additional peak energy and ancillary services, similar concepts can apply to other existing and future SHP. Consequently, the know-how gained within this project will enable to provide high-end engineering services in Switzerland and abroad. The corresponding potential increase of revenues and energy generation could be assessed using for instance the tools currently being developed within the RENOVHydro Project, co-funded by CTI-KTI and SFOE under the SCCER-SoE umbrella. Indeed, the RENOVHydro multi-disciplinary project aims at developing a software library to explore various alternative scenarios for hydropower plants regarding their production capacity and the ancillary services they can provide. This tool is targeting the optimization of renovation of existing hydroelectric plant where several electromechanical and civil engineering options are possible, leading to several scenarios that cannot be explored with limited available resources. Nevertheless, it could also be used to assess the added value resulting from extended storage reserves that the headrace tunnel may represent, through a systematic approach using the RENOVHydro tools. Such assessment of new services will then be achieved considering detailed simulations of the SHP including hydraulic, mechanical and electrical system and their related control systems, taking into account the new operating strategies in the proposed project. The Swiss Hydro Asset Modernization Assessment project (SHAMA) funded by the SFOE aims at studying the impact of the political, economic and environmental contexts on the best technical solutions for hydropower plant renovation resulting from a systematic assessment process using the RENOVHydro Library. The various Swiss and European political strategies, the evolution of electricity price, climatic changes and environmental constraints are factors that have a direct impact on profitability of the hydropower renovation for which the best technical-economic solution can be significantly different. In this context, the present project may lead to new opportunities for Small Hydro Plants whose impacts could be further assessed with the methodology developed in the SHAMA Project.

## 1.2 Context of the project

SHP in Switzerland represents 10% of the hydroelectricity production with 3.4 TWh per year, and an existing potential between 460 GWh and 770 GWh has been estimated, BFE 2019. Most of this potential concern “large” SHP with a mean installed power between 1 MW and 10 MW. In the framework of a post RPC or an open market situation, the research project aims at showing the ability of a SHP to produce clean, sustainable and renewable energy while producing ancillary services.

The optimized operation during the winter semester results in additional revenues from flexible operation, but not necessarily in more kWh. The fine coupling of water/sediment forecasts with the use of underground/surface intra-day storage and multi-nozzle Pelton group operation is the key to provide flexibility. At the outlet, the flow discharges variation must remain acceptable from the ecological point of view. Flexible operation can improve the economic viability of borderline power plants (or prospective projects) in a post-FIT (RPC) or open market condition, guaranteeing their continuity and/or integration in the fleet of hydropower plants needed for the energy transition.

Preliminary estimates of a full winter semester indicate that a 1-5% increase in annual revenues can be achieved with the addition of storage volumes equivalent to a few hours per day of operation at discharges multiple of the river inflows, considering reasonable electricity sell prices in post-FIT conditions, at peak or sub-peak hours.

The possibility to concentrate production on fewer hours per day also in wintertime may give the power plant the possibility to sell part of its future production for primary control. This means having the possibility to scale up production within 30 s response time. This service is presently subject of contracts with the grid operator, negotiated on a weekly basis and for different capacities. The power plant is thus remunerated for its readiness to provide a given power for a given time span, and only implicitly for the



energy produced. This potential remuneration is however even more difficult to estimate than that resulting from peak energy production. In fact, the economic utility of placing some of the available power in a primary control market is directly proportional to the role of a given scheme in the regional network and inversely proportional to the existence of larger or similar size schemes in the same region and of other competing control alternatives (e.g., curtailment, batteries).

There are at least two ways of increasing energy production by adding flexibility to high-head HPPs with no initial storage functionalities:

- 1) by reducing the residual flows (i.e., ecological discharges) during the winter semester, which requires extensive ecological and hydro-morphological studies, which are out of the scope of the current research project.
- 2) by reducing the water losses, i.e., reducing the percentage of useable water above the residual discharge threshold that is not captured (except floods). In fact, in many mountain rivers there is hardly any flow during several weeks or months during this semester, given the low temperatures, soil freezing and snow cover. As soon as there is some flow, this must remain in the river. However, above the residual discharge threshold not all “excess” inflows are used. In fact, only those above the minimum operational discharge (see Figure 1) are used, meaning that significant inflows are lost. Part of these inflows can be used by providing limited storage for these excess volumes (previously considered “non-diverted volumes”) or by changing the turbine design or combining both solutions.

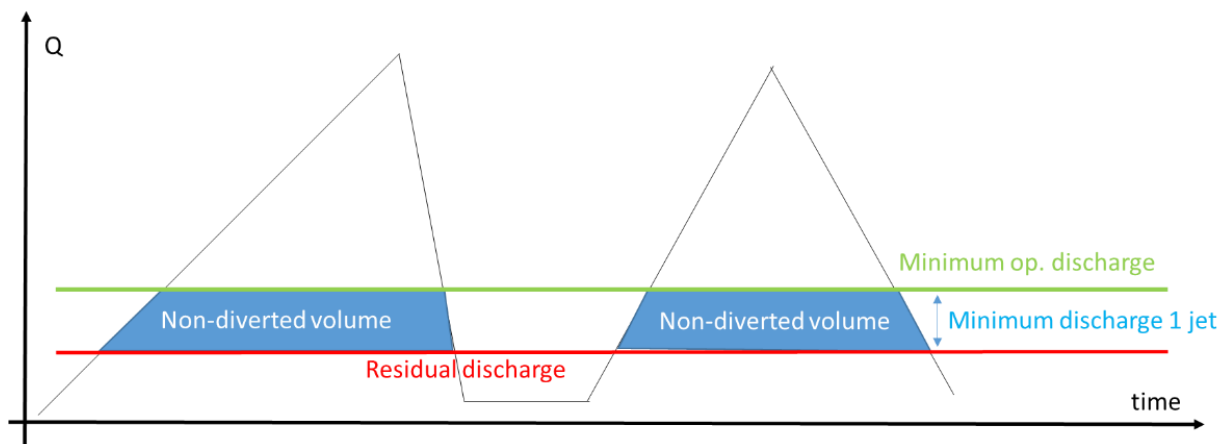


Figure 1– Definition of minimum operational discharge of a hydropower scheme with no storage.

This research project may affect positively several hundred high-head SHPs with no or little storage, (175 SHPs with an installed capacity between 1 MW and 30 MW with a discharge lower than 5 m<sup>3</sup>/s) resulting in an annual revenue increase of 1-5%. A small increase in energy production (< 5%) is foreseen, due to an improved use of excess waters at high-altitude intakes above the residual discharge releases. According to the WASTA Database 2015 from OFEN, this group of SHPs is providing more than 2'690 GWh per year, 815 GWh being produced during winter. This group of HPPs corresponds to an installed power of 758 MW; 10% of this installed power could be allocated for ancillary services at least during wintertime.

Moreover, according to FMV, above this limit of 30 MW, the methodology could be applied to 3 other power plants of their pool representing 120 MW of installed power and 650 GWh per year of production:

- Ernen: 32 MW (2 x 16 MW) producing 170 GWh per year.
- Mörel: 48 MW (3 x 16 MW) producing 260 GWh per year.
- Chippis-Rhône: 40 MW (4 x 10 MW) producing 220 GWh per year.

The demonstration of the SHP flexible capacities is carried out on the pilot facility of the SHP of Gletsch-Oberwald (KWGO) operated by FMV and commissioned end of 2017 (see Figure 3). The additional



flexibility is done by testing infrastructure and equipment or operational adaptation measures, assessing their impact in terms of outflows, electricity output and revenues.

The main investigated points are:

- How can intra-day, intra-week or intra-monthly storage be added to a given scheme?
- What are the consequences of enlarging the operational range of the machines?
- What can be the added value of meteorological forecast in terms of power generation and prediction of sediment inflows?
- What are the consequences of the hydropeaking resulting from a more flexible operation on the downstream river reach?

### 1.3 Objectives

For this demonstrator project, six different research tasks were defined, and one was dedicated to the management of the activities. The six tasks, which will be described hereafter, are:

- Task 0 - Management of the project: HES SO and FMV.
- Task 1 - Assessment of storage potential: EPFL LCH & FMV.
- Task 2 - Hydraulic machines flexibility: HES SO, EPFL LMH, PVE & FMV.
- Task 3 - Real-time hydrological forecasts: WSL & FMV.
- Task 4 - Short-term hydropeaking effects on ecosystems EAWAG & FMV.
- Task 5 - Experimental campaigns on site: HES SO & all the partners.
- Task 6 - Economical opportunities to provide ancillary services with SHP: FMV & acad. Partners

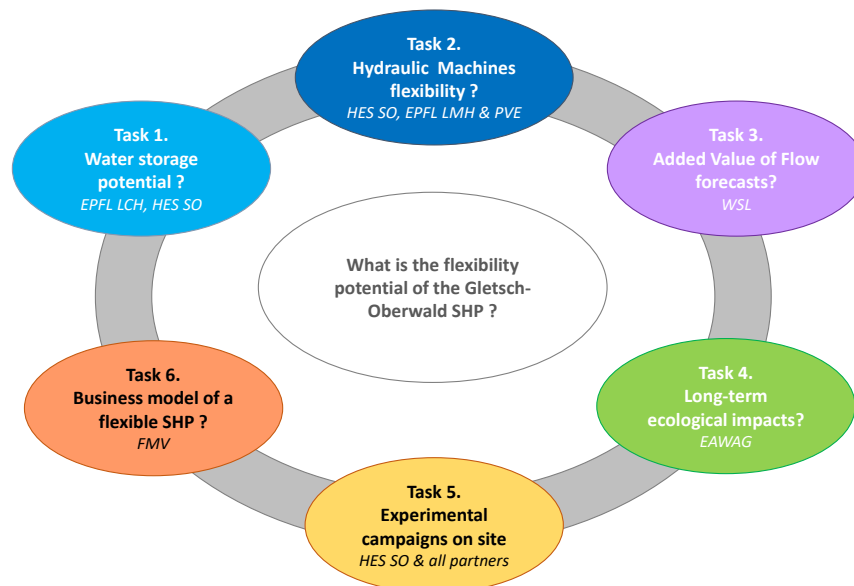


Figure 2: Project organization



## **Task 1: Investigation of the storage potential**

### *Overarching research question*

How can intra-day, intra-week or intra-monthly storage be added to a given run-of-the-river scheme, on the headrace side, on the tailrace side or both, to allow the scheme to generate peak energy and eventually contribute to grid regulation?

### *Workplan*

The aim of this task is to assess the possibilities of increasing storage to concentrate the production in periods with higher remuneration, preferably with best efficiencies. The assessed alternatives to increase storage will range from optimizing the usage of available space under-ground, partial dewatering of the headrace tunnel and exploring open air backwater options within the present concession limits. This may lead to borderline operation, the impacts of which must be identified, assessed, harnessed (if positive) or mitigated (if negative). The main activities planned are:

- Optimizing water diversion and desander operation (including flushing), with regards to available water resources and their variability, sediments inflows, environmental requirements, as well as safety and comfort margins in all hydraulic structures from intake to tailrace.
- Increasing storage volume underground or at open-air (e.g., intake, desander, tailrace).

## **Task 2: Hydraulic machines flexibility**

### *Overarching research question*

What are the consequences of enlarging the operational range of the Pelton turbines in case of large head variations?

### *Workplan*

The aim of the following task is to investigate the flexibility of a run-of-river hydropower plant case study. The SHP studied features two Pelton turbines with a maximum installed power of 2 x 7 MW for a net head of 288 m and a nominal discharge of 5.7 m<sup>3</sup>/s. The storage capacity will be assessed in Task 1, whereas in this task the operating range of the turbine will be investigated for low head operating conditions allowing to make more flexible the hydropower plant. This work will be performed in collaboration between HES SO Valais, EPFL-LMH and PVE.

Four main activities will be carried out:

#### *2.1 Estimation of the available power/energy for ancillary services*

- Complete 1D-Model of the power plant
- Calibration of the parameters
- Simulations of primary control scenarios
- Estimation of water level variations at the inlet & outlet
- Estimations of the pressure fluctuations in the tunnel

#### *2.2 Influence of the water level variation on the jet quality*

- 3D CAO from the intake to the injectors
- CFD simulations for different scenarios
- Influence on the jet quality



### *2.3 Influence of the jet quality on the runner*

- Coupling between CFD and SPH
- 3D SPH simulations of the flow in the Pelton runner for different scenarios

### *2.4 Monitoring of the power plant*

- Implementation of sensors & acquisition systems
- Hydro-Clone installation
- Consequence evaluation of the new operating conditions

## **Task 3: Real-time hydrological forecasts**

### *Overarching research question*

A flexible operation of a small alpine run-of-river plant will require accurate and timely forecasts of runoff and sediment transport in the stream at various time scales (few hours to weeks). What forecast accuracy can be achieved with an operational forecast system for the Rhone river at the inlet of HP Gletsch-Oberwald? And what is the added value of such forecasts for the flexible operation of the new HP plant and for the management of sediments at the basins of decantation?

### *Workplan*

The specific objectives of task 3 are:

#### *3.1 To design and set up a hydrometeorological forecast system specifically for the catchment of Gletsch*

- Fully automatic real-time operation for the duration of the project (2018-2021) and beyond
- Available/visible for all project partners

#### *3.2 To assess the forecast accuracy of this forecast system for various lead times*

- Short range forecasts – Nowcasts (lead time: 0 to 6 hours): The hypothesis is that these very short-range predictions will optimize the flexible management of SHP's and will allow the providers to react to within-day peak energy demands in a timely manner.
- Medium-term runoff forecasts (lead time: 1 to 5 days): These forecasts should be suitable to plan and prepare the detailed sequence of the flexible operation in the coming week.
- Extended range forecasts (lead time: 1 to 4 weeks): The goal would be to increase the flexibility of planning and managing long-term maintenance works like sediment removals.

#### *3.3 To use the hydrological forecasts for estimating sediment transport*

Application of state-of-the-art sediment transport formulas and comparison with sediment observations in the HP Plant

#### *3.4 To further explore the challenges imposed by snow and glacier melt for the runoff forecast at Gletsch*

- Installation and operation of specific winter-time measurements at Gletsch (a location that is unreachable by car and public transport in winter)
- High-resolution modelling of the snow cover



## **Task 4: Short term hydropeaking effects on ecosystems**

### *Overarching research question*

What are the effects of the short-term hydropeaks produced by the flexible power production of a small hydropower plant on the structure and function of the downstream alpine river ecosystem?

### *Workplan*

The study consisted of a series of controlled field experiments downstream the water release of the new SHP in Gletsch-Oberwald. The focus was on quantifying the effect of short-term hydropeaking with varying recovery times in between peaks on the abundance and drift of macroinvertebrates in the downstream floodplain. Specifically, we tested whether the hydropeaking experiment caused a reduction in abundance of hydropeaking sensitive taxa or a shift in community composition as compared to the upstream site unaffected by hydropeaking, and whether the observed response was different in pool and riffle habitats. Furthermore, we quantified the properties of the resulting hydro- and thermo-peaking and assessed them with standard indicators.

## **Task 5: Experimental campaigns on site**

### *Overarching research question*

What are the suitable experimental investigations required to assess the flexibility of this small run-of-river power plant?

### *Workplan*

The achievement of the on-site experimental campaigns requires to carry out several preparative tasks allowing the definition of a production program during the days of the tests that respects the power plant limitations and the owner wishes. To mitigate the risk, two campaigns have been scheduled. The first campaign focuses on the validation of the methodology implemented by keeping in the range of the operating points guaranteed by the manufacturer of the turbine. The second campaign focuses on the exploration of the whole range of flexibility identified.

### *5.1 Preparation of the campaigns*

- Risk assessment, i.e., identification of operation restrictions and mitigation measures.
- Laboratory tests.
- Mapmaking of the widest possible operating range of the turbine.
- Methodology to prepare the production programs.
- Setting up of a dedicated instrumentation to acquire the necessary data and to ensure the smooth running of the tests.

### *5.2 Analysis of the results*

- Post-processing of the on-site test data.
- Mapmaking of the turbine performances necessary for the business model assessment.



## **Task 6: Business model of a flexible small hydropower plant**

### *Overarching research question*

What is the business model of the flexibility for SHP even in case of run-of-the-river plants with a priori small storage capacity?

### *Workplan*

The outcome of the previous tasks investigated in this demonstration project is a set for business models allowing the detailed assessment of the added value of flexibility for small hydropower plants. The limitations due to storage capacities identified in task 1, to electro-mechanical operating range investigated numerically and experimentally in task 2 and to the effect of short-term hydropeaks on the eco-system assessed in task 4 and the opportunities linked to short-term forecasting identified in task 3 will be gathered to define the specifications of the new operating conditions to make more flexible the hydropower plant. New avenues for possible financial models for the flexibility of SHP will thus be identified. The following subtasks are planned:

#### *6.1 Business models*

- Definition of the technical and economic hypothesis
- Acquisition of the technical and economic data
- Proposal for one or more business models
- Comparative assessment of the business models

#### *6.2 Economic scenarios*

- Definition of economic scenarios
- Definition of the key parameters for the sensitivity analysis
- Definition of target value (or range of targeted values) for the key hypothesis
- Development of the calculation model
- Implementation of the scenarios and the sensitivity analysis

#### *6.3 Documentation*

- Report with synthesis of key hypothesis, results of the different scenarios and sensitivity analysis.
- Recommendations on methodology and key issues to be addressed for SHP to evaluate the added values provided by extended flexibility.





## 2 Description of facility

The demonstration site for this project is the run-of-river (ROR) SHP of Gletsch-Oberwald (KWGO) owned by FMV and commissioned end of 2017, see Figure 3. KWGO is in Wallis, the intake being at Gletsch, the water coming from the source of the Rhone River, while the power plant is at Oberwald.

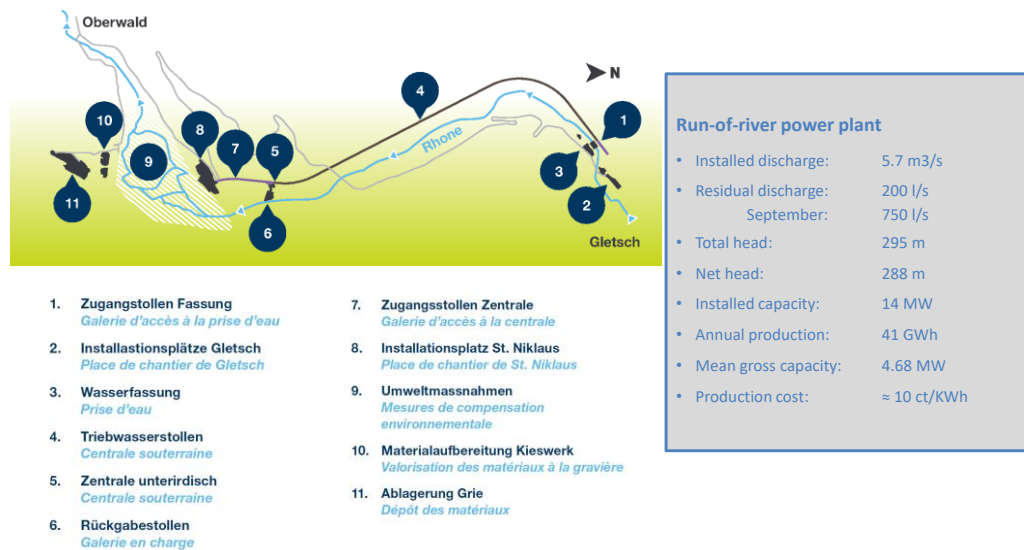


Figure 3: Sketch of the Gletsch Oberwald small hydropower plant, source: FMV.

This ROR SHP is equipped with two six-jets Pelton turbine units, see Figure 4 featuring a maximum power of 7.5 MW each for a net head of 287.45 m and a total discharge varying between 0.145 m<sup>3</sup>/s and 5.8 m<sup>3</sup>/s.



Figure 4. on the left: intake of KWGO, on the right: machinery cavern of KWGO. Source: FMV.

The inflow is maximum during the summer period after the snow melt and is very low during winter, see Figure 5, the mean capacity of the power plant being lower than 5 MW explaining the classification of “small” for this hydropower plant.



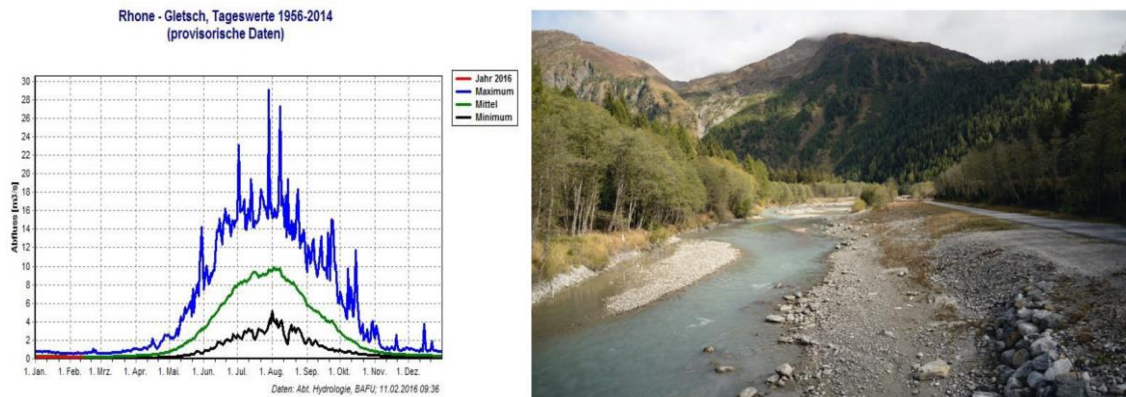


Figure 5. on the left: inflow variation of KWGO, on the right: alluvial area downstream of KWGO. Source: FMV.

### 3 Procedures and methodology

#### 3.1 Task 1: Investigation of the storage potential

The analysis of the possible volumes to be used for storing water has been conducted on a systematic way looking first and foremost to the components of the power scheme, therefore avoiding costly operations of new excavations. A ranking for the most interest components of the scheme to be used as reservoir, can be constituted by analysing the resulting energy coefficient and the use rate, which accounts for the number of times the reservoir is filled by water and how long it takes (a big reservoir may in fact be useless if the incoming water does not fill it completely and on a reasonable duration).

The additional storage volumes, shown in Figure 6, to be considered are:

- the pressurized headrace tunnel;
- the forebay tank;
- the settling basin;
- the access gallery;
- the intake works.

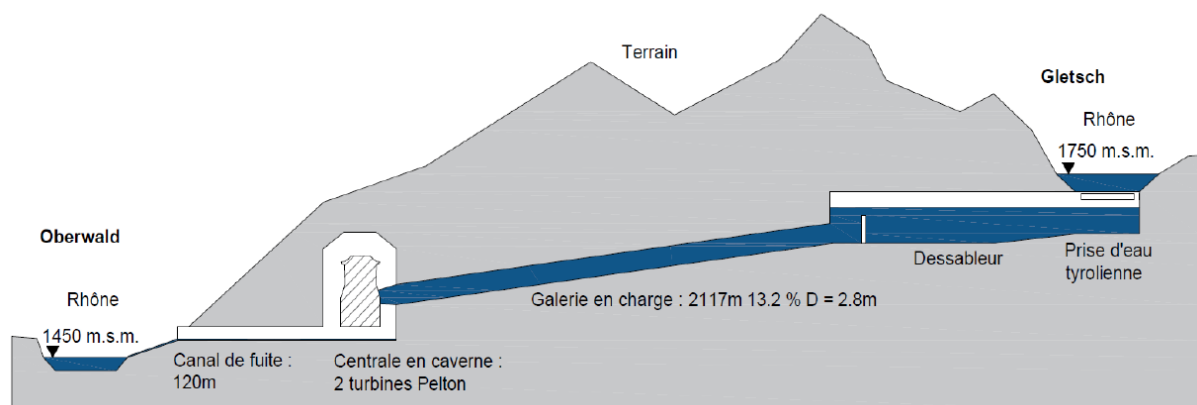


Figure 6: Scheme of the KWGO power plant.



At least, as built drawings are necessary to correctly calculate the available storage volumes, the calculations can be done directly using the 2D drawings or using a CAD software after a 3D reconstruction. If all the information cannot be extracted from the drawings, on-site measurements are required to avoid erroneous data.

The output must be a table giving the available storage volume as a function of the water level.

### 3.2 Task 2: Hydraulic machines flexibility

The task 2.1 and 2.4 concern the global investigations of the ancillary services capacities of the KWGO SHP and the monitoring of the power plant. In order to determine to what extent, the power plant may contribute to support the power network stability and assess the available power/energy for ancillary services, the KWGO SHP is modeled by means of the SIMSEN software to obtain a complete 1D-numerical model, as illustrated in Figure 7. This model also served as the basis of the power plant monitoring with the Hydro-Clone® real-time monitoring system. Hydro-Clone is a digital twin of the power plant based on a duly validated SIMSEN model of the hydroelectric scheme under consideration, which simulates in real time the dynamic behavior of the facility based on boundary conditions measured on site and transmitted to the numerical model via the SCADA system. Its deployment at KWGO SHP prior to commissioning allowed to monitor and exploit the commissioning tests to calibrate the parameters of the numerical model. This procedure ensured the validation of the numerical model of the layout by verifying that the transient behavior of the power plant is accurately reproduced by simulation. Once validated, the SIMSEN model was used to perform numerical simulation during the preparation phases of the 2 test campaigns to anticipate the transient behavior of the power plant during the tests. Then, the Hydro-Clone monitoring system was also used during the 2 hydro-peaking test campaigns performed at site to monitor the transient behavior of the KWGO power plant. The corresponding measurements and simulation results were used for the post processing of the measurement campaigns regarding the transient behavior of the hydro unit.

Among the ancillary services, the primary control ensures that the balance between production and consumption is restored within seconds following a disturbance. To be eligible to provide this service, the power plant must be pre-qualified by Swissgrid to ensure that it is able to provide the primary control capacity, which must be kept in reserve at all time. The 1D-numerical model is thus used to simulate several primary control scenarios to find out how much reserve power the power plant can provide, while meeting the Swissgrid qualification criteria. The dynamic limits of the power plant can thereby be determined, as well as the inlet and outlet water level variations induced by the provision of primary control. By replicating the hydraulic transients of the powerplant, the simulations yield the pressure fluctuations throughout the waterway, which can be post-processed to derive the penstock level of solicitation and assess the potential impact of the primary control on the service life of the penstock.

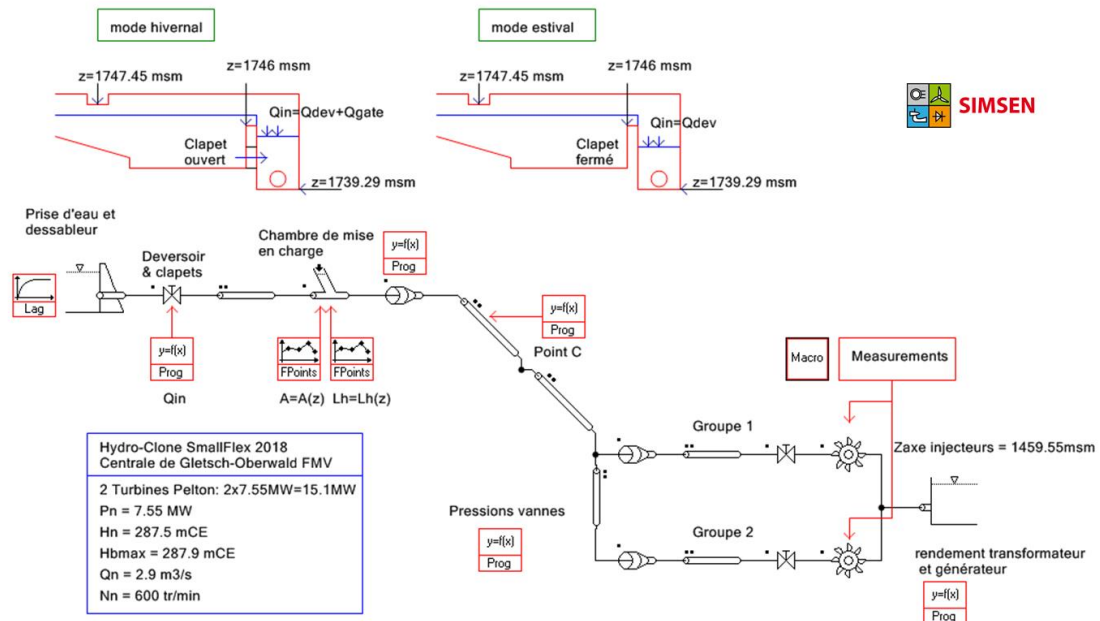


Figure 7: Simsen model of the KWGO SHP

The tasks 2.2 and 2.3 focus on the influence of the water level variation due to the dewatering of the head race tunnel on the jet quality and its impact on the runner buckets (pressure peaks, torque fluctuations, loss of efficiency, risk of erosion...).

A high jet quality is defined by an axisymmetric shape of the jet with a homogeneous velocity and a sharp straight interface between the water and the air. A jet that does not respect these features often leads to torque fluctuations, efficiency losses and premature erosion. In addition, by decreasing the water level, the velocity of the jet also decreases, and two phenomena can occur. A low velocity jet results in the inability of the water sheet inside the runner bucket to escape before the bucket is impacted by a second jet. Therefore, shocks occur between the jet and the water sheet leading to torque fluctuations, local mechanical stresses, and efficiency losses. This phenomenon is often referred as the “falaise” effect in the French literature. Below a critical water level, the jet is unable to reach the runner buckets and no energy is transferred to the Pelton runner. This last phenomenon can be estimated by analytical formula whereas the “falaise” effect can be only roughly estimated by analytical formula.

To investigate the jet quality and the occurrence of the “falaise” effect, a numerical approach is used. The numerical approach is preferred to an experimental study because its cost is lower and numerical simulations allow the detailed investigation of the flow inside the Pelton distributor and in the runner buckets.

However, there are still some challenges that must be tackled. The simulation of the flow in a Pelton turbine requires to deal with both a single-phase flow in the distributor and a two-phase (air and water) flow interacting with the rotating Pelton runner. In the distributor, the flow domain is well delimited, whereas it is not the case in the Pelton casing surrounding the runner. Finite volume solvers are well suited for delimited domain whereas particle-based solvers are more suited for undelimited flow domain with moving boundaries. Therefore, two different solvers have been used. The OpenFOAM toolbox, providing a finite volume solver for two-phase flows, is used to compute the jet. The GPU-SPHEROS solver, based on a finite volume particle method, is used to compute the interaction of the jet with the Pelton runner. A schematic representation of the domains of application of each solver is shown in Figure 8. The coupling between the two solvers is carried out by transferring the velocity, the volume fraction and the turbulence field from the OpenFOAM results to the GPU-SPHEROS simulations at the section 2 (see Figure 8).

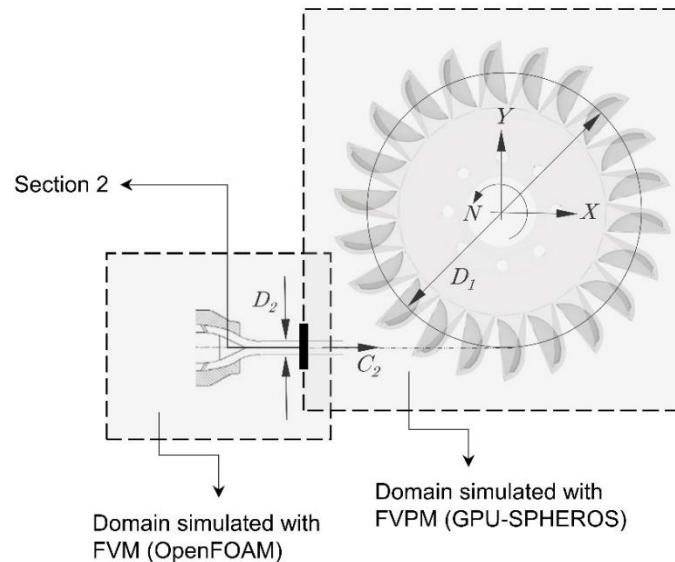


Figure 8: Domains of application of the OpenFOAM and GPU-SPHEROS solvers.

This methodology has been used to compute the flow for six different water levels corresponding to a head variation between 66% and 100% of the nominal head. The OpenFOAM simulations allow investigating the quality of the jet, while the GPU-SPHEROS simulations allow investigating the interaction of the jets with the Pelton runner.

### 3.3 Task 3: Real-time hydrological forecasts

For the purpose of supplying the project partners and operators with accurate forecasts of discharge and sediment transport at the inlet of the KWGO SHP, WSL developed and implemented the following methods:

#### *Short-term runoff forecasts (“Now-casting”)*

For the supply of highly accurate runoff forecasts at short lead-times of 0 to 6 hours, we used the INCA-CH now-cast system (Nerini et al., 2018), developed and provided by MeteoSwiss. It merges all the meteorological information available (from weather stations, precipitation radar and satellite data) in real-time and extrapolates this information into the near future. These data are interpolated to a 1 km resolution grid and updated every 10 minutes to yield predictions for the next 6 hours for the main meteorological variables like precipitation, temperature, wind. Finally, the INCA-CH forecasts were downscaled to the Gletsch catchment using a nearest neighbour approach by incorporating local lapse rates for adjusting temperature and precipitation data. A state-of-the-art hydrological model (PREVAH; Viviroli et al., 2009) was fed with the INCA-CH meteorological forecasts to calculate (at hourly time resolution and at a spatial scale of 100 m) all components of the water balance (including snow and glacier melt) and ultimately the total runoff of the Rhone river at the intake in Gletsch.

The forecast system was fully automated (running on servers at WSL), and the results are displayed on a web platform (<https://hydro.slf.ch/sihl/gletsch>). The coupling of the INCA-CH nowcasts and the PREVAH model was done hourly and results in streamflow, resp. inflow forecasts at Gletsch for the next 6 hours. Beyond the 6 hours COSMO-1 forecasts were assimilated seamlessly and provided forecasts for lead-times from 6 to 30 hours (see following chapter) – according to the schematic in Figure 9.

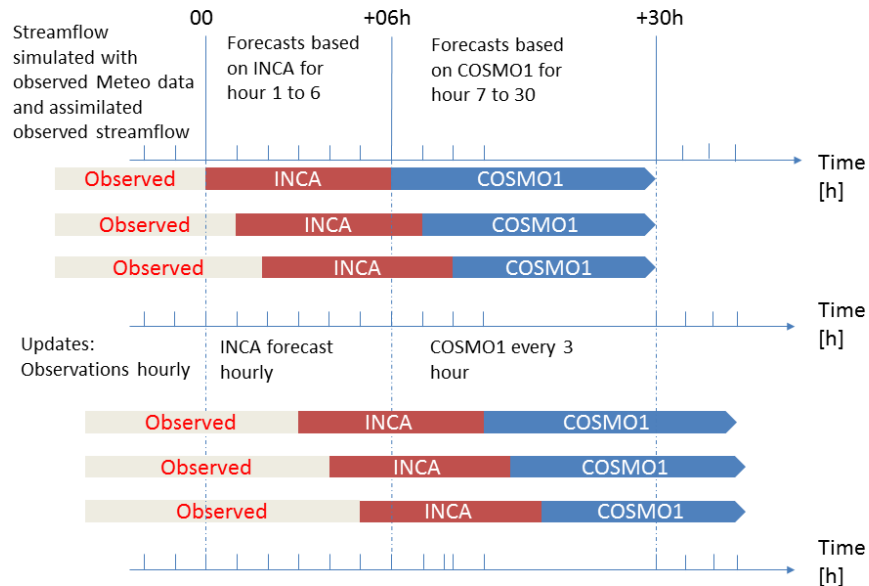


Figure 9: Schematic of the operational implementation of the now-cast INCA + COSMO-1 forecasts at WSL.

#### *Medium-term runoff forecasts ("5-day lead time")*

For the scheduling and design of the two SmallFlex test campaigns, runoff forecasts with lead-times of several days were requested from the project partners, because of the time span needed for preparing the operational work. For this purpose, WSL set up an operational forecast chain using the MeteoSwiss weather model COSMO E, which generates an ensemble of 21 runoff forecasts with lead-times from 1 hour up to 5.5 days. The COSMO E forecasts are initialized twice a day, at 12:00 and at 24:00 and are usually available about 6 hours later at WSL. The horizontal grid size is about 2.2 km. The usage of an ensemble system allows the estimation of the probabilities for the occurrence of events and their uncertainty ranges. As in the case of the short-term forecasts, these meteorological data were automatically transferred to the PREVAH model to produce runoff forecasts for the Rhone river at the intake in Gletsch.

#### *Long-term runoff forecasts ("lead time 1 month")*

For a longer-term planning of the (flexible) operation of the KWGO SHP we also set up a model chain for meteorological extended-range forecasts (provided by ECMWF/MeteoSwiss) covering the range of lead-times between several days and four weeks. The spatial resolution of the meteorological extended-range forecasts changes from 18km for the first 15 days to 36km for the weeks three to four. When looking at forecast horizons beyond seven to ten days the skill of an exact deterministic prediction is small because of the chaotic nature of the atmosphere and the increase of uncertainty. However, with the help of ensembles it is possible to describe the probability that runoff will be below or above a certain threshold for specific weeks ahead. Usually, the thresholds are based on climatological long-term observations. For example, for tercile forecasts two thresholds are defined, which divides the historical data in 1/3 below normal (lower tercile), 1/3 above normal (upper tercile) and 1/3 between these lower and upper tercile. Monthly tercile forecasts were implemented into the Gletsch forecast model in 2019 allowing the estimation of possible trends in the streamflow for the upcoming 2 to 4 weeks (see example of a tercile forecast for Gletsch in Figure 10).

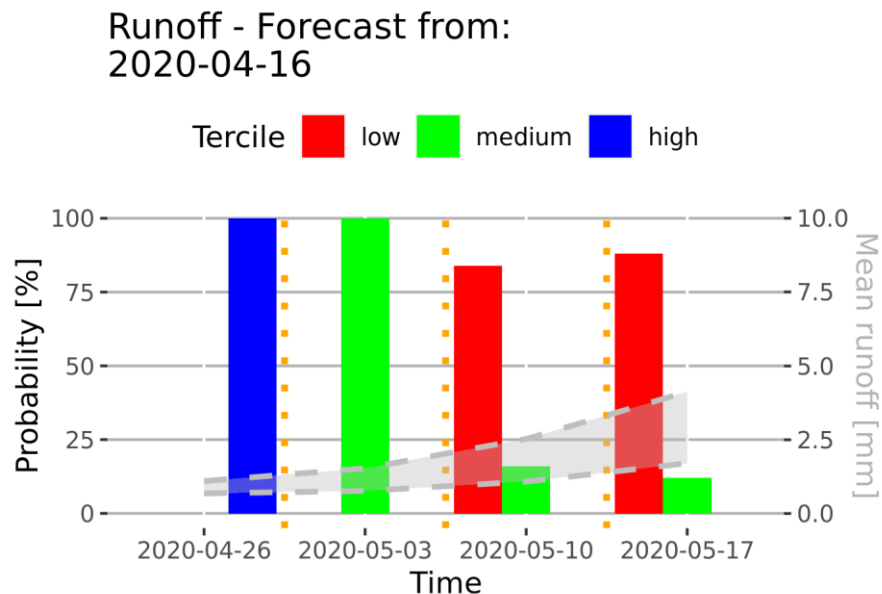


Figure 10: Example of the tercile forecast for the upcoming 4 weeks. The probability for each tercile is estimated by the number of ensemble members falling into each category. For example, at week 1 all 51 ensemble members are in the 3<sup>rd</sup> tercile indicating streamflow conditions above the normal climatological range for that week of the year.

#### *Estimations/Forecasts of sediment transport*

For the purpose of estimating and forecasting sediment transport in the Rhone river at the intake of the KWGO SHP, we combined our runoff forecasts with a sediment-transport formula. The Gletsch catchment is dominated by a glacial runoff regime with steep slopes and pronounced seasonal and diurnal variations in flow discharge and sediment transport rates. In general, bed load transport rates are typically calculated as a function of the hydraulic forcing, which can be expressed by, e.g., flow discharge, stream power or shear stress. In order to accurately predict bed load transport rates at steep slopes, one has to consider the increased flow resistance and critical conditions for initiation of motion as additional controls on bed load transport.

Based on a state-of-the-art formula by Rickenmann (2012) the critical discharge for sediment transport was calculated as a function of slope, grain size and channel width. If the observed/forecasted streamflow is above this critical discharge sediment transport will occur, which is called the effective runoff volume. The total bedload volume is a function of the effective runoff volume and slope and a correction factor. To account for energy losses due to form roughness, a reduced energy slope is used instead of the real channel slope.

However, direct observations of bed load transport and hydraulic conditions in such steep streams are rare, complicating the model development and validation. For the period of this project only rough estimates of accumulated sediment volumes were available for the Rhone river at the intake in Gletsch counting the sand trap emptying during summer 2018. This information was used as guidelines for verifying the results of the formula of Rickenmann.





### 3.4 Task 4: Short term hydropeaking effects on ecosystems

#### *Introduction*

An experimental field study was performed in November 2018 to investigate the effects of hydropeaks with varying recovery time in between on the abundance and drift of macroinvertebrates in the downstream floodplain. The set-up and methods are described in detail in Aksamit et al. (2021a) and shortly summarized in the following.

#### *Experimental set-up*

The experimental field study was scheduled in November 2018, during near representative late autumnal conditions. It included five experimental hydropeaks of 15 minutes duration. The hydropeaks were performed on 8, 16, 19, 21 and 22 November at 13:00, resulting in progressively shortened recovery times of 8, 3, 2, and 1 day between the peaks (Table 1). Sampling was performed in the residual flow reach upstream of the outflow of the hydropower plant and within the floodplain of national importance downstream of the outflow (Figure 11). At both sites, sampling was performed in a riffle and a pool habitat.

Table 1: List of experimental hydropeaks including information on average water temperatures, weather in the previous 48 hours and air temperature. The recovery time >100 for the first peak indicates that there has been no previous experimental hydropeaking in this river reach.

Peak	Date	Recovery time [days]	Average water temperature [°C]	Air temp min/max [°C]	Weather (previous 48 hours)
1	08.11.2018	> 100	4.48	7 / 15	Sunny; 34.5 mm of rain
2	16.11.2018	8	2.96	-1 / 11	Sunny; no precipitation
3	19.11.2018	3	1.33	-9 / 5	Snow; 2 cm of snow
4	21.11.2018	2	1.50	-6 / 4	Overcast; 5 cm of snow
5	22.11.2018	1	2.46	-10 / -1	Sunny; 2 cm of snow



Figure 11: Sampling locations (Figure modified from Aksamit et al. (2021a)).



### Macroinvertebrate sampling

Two macroinvertebrate collection methods were employed at the two measurement sites:

- Drift-net sampling: Drifting macroinvertebrates were collected in both the pool and the riffle habitats using triplicate nets placed above the stream substrate to allow water to flow through. Samples were collected during baseline conditions before each peak, and during different phases of each peak (Figure 12).
- Kick-net sampling: Benthic macroinvertebrates were sampled by agitating the stones, sediment, and organic matter of the stream bed by foot and catching the sample in a net held next to the disturbance. Samples were taken during baseline conditions before each peak. Sampling was performed in the pool and the riffle habitat at the downstream site, but only at one combined habitat at the upstream site.

The collected macroinvertebrates were preserved using 70% ethanol and subsequently determined to family level in the laboratory.

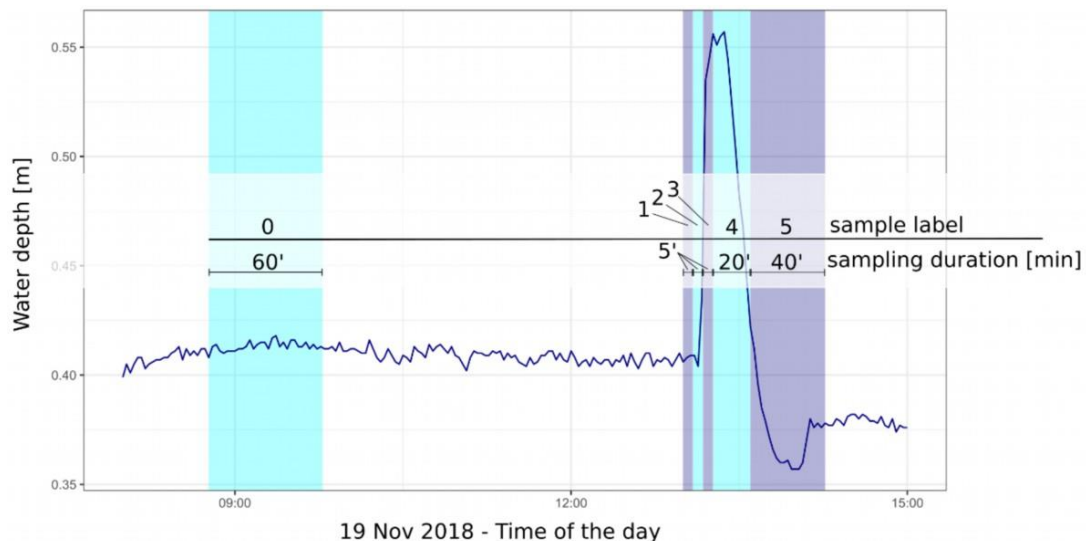


Figure 12: Timeline of drift samples taken during each hydropeak. The baseline sample 0 was taken during 60 minutes in the morning before each peak. Two 5-minute samples were taken during the rising limb (samples 1 and 2) and one at the peak (sample 3). The 20 minute-sample 4 was taken during the falling limb, and subsequently, 60-minute post-peak sample was collected. The blue line indicates the water depth recorded in the main channel at the downstream measurement site (Figure from Aksamit et al., 2021a).

### Sampling of physical and chemical parameters

The following physical and chemical parameters were recorded to calculate the filtered water volume during the drift samplings and to characterize the physical and chemical conditions of the experiments:

- Flow velocities in front of each net were measured with a MiniAir2 velocity meter (Schiltknecht AG, Gossau, Switzerland).
- Water depths in front of each net were measured with a rigid meter.
- Water temperature and pressure (as a proxy for the water level) in the main channel at the upstream and downstream sites as well as directly downstream of the outflow of the power plant were recorded using HOBO U20L-04 temperature loggers.
- Water temperature, specific conductivity, dissolved oxygen, pH, and turbidity at the measurement sites were measured with a WTW MultiLine® 3630 IDS portable meter, and a Hach 2100Q Turbidity meter, before, during and immediately after each peak.
- Grain size distribution of the substrate was sampled before each experiment in each habitat with a Wildco Gravelometer.





### Statistical analysis

Before statistical analysis, observed macroinvertebrate abundances were converted to densities by dividing them with the filtered volumes. Statistical analyses were performed using PRIMER Version 7 with the PERMANOVA+ add-on.

## 3.5 Task 5: On-site tests

Before performing the on-site tests, studies and works are necessary to avoid damaging the power plant and to collect the maximum valuable information for assessing the possibility to operate the power plant by dewatering the head race tunnel safely and efficiently. These works cover different topics, the most important ones are described.

One study must focus on the risk assessment related to the tests scheduled, i.e., hydropeaking and dewatering of the head race tunnel. The risk assessment and the corresponding actions taken to mitigate the risk are summarized in Figure 13.

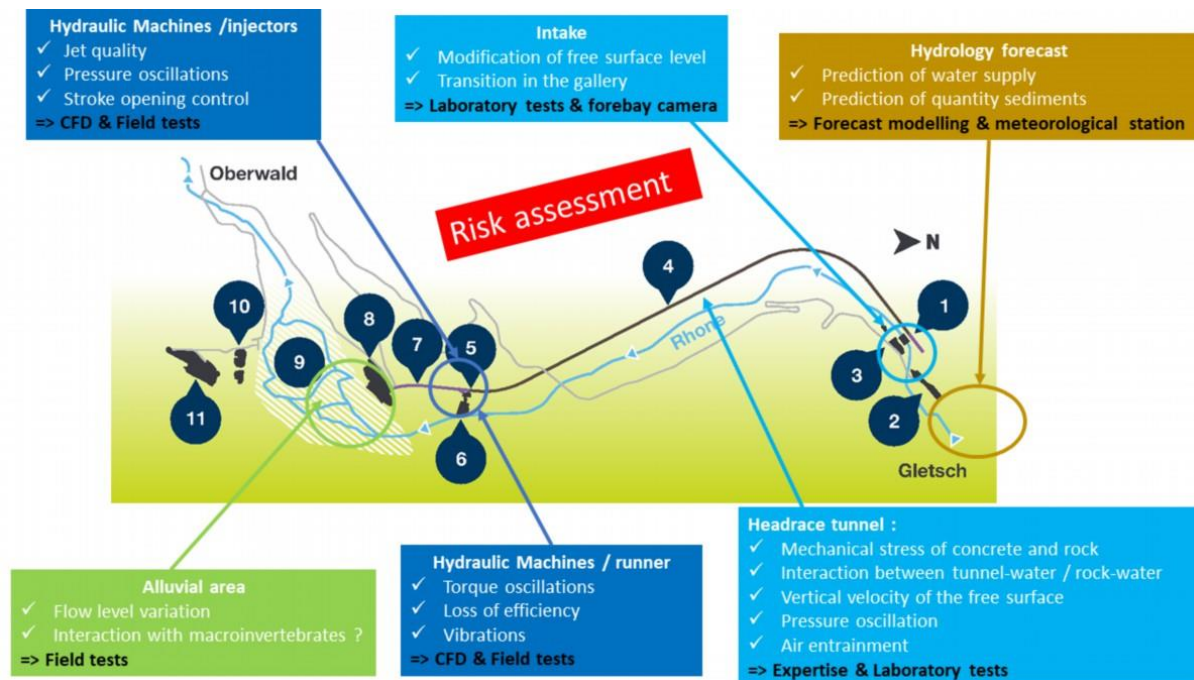


Figure 13: Risk assessment due to the dewatering of the head race tunnel. Bold black text refers to the actions taken for mitigate the risks.

The most important risks are:

- the mechanical stresses and pressure oscillations in the head race tunnel.
- the air entrainment inside the penstock.
- the vibrations of the Pelton unit usually accompanied by an efficiency loss.
- the environmental impact (see task 4).

To address the first three risks, specific actions have been undertaken.

Regarding the mechanical stresses in the rock, the investigation has been done by a third party based on a design brief written by the partners describing the duration of the peaks, the number of peaks wished, the lowest head targeted... Furthermore, PVE checked the possibility to do an emergency shutdown of the power plant whatever the water level in the head race tunnel and particularly at the lowest head scheduled.



For the risk of air entrainment, experimental studies have been carried out on a reduced scale model of the forebay tank and the head race tunnel built at the HES-SO laboratory (see Figure 14).

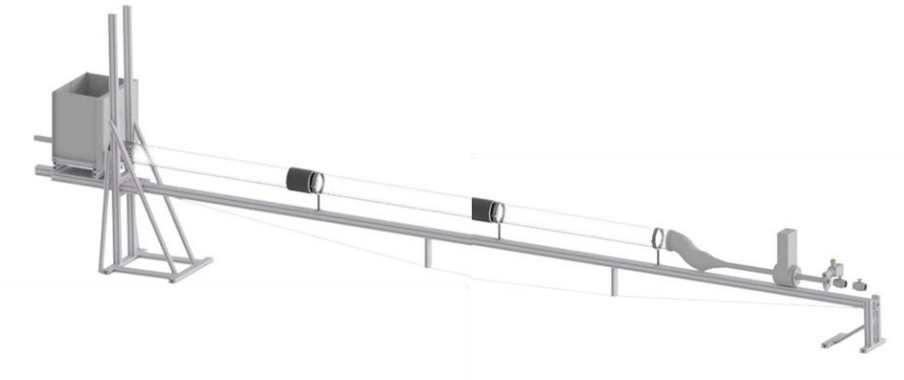


Figure 14: 3D view of the reduced scale model of the forebay tank and the head race tunnel.

Using a high-speed video camera, the free surface of the flow is observed and the risk of air entrainment assessed. Two cases can be critical: firstly, the presence of a vortex in the forebay tank that can suck air inside the flow and secondly the entrainment of bubbles downstream the hydraulic jump in the head race tunnel. These two cases are shown on Figure 15 for a flow discharge 50% higher than the maximum flow discharge of the power plant. For lower flow discharges no vortex or air bubbles entrainment are observed. Consequently, no air entrainment is expected during the on-site tests.

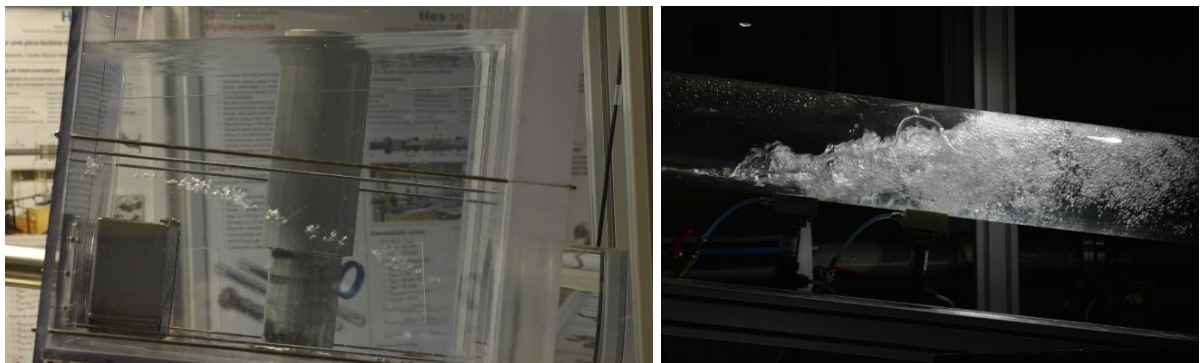
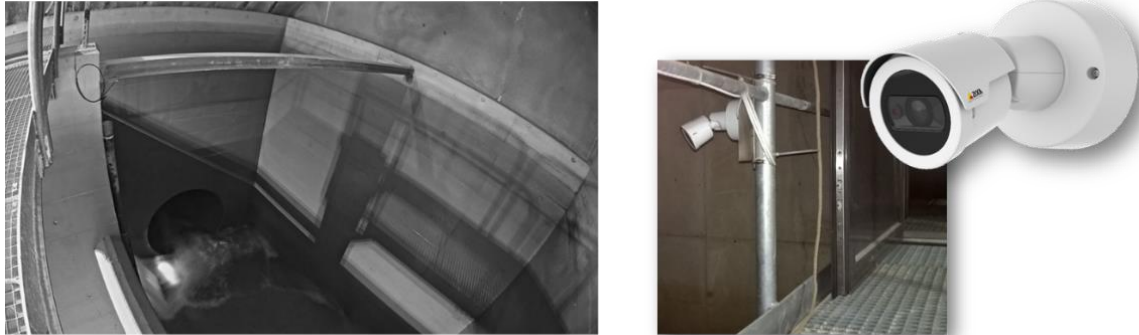


Figure 15: Risk of formation of an air vortex in the forebay tank (left) and of air entrainment downstream a hydraulic jump. Model tests at a flow discharge corresponding to 150% of the maximum flow discharge of the power plant.

In addition, on site, an IR camera (see Figure 16) has been installed above the forebay tank to film the water surface during the dewatering. The camera allows to view the formation of vortices or waves at the free surface.



Regarding the vibrations, the Pelton unit has been equipped with six sensors: a flow meter, two pressure sensors, a tachometer, an accelerometer 3-axis and a microphone. The flow meter and the pressure sensors allow calculating the hydraulic power and detecting the flow perturbations. The microphone, the tachometer and the accelerometer allow assessing the vibration level and identifying the instabilities that occur during the tests.

The diagram illustrates the timeline of the test phase, showing the preparation of the program for day J (LCH) and the prediction of the debit (WSL) on day J-2, followed by the verification of the program on day J-1, and the final test on day J.

**Timeline:**

- Jour J-2:**
  - Préparation du programme pour le jour J (LCH):** Indicated by a double-headed arrow.
  - Prediction du débit (WSL):** Indicated by a green vertical line.
  - Vérification du programme:** Indicated by a brown vertical line.
  - Jour J-2 à 18h:** Envoi du programme du jour J à FMV.
- Jour J-1:**
  - Jour J-1 à 7h:** Envoi du programme du jour J à FMV corrigé avec les nouvelles prédictions du WSL si nécessaire.
- Jour J:** Jour du test.

For the first on-site tests in November 2018 (Figure 18), seven peaks have been scheduled over three weeks. The first two weeks are dedicated to the investigation of the influence of the hydropeaking events on the alluvial area by imposing a power of 6.5 MW for 15 minutes. Only the duration between two peaks is changed. The third and last week of tests focuses mainly on the production capacity by changing the duration and the amplitude of the peaks.

27/75

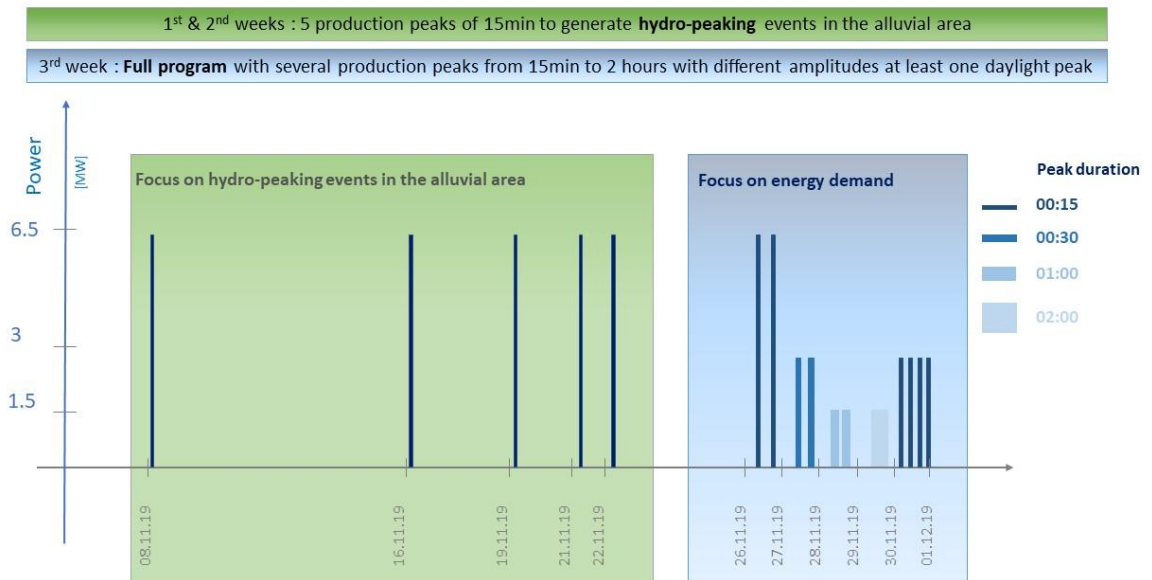


Figure 18: Schematic representation of the program achieved during the first field tests.

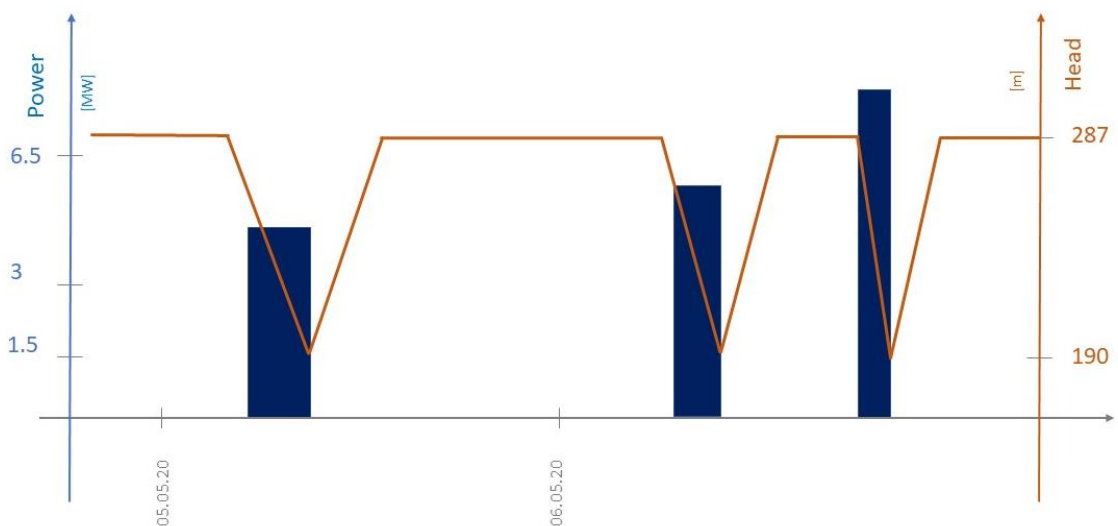


Figure 19: Schematic representation of the program achieved during the second field tests.

Contrary to the first campaign of on-site measurements, the dewatering of the head race tunnel required a deeper understanding of the feasible operating point range. Therefore, several maps have been drawn. An example is shown on Figure 20 for an incoming flow discharge of  $1.5 \text{ m}^3/\text{s}$ . The feasible operating points are in the region located below the thick black line that corresponds to the maximum flow discharge. The yellow dotted line represents the trajectory of a possible peak of two hour long. Following this line, the peak of production starts with a water level corresponding to the nominal head of 287 m. The power is set to 6.3 MW. Then, after one hour, the power is shifted to 5.8 MW for one hour. At the end of the peak, the head race tunnel is dewatering with a head of 220 m approximately.

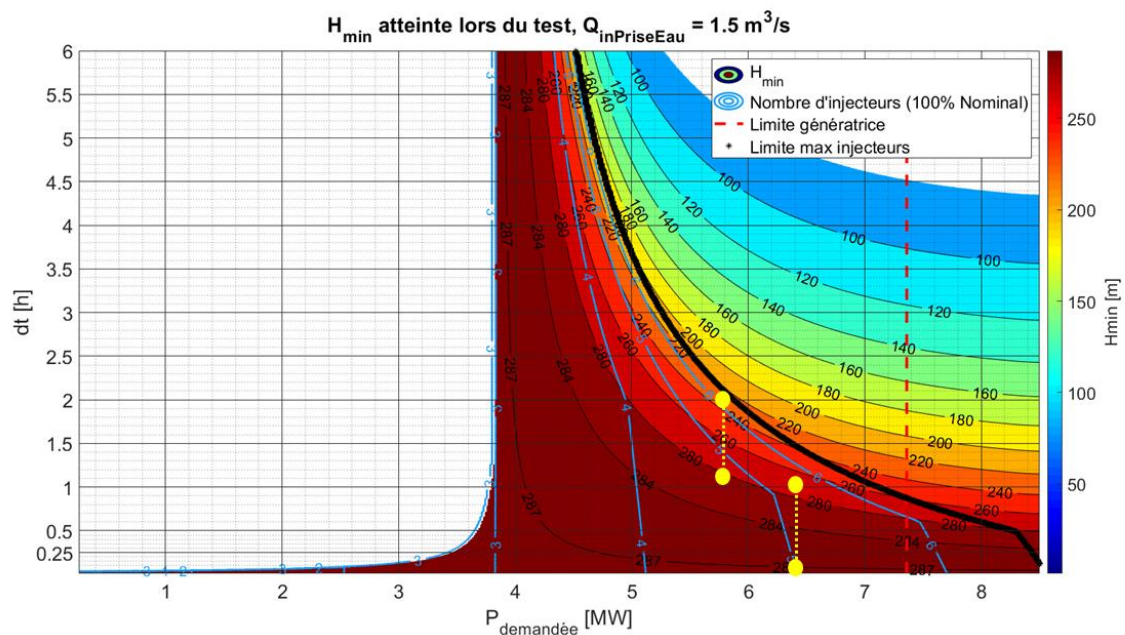


Figure 20: Example of a map representing the available range of operating points feasible for the peaks of production. The yellow lines show the trajectory of a possible peak.

Finally, a day has been dedicated to the manual control of the power plant to check for instance the possibility to set the needle stroke independently for each needle and on the entire stroke range. Manual control is necessary to investigate specific configurations that cannot be observed using an automatic pilot.

### 3.6 Task 6: Business model of a flexible small hydropower plant

The investigation of the possible economic benefits is based on the use of the storage volumes shown on Figure 21 corresponding to:

- 4'050 m<sup>3</sup> (volume 2 and 3) and approximately 2.5 MWh in summer mode from the 15<sup>th</sup> of May to the 15<sup>th</sup> of October.
- 6'180 m<sup>3</sup> (volume 1, 2 and 3) and approximately 4 MWh in winter mode from the 15<sup>th</sup> of October to the 15<sup>th</sup> of May.

Today the power plant operates at a fixed water level corresponding to an altitude of 1'747 masl. Consequently, the turbined flow discharge must be adjusted continuously depending on the incoming flow. The Pelton turbine can be run only for a flow discharge larger than 145 l/s. Since a minimum flow of 200 l/s (750 l/s in September) must be released for environmental purposes, the power plant can be operated only if the inflow is larger than 345 l/s (895 l/s in September). The use of the storage volume is a possible solution to avoid such a limitation.



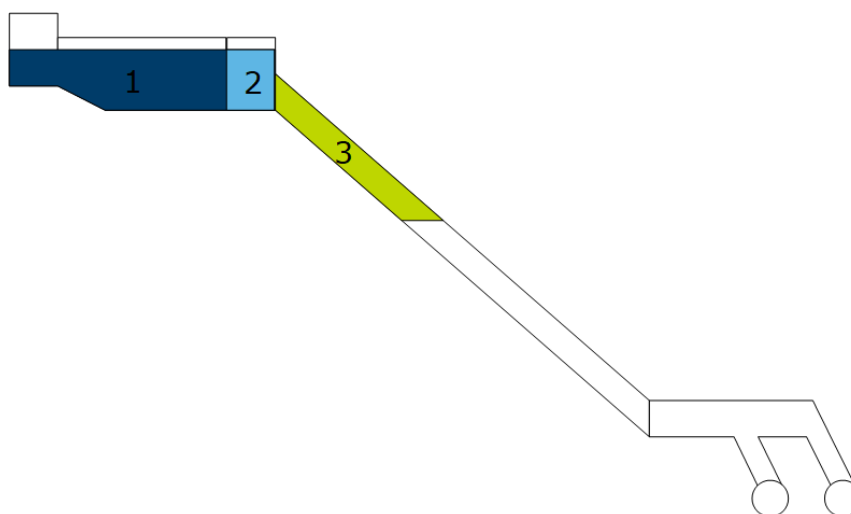


Figure 21: Identification of the volume storage: volume 1, the grit settling basin; volume 2, the forebay tank; volume 3, the head-race tunnel.

The Time-Step Energy (TSE) software is used to optimize the production depending on the incoming flow, the energy price on the electricity market and the available storage volumes. Following the results of the on-site campaign of measurements, limitations have been set to:

- a minimal head of 232 Water Column meter (WCm).
- a maximum power of 5 MW for a Pelton group.

Furthermore, a table linking the required flow discharge as a function of the available storage volume (determined in task 1) and the power requested has been provided to the TSE software (Table 2). The volume capacity of 100% corresponds to the volume in the winter mode, therefore the volume available in summer mode is limited to 66%.

Table 2: Flow discharge as a function of the available storage volume and power requested.

Volume [%]	Power [MW]	Q in winter mode [m <sup>3</sup> /h]	Q in summer mode [m <sup>3</sup> /h]
0	5	9 689	9 689
10	5	8 855	8 886
20	5	8 367	8 387
30	5	8 004	8 032
40	5	7 705	7 731
50	5	7 475	7 487
60	5	7 425	7 372
70	5	7 398	7 292
80	5	7 374	7 292
90	5	7 352	7 292
100	5	7 328	7 292



The optimisation of the energy produced is carried out separately for two different objectives:

- i. to maximize the revenue depending on the electricity price,
- ii. to maximize the revenue depending on the primary frequency control (PFC) ancillary service.

For the first objective, the storage volumes are used to increase the production of energy during the periods with the highest purchase prices. Then the volume storage that has been used is filled during the period of low purchase prices by operating the turbines at their minimum power or even by switching off the turbines. The optimization has been carried out over the years 2018 and 2019, for which the incoming flow discharge and the SPOT price in € are known.

For the second objective, the power and the storage volume required are known from the study performed by PVE (task 2.1). The maximum power is of 1.5 MW corresponding to a volume equal to 540 m<sup>3</sup> that is slightly higher than the volume of the forebay tank, which requires in summer mode to empty partially the head race tunnel. The optimization has been carried out for the years 2018 and 2019 in two steps: firstly, the production of the power plant operated at a constant water level is optimized without primary control ancillary service; secondly, the primary frequency control is considered over periods of 4 hours. However, Swissgrid required a power in whole number between 1 MW and 25 MW. Therefore, the analysis has been extended to the regulation control pool of FMV that includes the power plants of Ernen, Bramois, Gletsch-Oberwald and Pissevache.

The PRL prices considered for the study are the ones of the year 2020 due to the strong changes that occurred on this market for the last 2 years.



## 4 Results and discussion

### 4.1 Task 1: Investigation of the storage potential

Based on the power plant scheme and the storage volumes selected for the study, a preliminary ranking has been defined by listing the advantages and drawbacks for each volume. Table 3 lists the storage volumes selected with their advantages and drawback. Obviously, the construction of an external reservoir is costly and not easy to carry out. The three other options can be explored even if the use of the access gallery requires more works and can lead to safety issues.

Table 3: List of the selected storage volumes with their advantages and drawbacks.

Volume	Advantages	Drawbacks
Head race tunnel	<ul style="list-style-type: none"><li>• No modifications of the scheme</li></ul>	<ul style="list-style-type: none"><li>• Risk of air entrainment.</li><li>• lower turbine efficiency</li></ul>
Settling basin	<ul style="list-style-type: none"><li>• Minor work for geometry adaptation</li></ul>	<ul style="list-style-type: none"><li>• Risk of sediments passing through the waterways to the turbines</li></ul>
Access gallery	<ul style="list-style-type: none"><li>• Acceptable work for geometry adaptation (waterproofing of the gallery, gates)</li></ul>	<ul style="list-style-type: none"><li>• Temporary no access to the intake underground facilities.</li></ul>
External reservoir	<ul style="list-style-type: none"><li>• Large storage volume</li></ul>	<ul style="list-style-type: none"><li>• Major geometry changes</li><li>• Environmental impact</li><li>• Ground acquisition</li><li>• Snow and ice on the reservoir during winter</li></ul>

In order to select the most suitable components of the power scheme to be used for water storage, the power production at KWGO is simulated. The smart storage operations are reproduced considering an average winter and the inflow is calculated on the base of hourly mean discharge data at the federal hydrometric station (river gauging) of Gletsch, from 1974 to 2016. The energy value of each combination of power plant components considered for water storage is calculated on the base of the hydraulic head and the volume available. An energy coefficient  $EC$  is therefore defined as the cumulated energy produced per unit volume of stored water:

$$EC = \frac{\eta \gamma_w H V_{cum}}{V_{tot}}$$

Where:

- $\eta$  is the global efficiency ratio (usually between 0.7 and 0.9, here an average value of 0.8 has been used).
- $\gamma_w$  is the specific weight of the water.
- $H$  is the water elevation.
- $V_{cum}$  is the cumulated water volume in the scheme, going from downstream to upstream.
- $V_{tot}$  is the total water volume of the power scheme component (e.g., the top 1/3 of headrace tunnel length).





Figure 22 shows the water elevation corresponding to the cumulated water volume, starting from the most downstream component.

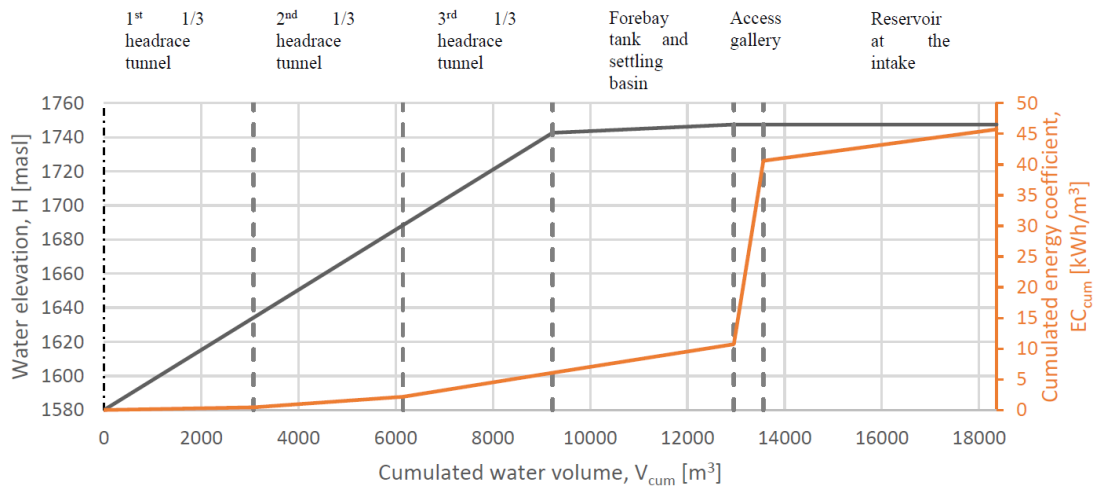


Figure 22: Water elevation in the power scheme and cumulated energy coefficient  $EC$  vs cumulated water volume. The combinations of components of the power scheme have been considered from downstream to upstream.

The economical valuation of each combination is also explored by comparing the cost generated by the works for the geometry adaptation (the investment) and the cumulated relative value of the kWh per unit stored water volume  $UV_{cum}$  which is defined as:

$$UV_{cum} = \frac{EC_{cum}}{V_{cum}}$$

Figure 23 shows that the two most expensive solutions are the construction of an external reservoir and the adaptation of the access gallery while the use of the headrace tunnel and the settling basin require only minor expenses. The unit value of each stored unit volume of water [kWh/m<sup>3</sup>/CHF] are the most interesting for the top part of the headrace tunnel and the settling basin.

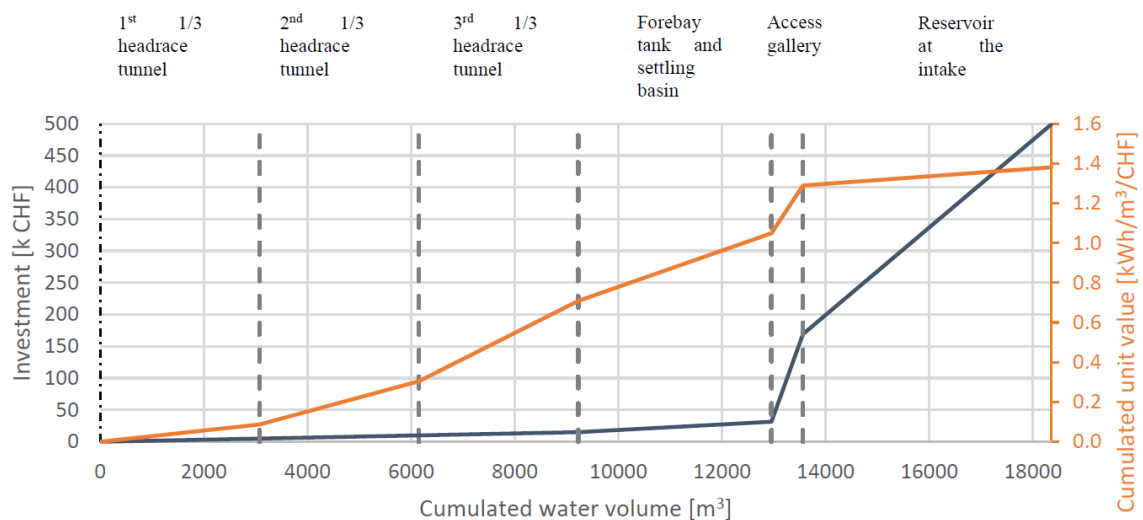


Figure 23: Cost for the adaptation of the power scheme component to the new operations (investment) and profit per unit water volume vs Cumulated water volume.



The screening proves that the settling basin and the forebay tank are the most profitable parts for the implementation of the smart water storage operations at KWGO. Therefore, two opening gates between the settling basin and the forebay chamber have been created (see Figure 24). These gates allow the use of the settling basin as a storage volume during the winter period for which the transport of sediment is low. In the summer period, the gates are closed and the only storage volume available is the forebay tank. Therefore, a storage volume curve has been defined for each period of operation (see Table 2).



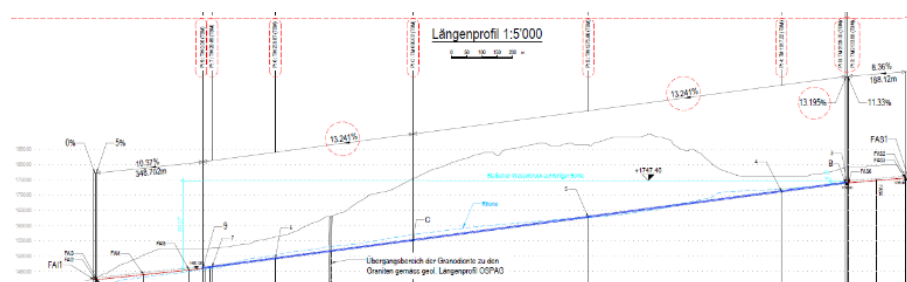
Figure 24: KWGO forebay tank with the two openings created on the downstream wall of the settling basin. The picture was taken the 24<sup>th</sup> of September 2018.

## 4.2 Task 2: Hydraulic machines flexibility

### *Estimation of the available power/energy for ancillary services*

The objective of this task is to evaluate the potential of available power to provide ancillary services, based on simulations of primary control scenarios using a SIMSEN 1D-numerical model of the KWGO SHP, as illustrated in the **Erreur ! Source du renvoi introuvable..** Particular care was taken to correctly model the desander and the forebay chamber, by taking into account the discharges exchange through the bottom gates and the weir, as shown in Figure 25c. The SIMSEN model can be configured to be either in "summer" operating mode, where the bottom openings are blocked and all the flow passes through the weir, as well as in "winter" operating mode, where the gates are open to allow the exploitation of the additional volume represented by the desander. It is worth mentioning that this model is also used by the Hydro-Clone® real-time monitoring system, which has been operational since June 2018. Consequently, its calibration and accuracy have been duly validated during commissioning tests. For instance, Figure 25d shows the comparison of measured and simulated pressures at the penstock bottom during an emergency shutdown of both units. It can be observed that the accuracy of the model is remarkable as it replicates almost perfectly the pressure transient in front of the turbines.

a)



b)

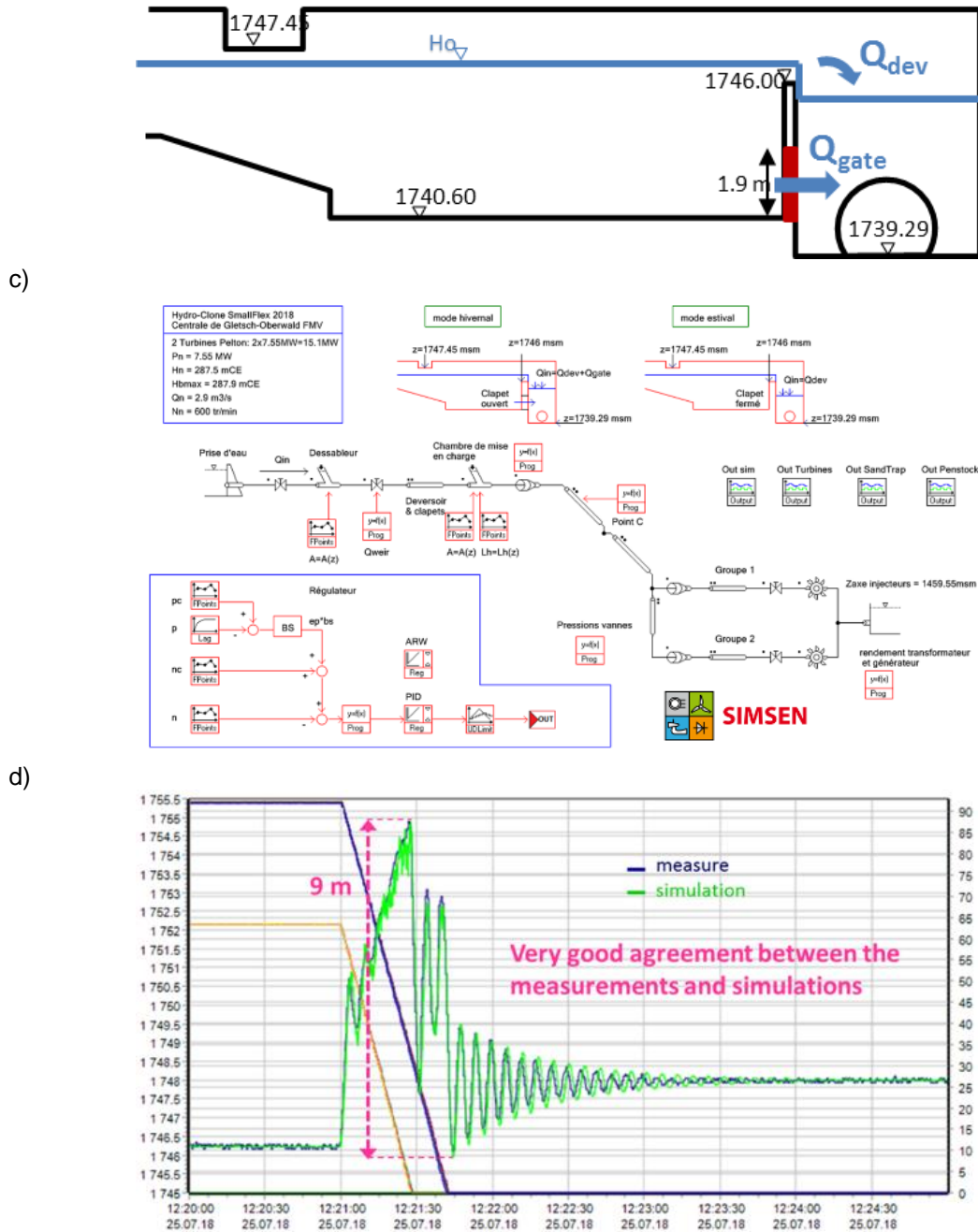


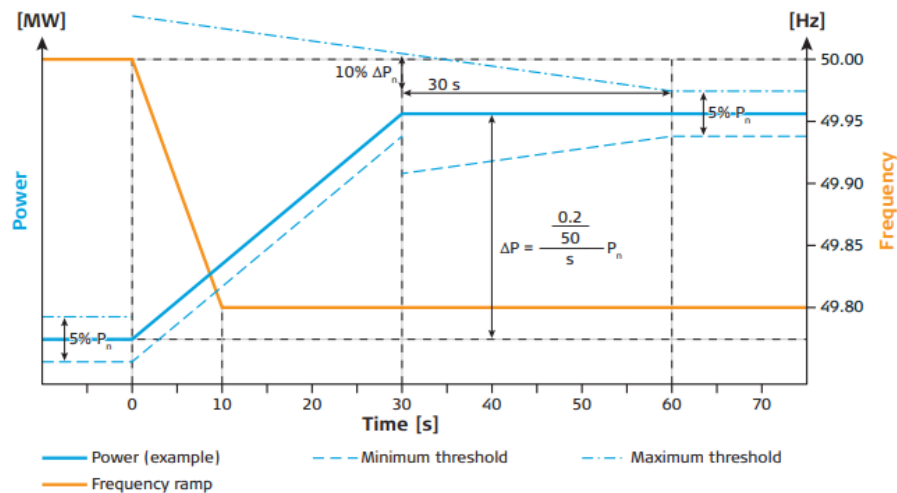
Figure 25. a) Layout of KWGO. b) Schematic view of the desander and forebay chamber with the flow through the gate and weir. c) SIMSEN model of the SHP KWGO with the regulator. d) Comparison of measured and simulated pressures at the penstock bottom during an emergency shutdown.

Among the ancillary services, the primary control ensures that the balance between production and consumption is restored within seconds following a disturbance. This activation is carried out directly and automatically in the power plant using the turbine controllers. According to Swissgrid's requirements, it must be possible to consistently activate the primary reserve power within 30 seconds and deliver it for at least 15 minutes for any quasi-stationary frequency deviation of  $\pm 200$  mHz. In addition, the power production must be within the tolerance bands shown in Figure 26. The amount of power delivered by a generating unit as a function of the frequency deviation in the network is typically characterized by the value of the permanent droop, defined as  $BS = (\Delta f / f_{ref}) / (\Delta P / P_{ref})$ . For instance,

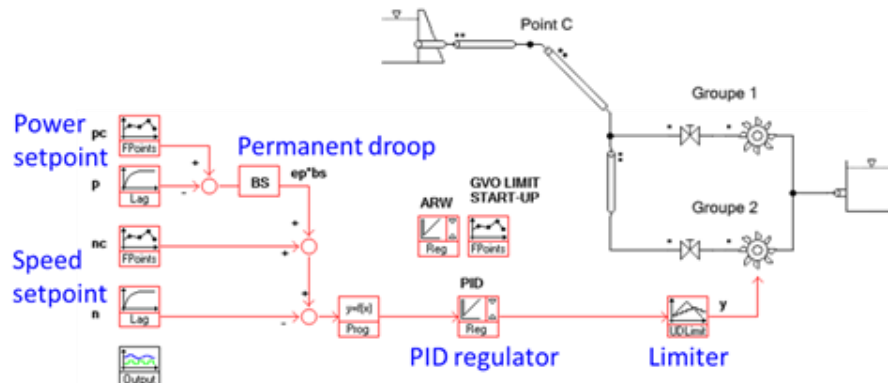


a permanent droop of  $BS=4\%$  corresponds to the provision of  $\pm 10\%$  of the nominal power in case of a frequency deviation of  $\pm 200$  mHz. In the case of the SHP KWGO, the analysis of the primary control potential consists first in evaluating the energy reserve available to provide ancillary services without exceeding the turbine guarantee limits. In a second step, the dynamic response of the facility is simulated for various permanent droop values by incorporating the turbine governor into the SIMSEN model of the power plant. This SIMSEN implementation of this PID type governor is shown in Figure 26d, with the speed and power control loops being combined via the permanent droop. The parameters of this controller have been optimized to obtain the most dynamic and stable response possible. Numerous frequency response scenarios were simulated to find out how much reserve power the power plant could provide, while meeting the Swissgrid qualification criteria (frequency response), see Figure 26c. Finally, the model was used to define the maximum permanent droop value that would guarantee a stable operation for a set of PID parameters. Indeed, the permanent droop acts as a gain on the regulator power control loop as illustrated in Figure 26b. Consequently, for an active power setpoint change, a low permanent droop can lead to a more stable behavior than a high permanent droop value, although the corresponding contribution to the primary control is more important. The stability of the system response to active power setpoint changes was therefore checked by simulating several permanent droop values in combination with the selected PID parameters, as shown in Figure 26d.

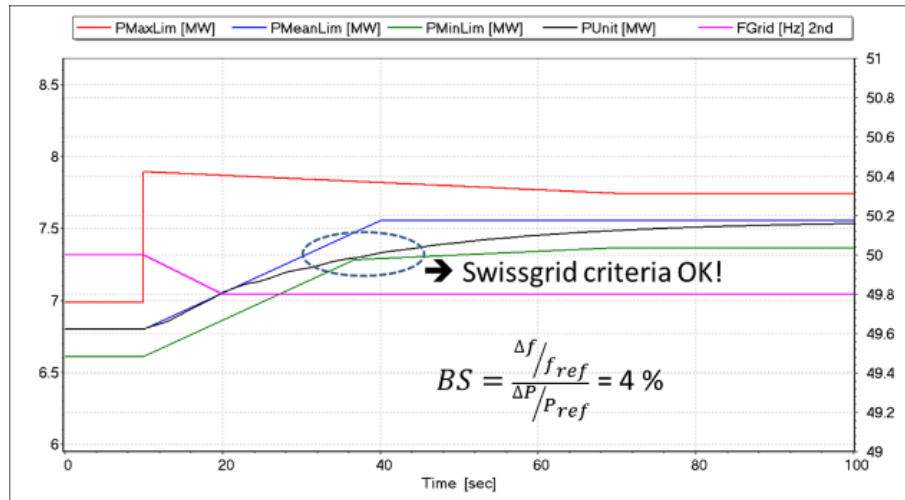
a)



b)



c)



d)

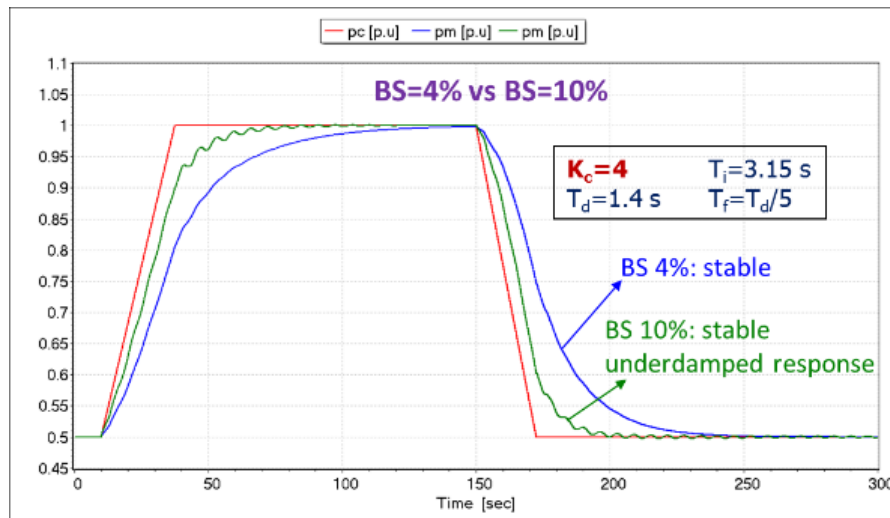


Figure 26. a) Tolerance band of the Swissgrid qualification test. b) SIMSEN modeling of the turbine governor. c) Simulated frequency response scenario meeting Swissgrid criteria with a permanent droop of 4%. d) Stability of the response when the power setpoint is changed with the permanent droop up to 10%.

The results of the estimation of the available power for ancillary services can be summarized as follows:

Considering the available water volume in the desander, the capacity of the primary control is  $\Delta P=2x \pm 4$  MW, corresponding to a permanent droop of  $BS=0.755\%$ .

Considering the ability to pass the Swissgrid qualification test (frequency response), the capacity of the primary control is  $\Delta P=2x \pm 3$  MW, corresponding to a permanent droop of  $BS=1\%$ .

Considering the stability during a change of the active power setpoint, the capacity of the primary control can be selected between  $\Delta P=2x \pm 0.5$  MW and  $2x \pm 0.75$  MW, corresponding to a permanent droop between  $BS=4\%$  and  $BS=6\%$ .

The pressure fluctuations resulting from the primary control have also been estimated by simulating the response of the power plant to a realistic Swissgrid signal representative of the frequency variations in the grid. As shown in Figure 27a, the pressure fluctuations induced by this ancillary service do not exceed 2.4% of the nominal head at the bottom of the penstock. In addition, the pressure fluctuations amplitude, along the entire penstock generated by the grid frequency control never, exceed 3% of the design static pressure, as shown in Figure 27b. Since these fluctuations are smaller than 5% of the design pressure, the British Standard EN 13445-3 (EN BS 2009) suggests that they do not contribute



to the fatigue of the pipe structure. It is therefore concluded that the impact of the primary control on the service life of the penstock is insignificant.

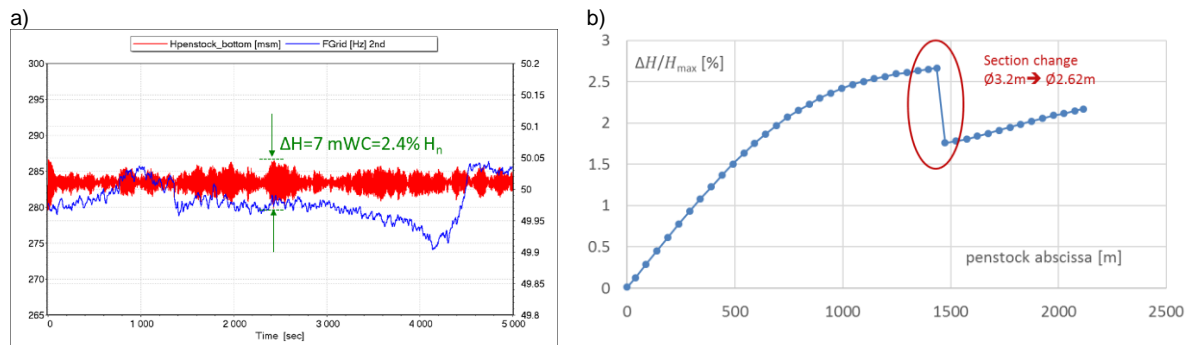


Figure 27. a) Simulation of the pressure fluctuations at the penstock bottom generated by the grid frequency control. b) Relative pressure fluctuation amplitude along the penstock generated by the grid frequency control.

### *Monitoring of the power plant*

Power Vision Engineering Sàrl has developed an innovative real-time monitoring system for the transient regimes of hydropower plants called Hydro-Clone® (Nicolet 2017 and Nicolet 2020). This digital twin is based on a duly validated SIMSEN model of the hydroelectric scheme under consideration, and simulates in real time the dynamic behavior of the facility on the basis of boundary conditions measured on site and transmitted to the numerical model via the SCADA system, see Figure 28a. Hydro-Clone is therefore able to replicate the power plant operation in real time and offers the possibility of detailed monitoring of transient phenomena and identification of possible malfunctions or extreme loads. This monitoring system has been deployed at the SHP KWGO and has been continuously operational since June 2018. The benefits of this real-time monitoring have already been used during the plant's commissioning tests in the summer of 2018, allowing detailed follow-up of the tests and a close monitoring of the turbine operation.

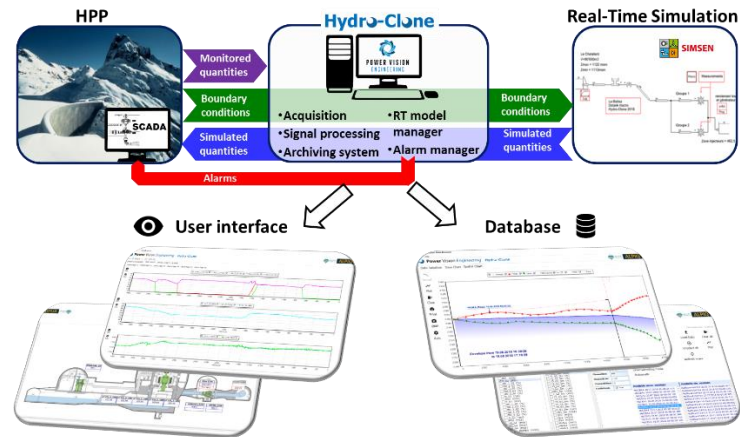
Figure 28 details the implementation of the Hydro-Clone system which includes:

- A PC running the real-time simulation of the SIMSEN model of the hydropower plant, including upstream and downstream reservoirs, intake galleries, penstocks and manifold, generating units, etc.;
- A remote access to the PC, via VPN or TeamViewer, allowing an efficient deployment and maintenance of the system for Power Vision Engineering Sàrl;
- The Hydro-Clone system which ensures the real-time operation of the simulation and the exchange of data between the SIMSEN simulation and the SCADA system at a minimum rate of 10 Hz to simulate the dynamic behavior of the development on the basis of measured boundary conditions, see Figure 28b;
- A user interface that allows to visualize and analyze the transient phenomena occurring in hydropower plant, illustrated in Figure 28c;
- A tailored made database allowing at any time the access, the visualization and the analysis of simulation results and measurements.





a)



b)



c)

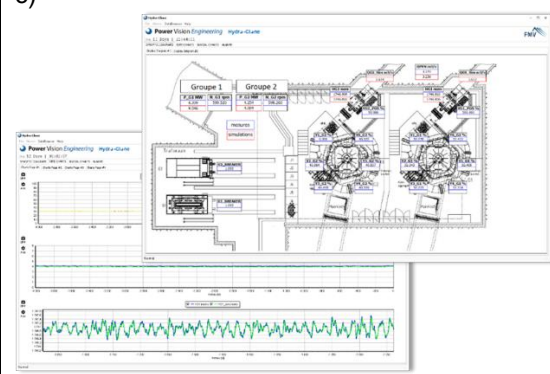


Figure 28 a) Hydro-Clone® general concept with dataflow exchange. b) Practical implementation of Hydro-Clone with the power plant PLC. c) Snapshots the Hydro-Clone interface as implemented for KWGO.

The objectives of the Hydro-Clone system are as follows:

- **Monitoring of transient phenomena** such as water hammers, surge tanks mass oscillations and transient behavior of the units;
- **Detection of significant pressure variations** along the water conduits, that could pose a risk to equipment if the same sequence were to occur at a different reservoir level, even before reaching the allowable limits of the arrangement, enabling to:
  - Identify improper sequence or parameterization of the control and regulation system;
  - Identification of resonance or self-excitation phenomena;
- **Detection of anomalies** in the event of a significant deviation between the simulated and measured quantities, such as:
  - Unexpected air admission from air-valves;
  - Unexpected gate or valve closures;
  - Flow obstruction by external body;
  - Surge tank sediment deposit;
  - Water column separation;
  - Sensor failure;
  - Breaking or failure of a component;



- **Monitoring of non-measurable quantities** such as:
  - Pressures and discharges values in galleries and penstocks;
  - Mechanical torque in couplings;
- **Degradation of physical quantities** such as:
  - Head losses in galleries and penstocks;
  - Efficiency of turbines, pumps and motor-generators;
  - Operating laws for regulating and safety devices such as safety valves, turbine distributors or injectors, axial turbine blade angles, etc. ;
- **Ahead-of-time projections** of the state of the system (what-if), to identify possible risks related to pre-defined scenarios such as emergency shutdown, unit loading, or unexpected valve closure;
- **Anticipation of significant damage** by long-term monitoring of phenomena such as:
  - Fatigue of penstocks and pressurized components;
  - Penstock buckling.

This monitoring system made it possible to keep track of the correct course of operations during the first and second test campaigns. For example, Figure 29 illustrates the water level in the desander and the turbine discharge during hydropeaking production on November 27, 2018. This permitted to check that the production program was correctly executed and to deduce the inflow rates as a function of the filling rate of the desander. In addition, the recording of all the test results in a dedicated database permitted the fine post-processing and analysis of the test campaign outcomes to assess the consequence evaluation of the new operating conditions.

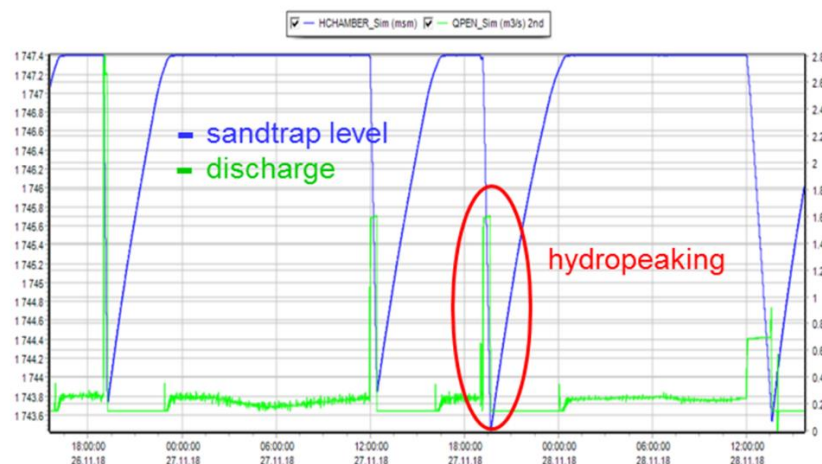


Figure 29. Example of discharge and desander level monitoring during the hydropeaking tests of November 27, 2018, carried out as part of the first test campaign.

The digital twin of the power plant was also used to carry out some predictive analysis prior to the second test campaign, which aimed to partially dewater the headrace tunnel to exploit the corresponding volume of water. This partial dewatering induces however some large head variations on the Pelton runner, which leads to changes in the transient behavior of the system and the controller. It was therefore crucial to anticipate the behavior of the power plant prior to on-site tests by performing prospective simulations using the numerical model. The Figure 30a illustrates one simulated scenario with a power peak of 1 hour, leading to the partial dewatering of the headrace tunnel, which was used to anticipate the water level variations at the inlet and outlet of the power plant for a given water inflow. The simulations also showed the possibility of carrying out an emergency shutdown during the dewatering of the headrace tunnel without any major risk for the power plant, see Figure 30b.



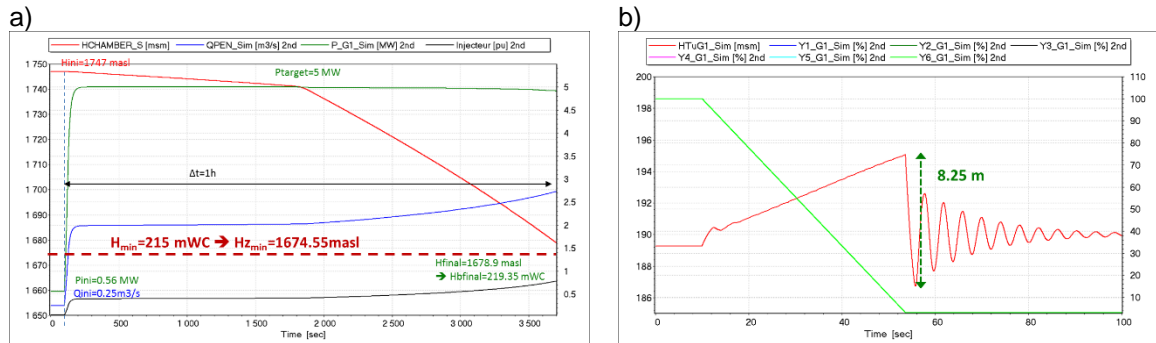


Figure 30. a) Simulation of the power peak with dewatering of the tunnel. b) simulation of an emergency shutdown at low head.

Finally, the numerical model was used to estimate the occurrence of the so-called “falaise” effect which is characterized by an abrupt drop of the machine efficiency when the turbine net head is lowered. This effect is well known in the case of multi-jet facilities, where the drop of the jet velocity, induced by the lowering of the head, leads to a detrimental operation of the turbine since as the buckets fail to empty completely before reaching the next injector. Using the calibrated turbine characteristic of the digital twin, the limit net head at which the machine can operate without encountering this effect was calculated. As illustrated in Figure 31, it is estimated that the «Falaise effect» occurs as soon as the net head falls below 215 mWC, which corresponds to 75% of the nominal head.

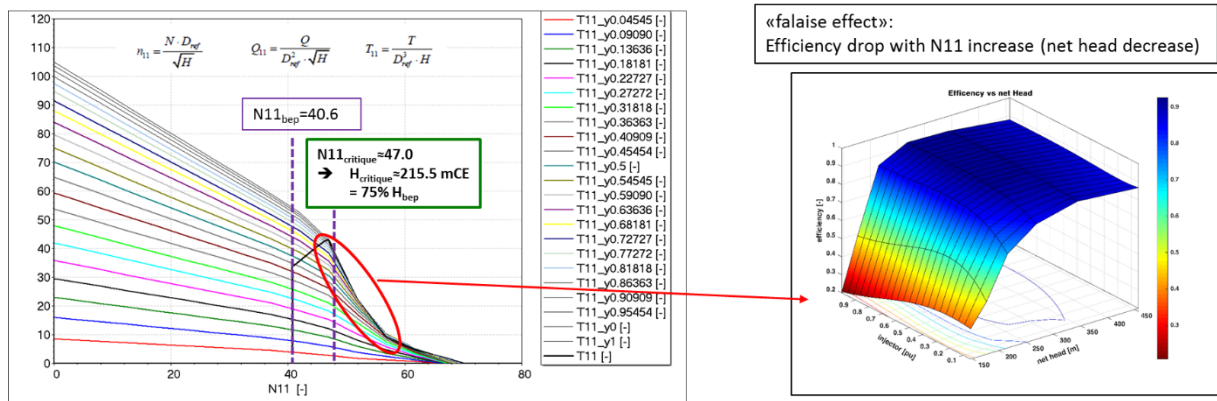


Figure 31. Estimation of the «Falaise effect» occurrence based on the turbine characteristic.

### Influence of the water level variation on the jet quality

As described in the Procedure and Methodology section, the influence of the water level on the jet quality has been investigated by numerical simulations. Figure 8 sums up the methodology followed with the use of the OpenFOAM toolbox to simulate the jet at the outlet of the needle and the GPU-SPHEROS solver to simulate the interaction between the jets and the runner buckets.

The simulation of the jet at the outlet of the needle is carried out for six different heads. The six heads can be split in three sets. A first set with the heads of 287 m and 282 m for which the head race tunnel is filled by water and only the settling basin and the forebay tank are partially emptied. A second set with the heads of 275 m and 255 m for which the head race tunnel is partially dewatering and the third set with the heads of 215 m and 190 m for which more than 25% of the head race tunnel is dewatering and for which the “falaise” effect occurs. For each head, three needle strokes are considered: 20%, 49% and 90% of the maximum stroke. In overall, eighteen simulations have been performed.

Before launching all these simulations, the influence of the computational domain is investigated. Two computational domains are considered: one with the complete Pelton distributor and the six needles, a



second with only one needle (see Figure 32). Downstream the needles, a box is added to allow the development of the jet.

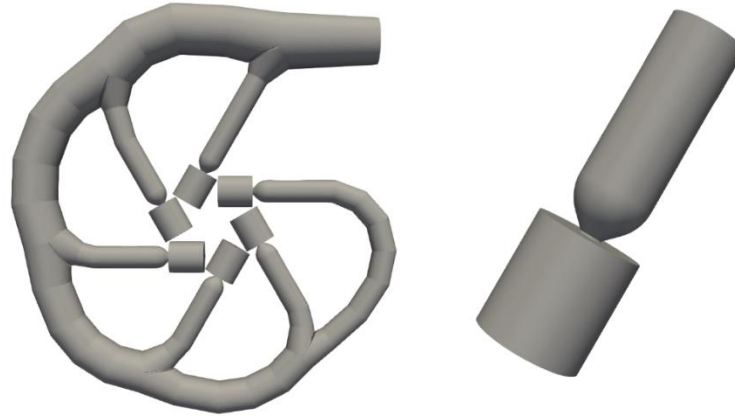


Figure 32: View of the two computational domains considered: the full domain with the Pelton distributor and the six needles (left), the reduced domain with only a single needle (right).

Simulations are carried out for a needle stroke of 49% and two heads: 287 m (the nominal head) and 215 m (occurrence of the “falaise” effect).

The contours of the volume fraction for the nominal head of 287 m are displayed on Figure 33. No strong differences are noticeable between the two computational domains. Figure 34 compared the velocity and the water volume fraction profiles in section 2 between the full computational domain (the six jets are considered) and the reduced domain. No large differences are observed for both quantities.

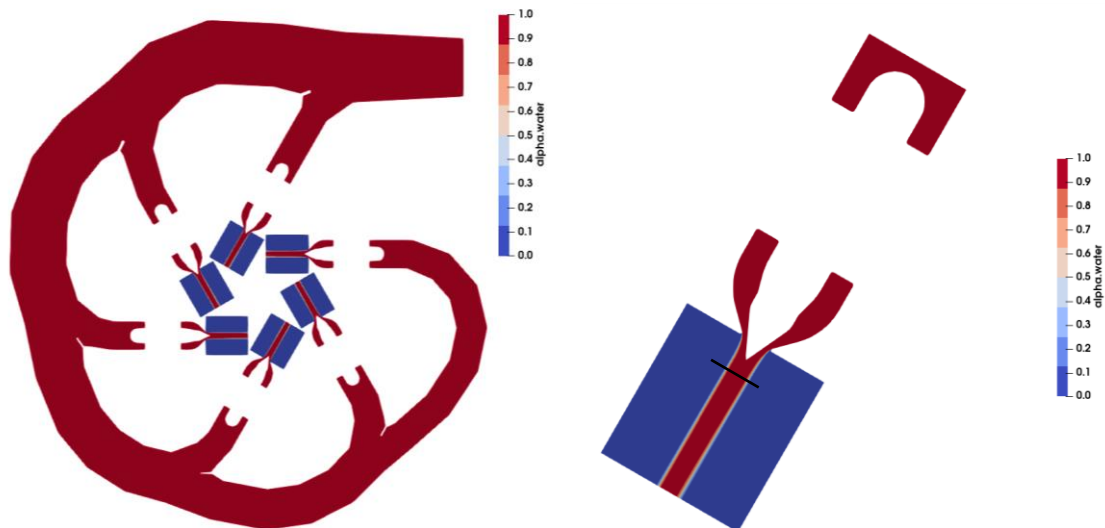


Figure 33: Plane view of the water volume fraction ( $\alpha_{\text{water}}$ ). Head of 287 m. The black line on the right picture refers to the section 2 at which the data are transferred between the OpenFOAM and the GPU-SPHEROS simulations.

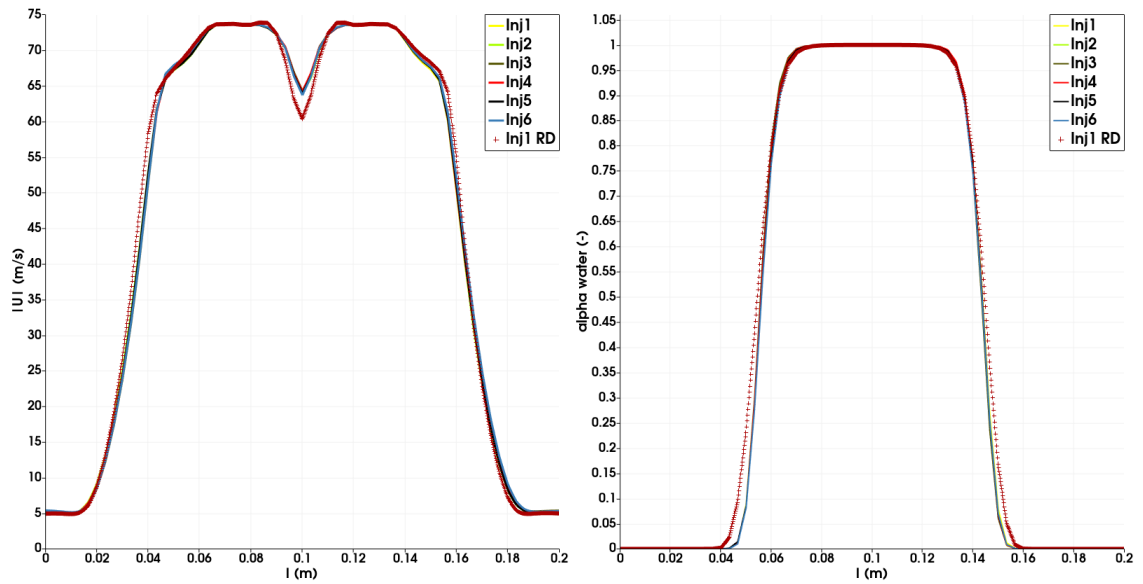


Figure 34: Velocity (left) and water volume fraction (right) profiles in section 2 (see Figure 33 for the definition of section 2) for a head of 287 m. The solid lines refer to the simulation on the full domain. The crosses refer to the simulation on the reduced domain.

For the head of 215 m, the simulation on the full computational domain does not change the shape of both profiles compared to the head of 287 m (see Figure 35). The velocity decreases by approximately  $10 \text{ m s}^{-1}$  according to the lower head.

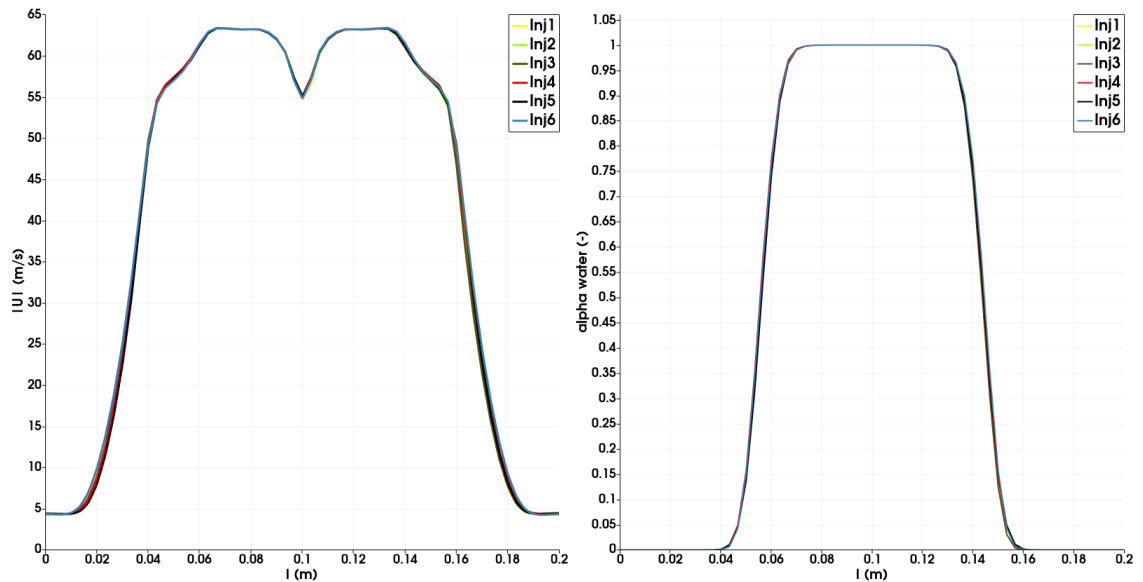


Figure 35: Velocity (left) and water volume fraction (right) profiles in section 2 (see Figure 33 for the definition of section 2) for a head of 215 m. Simulation on the full computational domain.

Since the influence of the computational domain is small and due to the lower CPU resources required by the simulation on the reduced domain, the eighteen simulations have been carried out using the reduced domain.



For the four highest head, an estimation of the flow discharge as a function of the needle stroke and the head are provided by PVE. Table 4 compares the flow discharge predicted by the CFD simulations with the ones provided by PVE. The last column gives the difference in percentage that is lower than  $\pm 3\%$  with the largest discrepancy for the lowest stroke. The accuracy of the simulations can be considered as sufficiently good to investigate the flow at lower heads, for which no data are available before performing the on-site tests.

Table 4: Comparison of the flow discharge between the CFD (OpenFOAM simulations) and the data from PVE for the different strokes and heads considered.

S [%]	Head [m]	Q CFD [m <sup>3</sup> /s]	Q PVE [m <sup>3</sup> /s]	Delta Q [%]
49	287	0.386	0.388	-0.5
	282	0.382	0.385	-0.8
	275	0.377	0.380	-0.8
	255	0.363	0.366	-0.8
90	287	0.548	0.554	-1.0
	282	0.542	0.548	-1.1
	275	0.536	0.542	-1.1
	255	0.515	0.522	-1.3
20	287	0.188	0.184	2.4
	282	0.186	0.182	2.4
	275	0.184	0.180	2.3
	255	0.177	0.173	2.2

For the lowest heads of 215 m and 190 m, there are not differences between them, therefore only the results for a head of 215 m are used for comparison with the nominal head of 287 m.

Figure 36 and Figure 37 show respectively the contours of the axial velocity of the jet and the water volume fraction in a plane parallel to the axis of the jet. The patterns of the contours are not influence by the head. The velocity decreases according to the head variation as expected. It is noticeable that the jet is more influenced by the stroke than the head. For the smallest stroke, the jet is a mixture of air and water since the water volume fraction is lower than 1. As far as the stroke increases, the jet is filled only by water with a shaper interface.

In addition to the contours, the profiles of the axial velocity jet and the water volume fraction in section 2 are plotted in dimensionless form on Figure 38. The dimensionless profiles superimpose one to each other whatever the head demonstrating that the water level does not influence the quality of the jet (only the velocity decreases according to the lowering of the head).

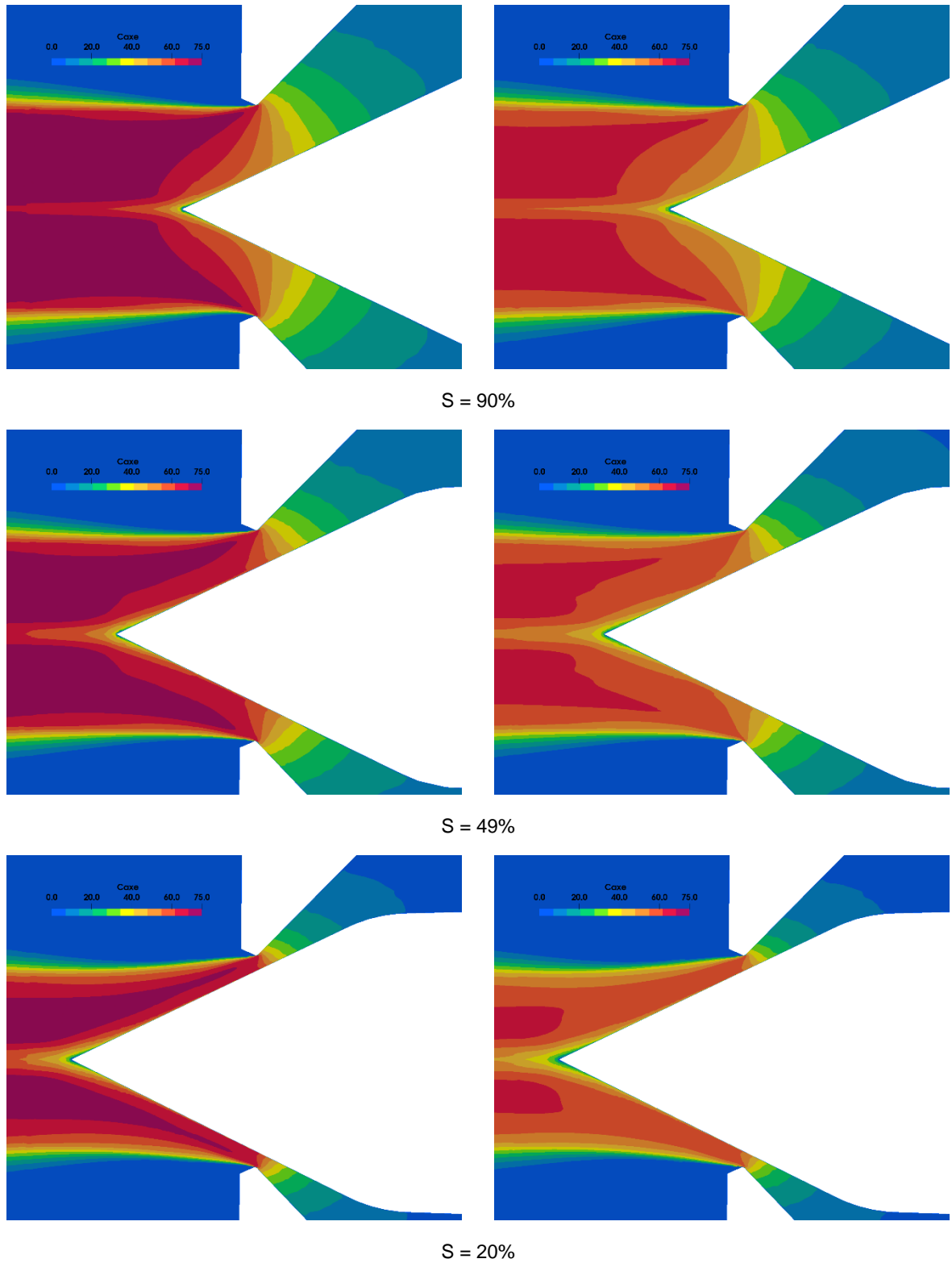


Figure 36: Contours of the axial velocity of the jet for a head of 287 m (left) and 215 m (right) in a plane parallel to the jet axis.

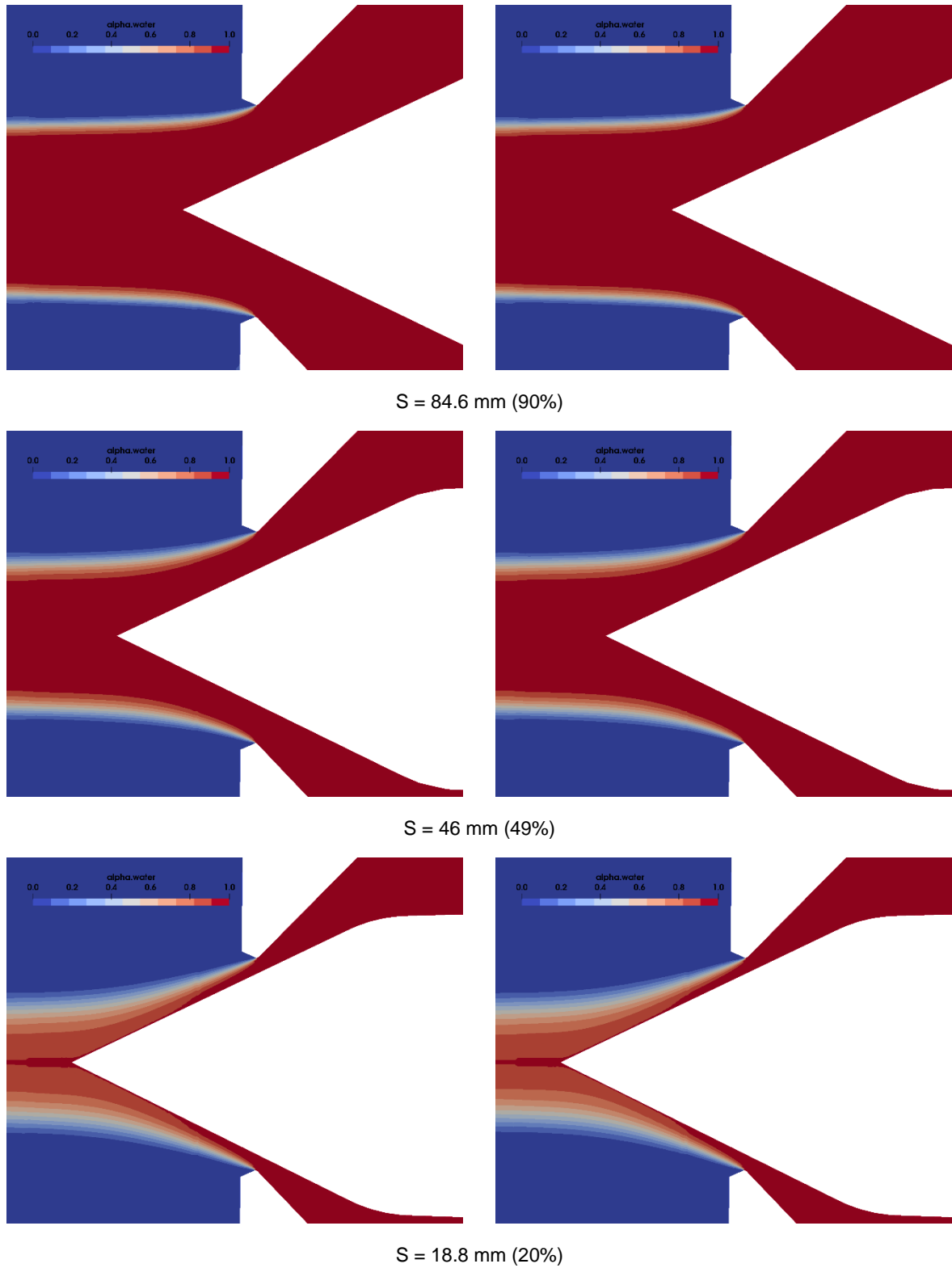


Figure 37: Contours of the water volume fraction for a head of 287 m (left) and 215 m (right) in a plane parallel to the jet axis.

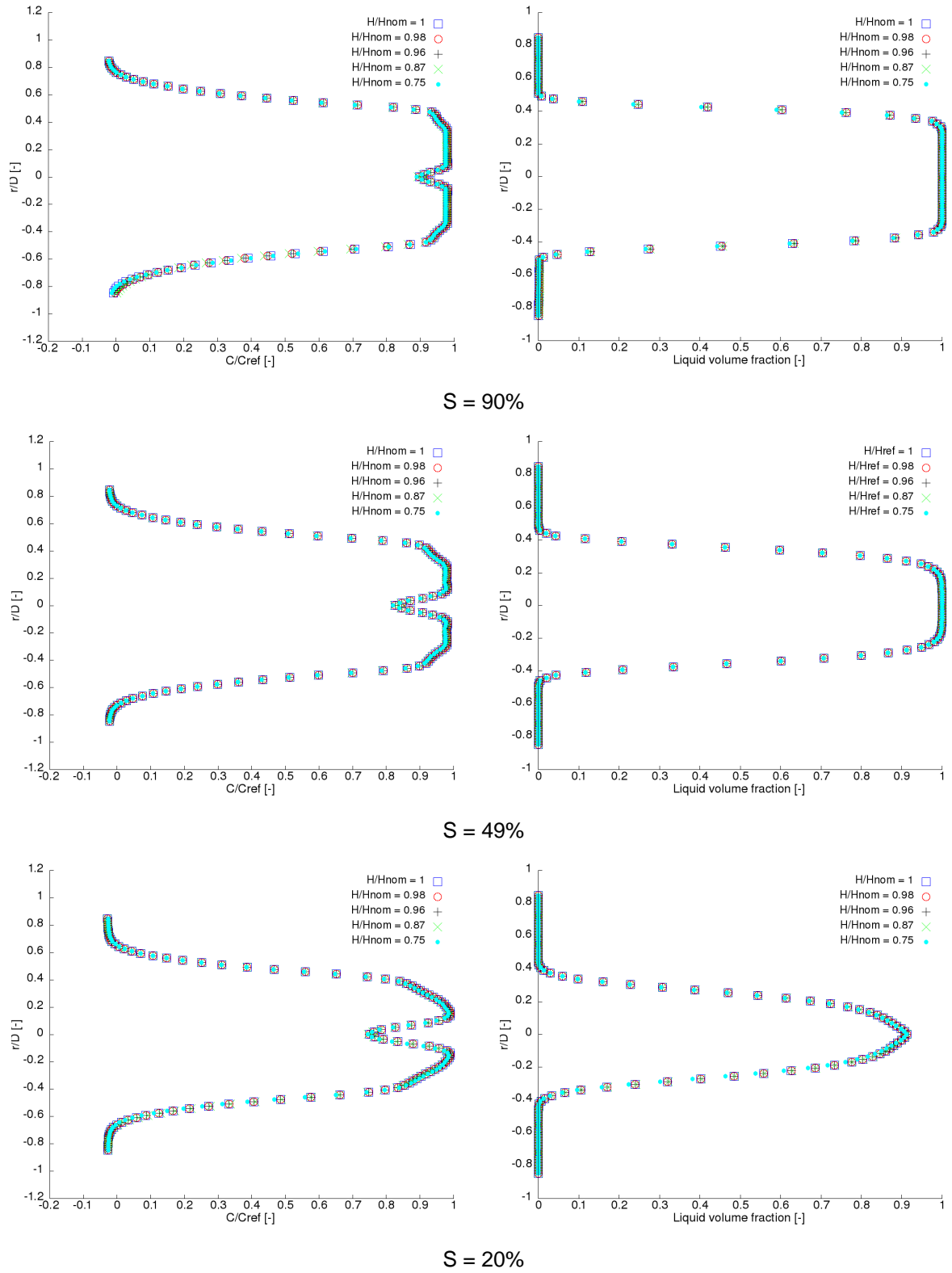


Figure 38: Dimensionless axial velocity (left) and water volume fraction (right) profiles in section 2 for five different heads.





### *Influence of the jet quality on the runner*

The velocity, the water volume fraction and the turbulence fields are extracted from the OpenFOAM simulations in the plane perpendicular to the jet at section 2 (see Figure 33). They are transferred to the GPU-SPHEROS solver as shown on Figure 39 for the velocity.

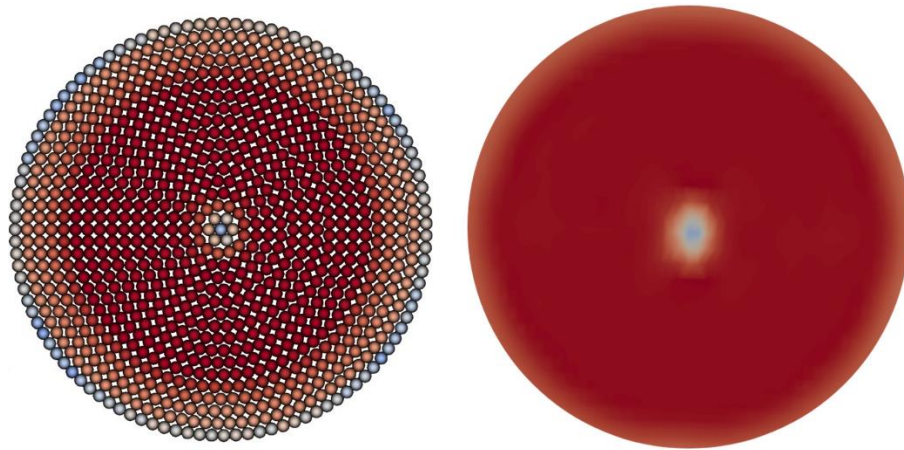


Figure 39: Contours of the velocity exported from the OpenFOAM simulation (right) to GPU-SPHEROS (left).

For the simulations using GPU-SHPHEROS two consecutive jets and three buckets are considered (see Figure 40). The main objective of the simulation is to investigate the interaction between the jets and the runner buckets for the heads computed with OpenFOAM. By lowering the head, the velocity of the jets decreases. Consequently, the water sheet inside the bucket due to the first jet does not move enough fast and is impacted by the second jet. This phenomenon known as the “falaise” effect is characterised by a sudden drop in efficiency, torque fluctuations and an increase risk of fatigue. The torque generated by the second jet, which is influenced by the first jet, is then used to compute the torque for the whole Pelton runner with six jets.

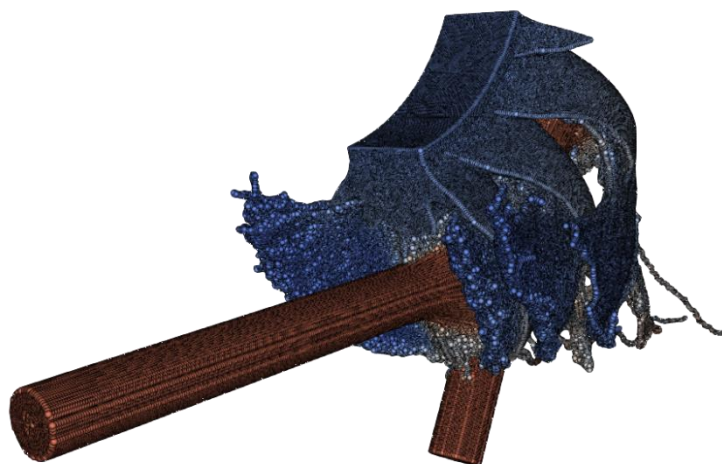


Figure 40: Water particles deviated by rotating Pelton buckets. GPU-SPHEROS simulation.

For a six jets configuration, the power and the efficiency as a function of the flow discharge are plotted on Figure 41 for four different heads: 287 m, 255 m, 215 m and 190 m. For the nominal head of 287 m, the power and the efficiency computed are in accordance with the available data. The maximum



efficiency measured is slightly above 0.9 and the minimum efficiency for a flow discharge of  $1 \text{ m}^3 \text{ s}^{-1}$  is around 0.6. Lowering the head leads to an efficiency drop with values between 0.3 and 0.6. These values agree with the measurements performed in May 2020 during the on-site tests with a minimum efficiency of 0.45 for a head of 190 m, a flow discharge of  $2.5 \text{ m}^3 \text{ s}^{-1}$  and six jets in operation.

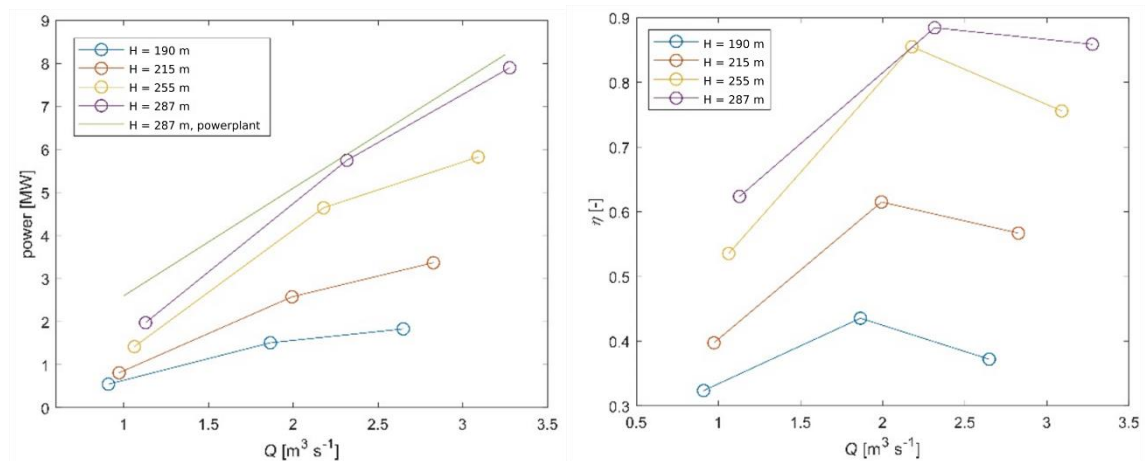


Figure 41: Power (left) and efficiency (right) as a function of the flow discharge for four different heads and six jets. GPU-SPEROS simulations.



### 4.3 Task 3: Real-time hydrological forecasts

#### *The hydrological forecast system for Gletsch-Oberwald*

At the beginning of the project, in May 2018, WSL set up a detailed hydrological forecast system specifically designed to the needs of the operators of the SHP KWGO and the project partners. The design of the operational online forecast system was based on the information platform Sihl developed at WSL for AWEL running operationally since 2010. The main focus of the Gletsch forecast system is the display of the latest available streamflow forecasts, see Figure 42, based on the three different meteorological short-term forecasts (COSMO-E, COSMO-1, INCA-C1). Additionally, a monthly outlook is provided indicating the probabilities that the upcoming weeks will be above, below or within normal climatological conditions.

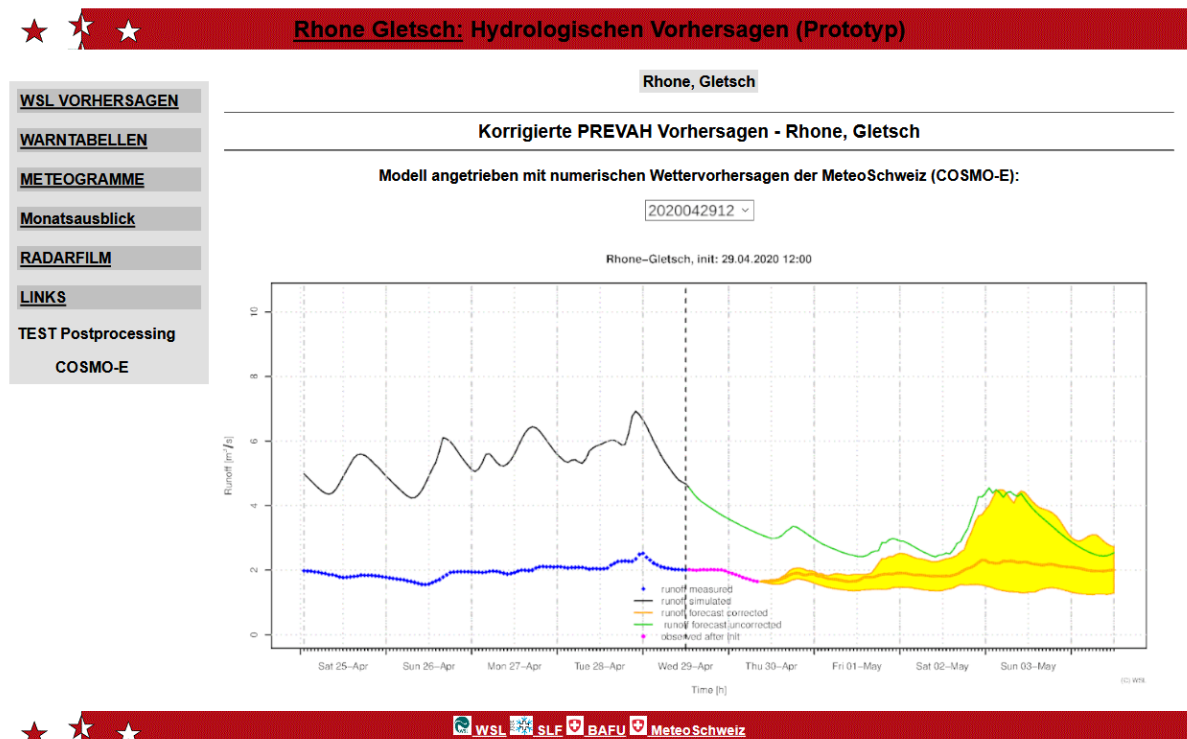


Figure 42: Visualization of the hydrological forecast system implemented for Rhone-Gletsch.

Usually, streamflow forecasts show two kind of errors, the hydrological model error and the meteorological forecast error. Although the hydrological model is well calibrated to represent runoff across all seasons (including extreme events), for specific situations the difference between the observed and the (transiently) simulated streamflow at the beginning of the forecast can be quite big. Especially in such small and steep alpine catchments, where snow and glacier melt processes are complex and crucial for the resulting runoff, the raw forecasts need to be assimilated with real observations of discharge. In our web platform we only show the so called post-processed forecasts as well for the COSMO-E forecasts.

#### *Application and verification of the hydrological forecast system for SmallFlex campaigns*

During the first SmallFlex campaign in November 2018 the hydrological forecast system for Gletsch was tested for the first time. Between 26.11.2018 and 30.11.2018 WSL provided the project partners with forecasts in real-time twice a day.

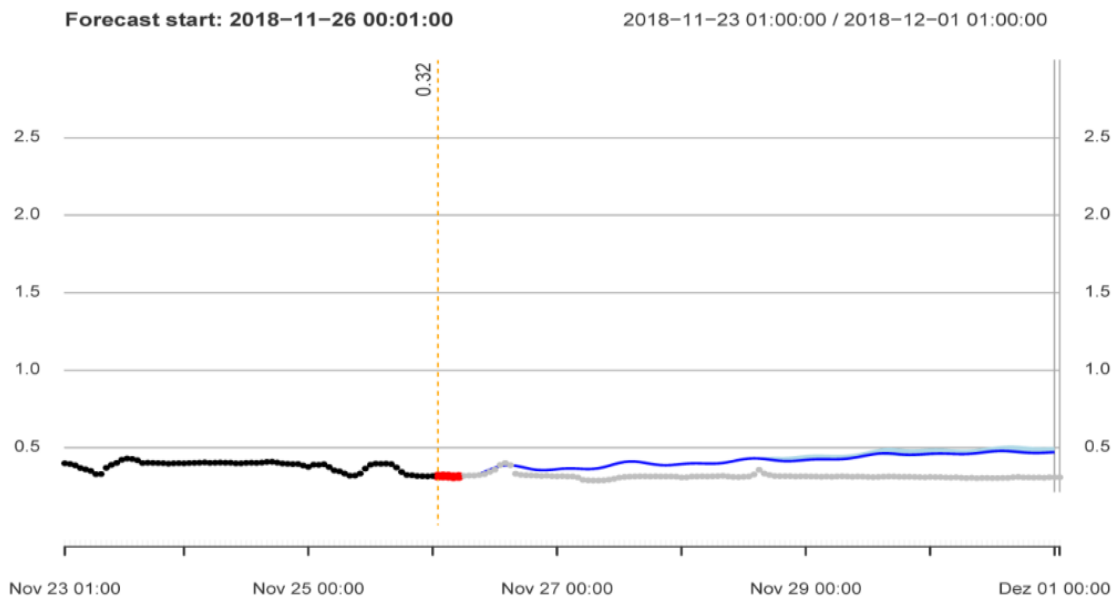


Figure 43: Example of an INCA-CH forecast extended with the COSMO-1 forecasts for the field campaign in November 2018

An example of a forecast during the week of the field campaign in November 2018 is shown in Figure 43. Black dots show the observed streamflow at the gauging station before the issuing of the forecast (blue line). The dots in grey are the true values, which were available in hindsight for comparison. The red dots are observations of runoff, which were retrieved in the time gap between the initialization of the meteorological forecast and the completion of the hydrological forecasts. Obviously, the runoff of the Rhone was very steady, before and during this SmallFlex field campaign; thus, the validation of the forecast was not very expressive.

For a more detailed verification of the INCA-CH system and its potential benefits for such small catchments like Gletsch, we used a rain-storm event from June 2019, and another one from October 2019. In June 2019, the raw INCA-CH + COSMO1 forecasts were producing much too high inflows, whereas the quality of the forecast for the event in October was fluctuating a lot between different forecast initializations. This results mainly from the complexity of the catchment and the difficulty in predicting the rain cells of highly localized convective thunderstorms within the right catchment. For example, a small shift in the movement of such storm cells would have hit neighbouring catchments and produced completely different runoff results for Gletsch. This was a clear indication that it is essential to apply some post-processing methods for producing reliable forecasts at such a small spatial scale.

Recently different machine learning methods (e.g., Gradient Boosting and Random Forests) and forecast combination methods have been tested in order to reduce the errors in the forecast system. These post-processing methods show some significant improvements (see Figure 44). However, these are preliminary results, which have to be analysed with longer time-series and more events.

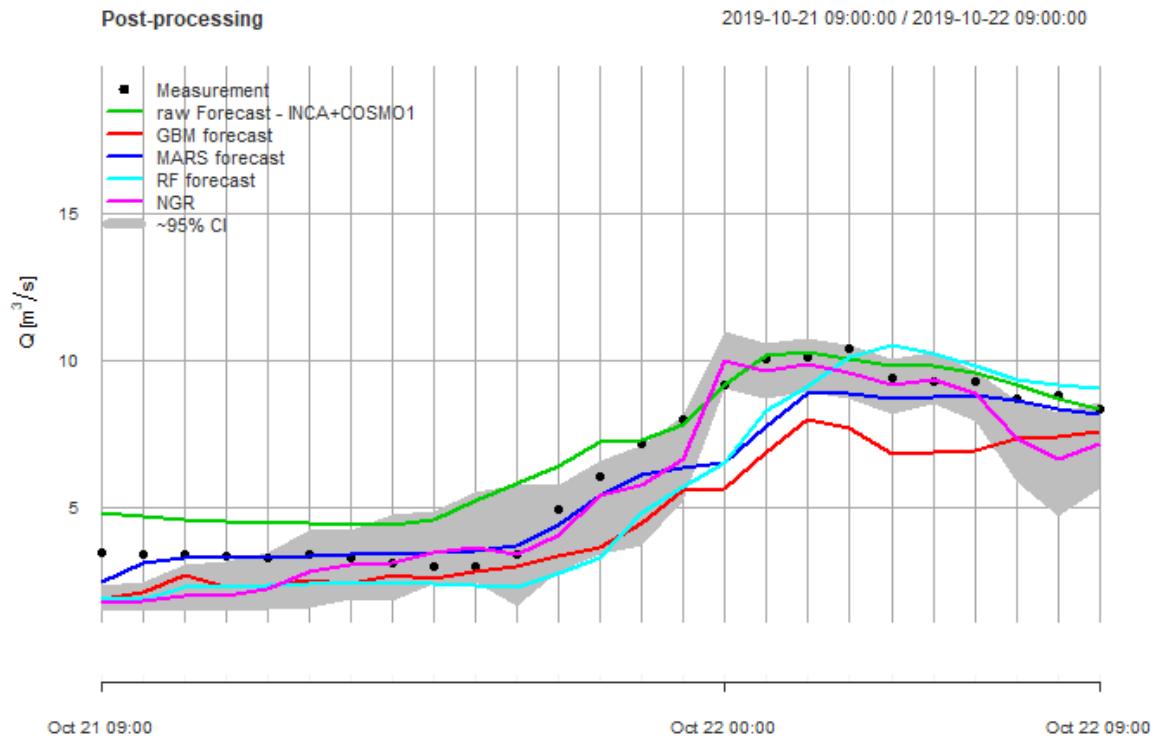


Figure 44: Example of different Machine Learning based post-processing methods for the INCA-CH + COSMO 1 based runoff forecasts at Gletsch during the rain-storm event of October 2019.

In Figure 45, the first forecast from the beginning of the second experiment in May 2020 is shown with meteorological initialization at the 1<sup>st</sup> of May at 24:00 and sent to the partners on the 2<sup>nd</sup> of May at 07:00 a.m. catchments. The mean of the forecast ensemble slightly underestimates the runoff, resulting in a mean absolute error of 0.3 m<sup>3</sup>/s on day 5.

Without correcting the hydrological model to the real initial runoff on May the 2<sup>nd</sup> – or in other words: with the model running throughout the whole year without assimilation of observations – the forecast system would have overestimated seasonal runoff by approximately 1 m<sup>3</sup>/s.

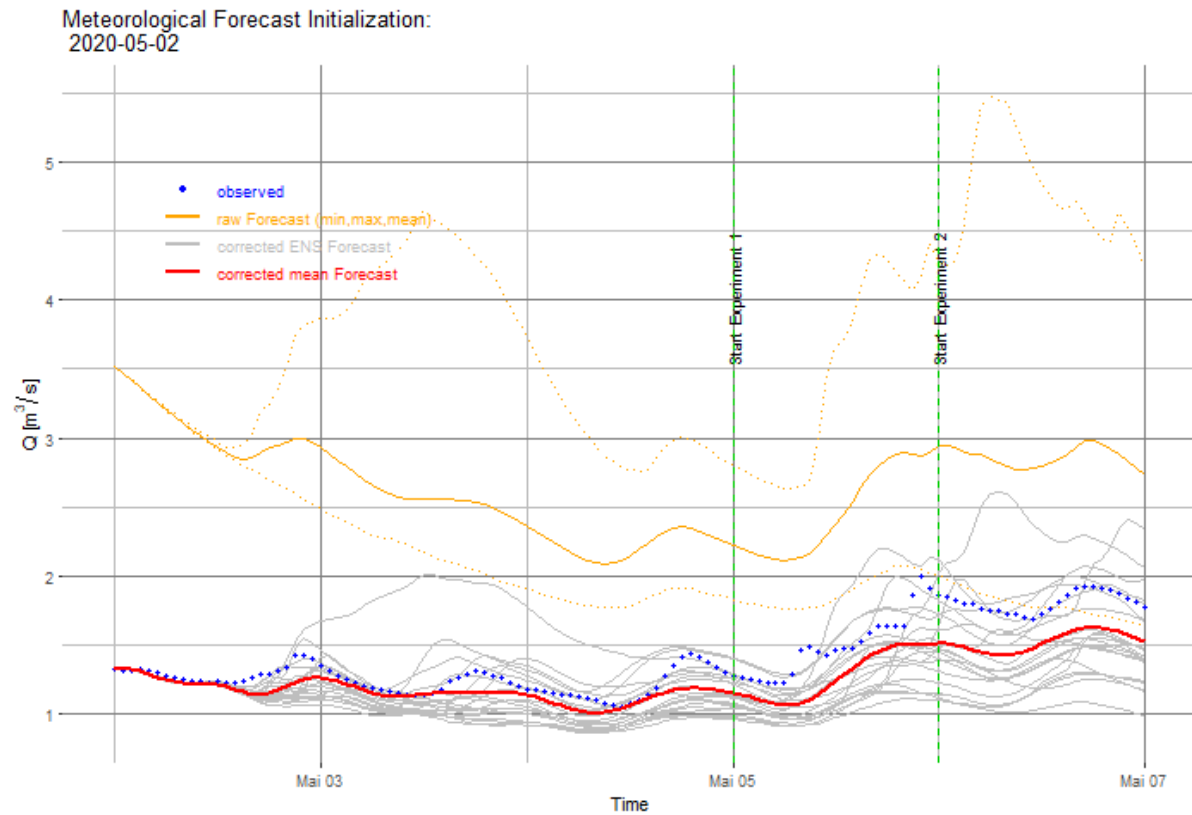


Figure 45: Streamflow forecast [m<sup>3</sup>/s] issued on 2nd of May for the raw forecast (orange) and the ensemble forecasts with corrected initial runoff (grey; ensemble mean = red) in comparison to the observed streamflow measured at the FOEN station in Gletsch (blue).

In Figure 46, the forecasts from the 4th of May (sent at 07:00 to the partners) are shown for the test runs planned for 5th and 6th of May. The ensemble mean forecast is very close to the true runoff with max deviations of 0.2 m<sup>3</sup>/sec; however, there are also single forecast members that clearly over- or underestimate runoff in the afternoon of 5 May. This is mainly caused by forecasts of too high precipitation amounts and/or too high air temperature, which will give raise to erroneously high melting rates.

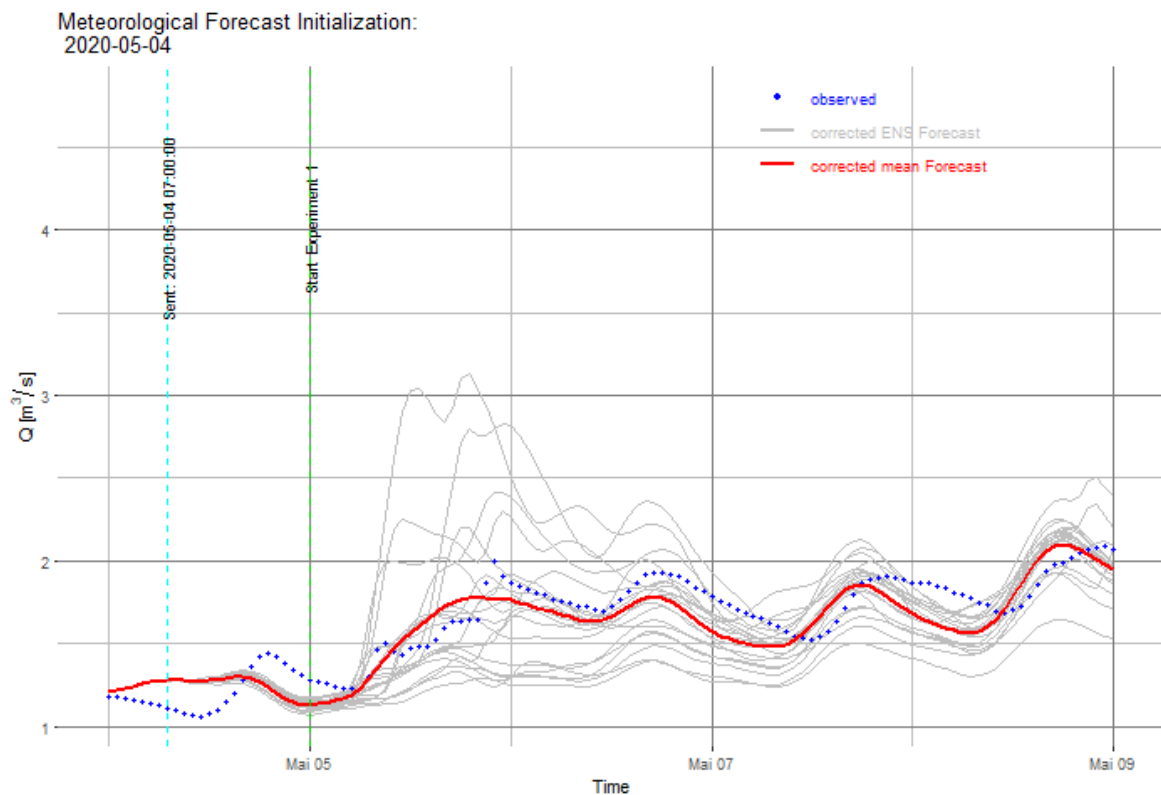


Figure 46: Forecast sent on 4th of May at 7:00 for preparing the test run on 5th of May.

The above results are only two snapshots of the performance of runoff forecasts issued on two specific days. However, for a more robust assessment of the forecast quality we need to evaluate longer time periods. To this end we used **all** runoff forecasts of May 2020 (issued twice every day) and plotted the mean daily runoff **predicted for lead-times of 3 and 24 hours**, together with the observed mean daily runoff (Figure 47). This comparison shows that the mean forecast error (difference between the observed and the predicted streamflow) increased from almost zero (lead-time 3 hours) to 0.7 m<sup>3</sup>/sec at lead-times of 24 hours (assimilating the model with observed runoff). In Table 5, the Mean Absolute Errors (MAE) for different lead-times are summarized.

Table 5: Mean Absolute Error (MAE) of the raw and the corrected forecasts of May 2020 for different lead-times.

Lead-time	MAE of the raw forecast	MAE of the corrected forecast
[h]	[m <sup>3</sup> /s]	[m <sup>3</sup> /s]
1	3.84	0.05
12	2.52	0.53
24	1.79	0.68
36	1.38	0.85
48	1.08	0.91



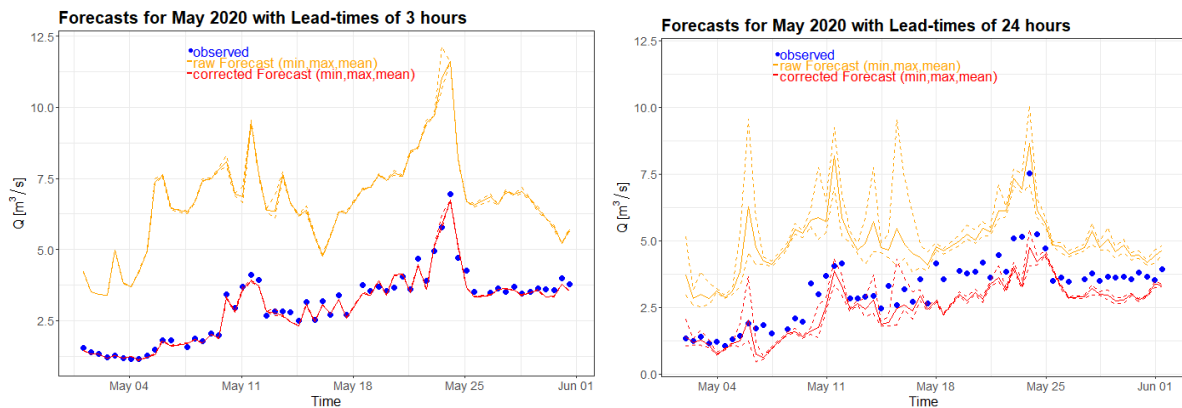


Figure 47: Evaluation of the forecast quality of May 2020 for lead-times of 3 (left) and 24 (right) hours with raw forecasts in orange (plus maximum and minimum), corrected forecasts in red and the verifying observations in blue.

How can this prediction accuracy be interpreted? What forecast error can be accepted in the present context?

First of all, the forecast uncertainty can be compared with the volume of water that can be temporally stored in the HP plant.

The storage volume in the settling basin and the forebay chamber is 2'500 m<sup>3</sup> and in the headrace tunnel 6'400 m<sup>3</sup> as estimated in Task 1. Typical low flows of the Rhone river in Gletsch in spring (before the big melt) are in the order of 0.5 to 1 m<sup>3</sup>/s. Considering a residual (ecological) water flow of 0.2 m<sup>3</sup>/sec that cannot be used for HP production, it takes 3 to 8 hours until the whole storage volume is filled up. In this low-flow case an over- or underestimation by 0.5 to 1 m<sup>3</sup>/sec would be very significant and hardly acceptable.

In the course of the snowmelt in May 2020, the inflow increased up to 6 m<sup>3</sup>/s, which would have led to a refilling of the available storage volume in about 25 minutes. In this case, an underestimation of the runoff by 0.5 to 1 m<sup>3</sup>/s would lead to a deviation in storage time by 3 to 5 minutes. This would probably be acceptable from an operational point of view.

#### *Estimation of bedload transport for the period of the SmallFlex project*

We calculated the sediment transport in the Rhone river at the HP intake in Gletsch for the entire project period (2018-2020). With an observed stream slope of 0.02% and a mean grain size of 0.057m (determined by EPFL) a total bedload volume of 95'000 m<sup>3</sup> was estimated for 2018. This volume was much larger than estimates by Mbenza (2020) who calculated for 2018 a total volume of ~3300 m<sup>3</sup> from the number of emptying and the total storage volume of the sand traps. Using a reduced energy slope of 0.01%, where the reduction factor is derived according to Badoux et al. (2008), resulted in a bedload volume of ~5000 m<sup>3</sup> (Figure 48), which is in a reasonable agreement with the “rough” field estimates from Mbenza (2020).

With the above assumptions of a reduced energy slope, we then calculated the daily sediment transport for 2019 and 2020 (Figure 49). This yielded a total bedload volume of ~10'000 m<sup>3</sup> for 2019 and 6'100 m<sup>3</sup>, respectively, for 2020. (However, no observation-based data were available for validating these periods.)

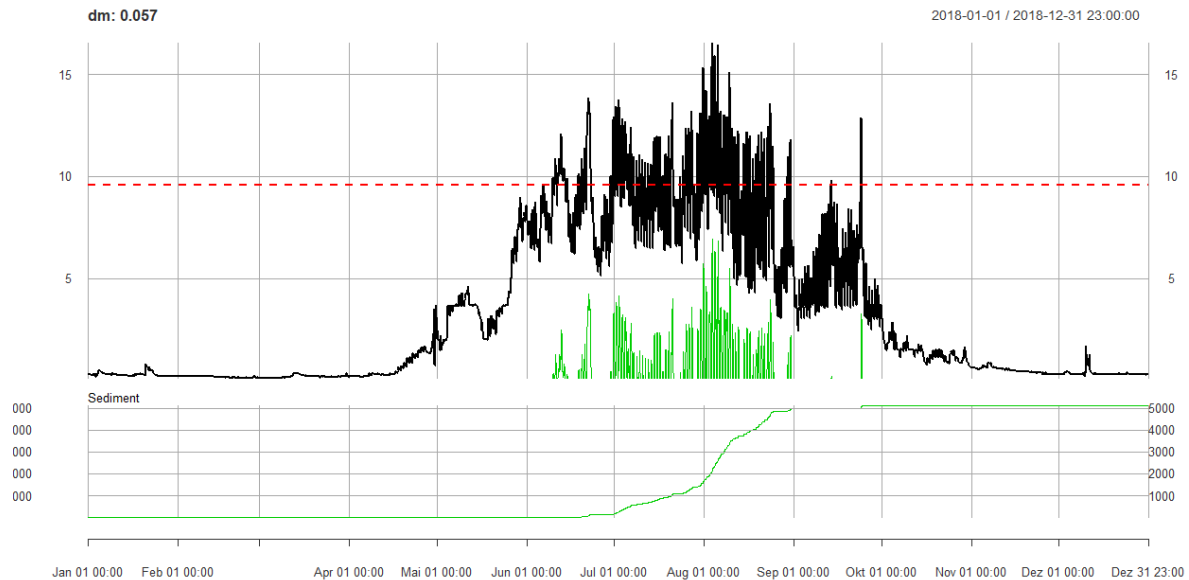


Figure 48: Hourly streamflow discharge  $Q$  of the year 2018 (black line). For a mean grain size of  $0.057\text{m}$  a critical discharge  $Q_{\text{crit}}$  of  $\sim 10\text{m}^3/\text{s}$  is estimated (dashed red line). In green the difference between  $Q$  and  $Q_{\text{crit}}$  is shown. Below the cumulated sum of the effective streamflow volume is shown, which yields about  $5000\text{m}^3$  for this year.

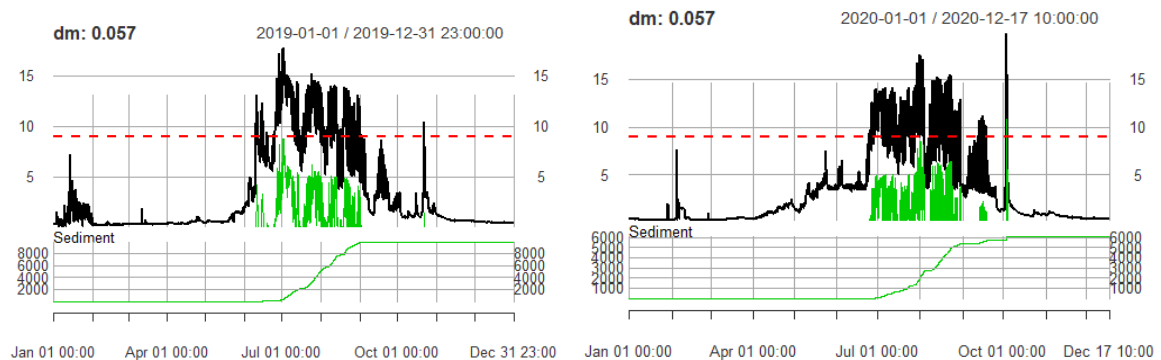


Figure 49: Hourly streamflow discharge  $Q$  of the year 2019 (left) and 2020 (right) in black and the difference between  $Q$  and  $Q_{\text{crit}}$  (red dashed line) is shown in green. Below the cumulated sum of the effective streamflow volume is shown.

Based on the results above, it is now possible to generate forecasts of hourly bedload transport rates. This raises the question of how much a prediction error in the runoff model affects the calculated bedload. This can be illustrated with Figure 50 showing two situations of summer 2020. The first example shows (on the left) a snowmelt period where runoff is exceeding the critical streamflow for sediment transport. The black line shows the observed streamflow and the green line the mean streamflow forecast for the next 5.5 days given the COSMO-E forecasts. The timing of the exceedance of the critical discharge is similar for forecasted and observed runoff, however the daily runoff maxima are slightly different in the beginning and towards the end of the forecast period. This would result in a difference in predicted accumulated bedload of approximately  $2\text{ m}^3$ , which is a very small volume. The second example shows a situation in midsummer 2020. Although the runoff forecasts follow quite closely the observed streamflow, the small differences in runoff leads to a rather substantial underestimation of the accumulated bedload of approximately  $60\text{ m}^3$  after 5.5 days. Given the huge uncertainties of all the sediment transport rate calculations these first tests of sediment forecasting are quite promising but



highlight the sensitivity of the sediment transport forecasts. We therefore strongly suggest that further analyses and tests are essential before making use of or even relying on such a sediment forecast. The most important requirement for a meaningful verification would be the availability of long time series of measured sediment transport rates.

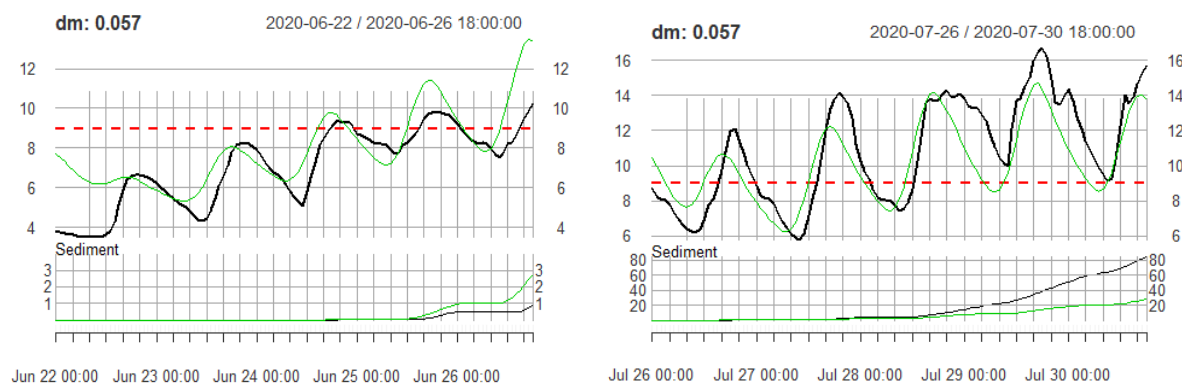


Figure 50: Two examples of runoff (upper figure) and corresponding accumulated bedload transport (bottom figure) for five days in summer 2020 (black line: using observed runoff; green line: using forecasted runoff).

#### *Further analyses in view of more robust and accurate hydrological forecasts*

In addition to the above analyses, WSL also took the opportunity of the SmallFlex project to investigate the spatial simulation of the snow cover accumulation and ablation in this steep and topographically challenging catchment. Also, the impact of climate change on the snow cover and the associated runoff in this specific catchment was studied using a very high-resolution weather generator and a complex snow model accounting for the full energy balance.

To this end, WSL also run a meteorological station at Gletsch during winters 2016-17 and 2017-18 because of a lack of other meteorological data within the catchment (see Figure 51). These data are available for the entire project team and for further analyses of the snow and hydrological forecast model. The data will be made available in the near future on [www.envidat.ch](http://www.envidat.ch).

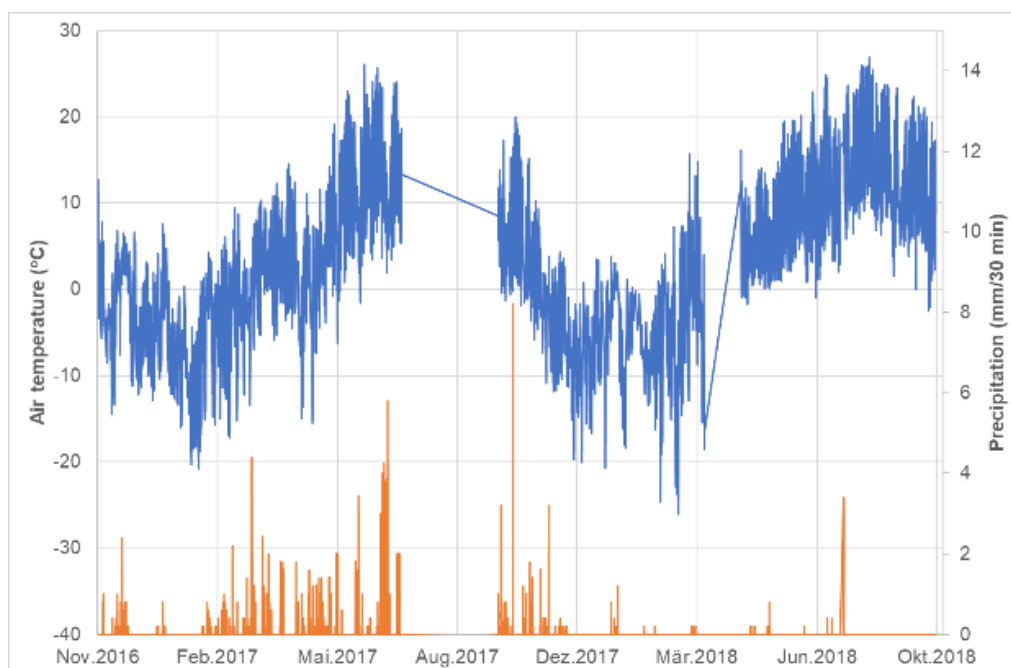


Figure 51: Air temperature (blue line) and precipitation (orange bars) measured at Gletsch parking slot during winters 2016-17 and 2017-18.

The analyses of the snow model simulation are still in progress; a corresponding publication is underway.

## 4.4 Task 4: Short term hydropеaking effects on ecosystems

### *Introduction*

The results presented and discussed here are a summary of the results presented in more detail in a separate hydrograph analysis report (Aksamit et al., 2021b) as well as a scientific publication on the impacts of the experimental hydropеaking on the macroinvertebrate communities (Aksamit et al., 2021a).

### *Effects of hydropеaking on hydraulic characteristics*

Figure 52 shows the discharge of the hydropower plant during the experimental field study in November 2018. The experimental peaks from 8 to 22 November were scheduled as proposed by Eawag in order to assess the effects of different recovery times on macroinvertebrates, those between 26 and 30 November were scheduled as proposed by EPFL and HES-SO, see Figure 17. The duration of the experimental peaks ranged from 15 to 120 minutes. The peak discharges decreased with increasing peak duration, as the same storage volume was used in all cases.

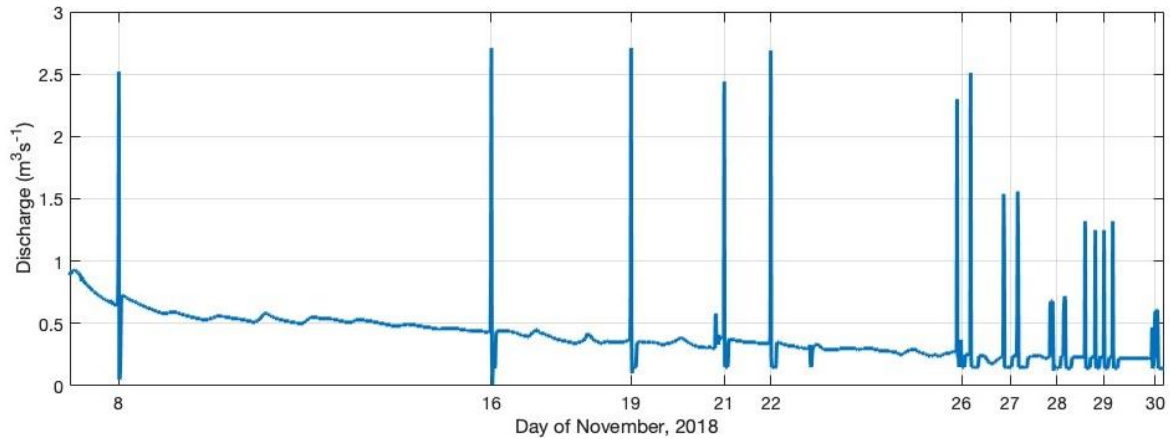


Figure 52: Discharge of the Gletsch-Oberwald power plant from 8 to 30 November 2018 (data provided by EPFL).

Following the criteria of Pfaundler et al. (2011), the impact of hydropeaking is considered substantial if the installed capacity is  $> 50$  kW and significant if the peak discharge during low flow (winter) conditions exceeds 25% of mean average annual discharge (MQ). MQ for the measurement location was estimated to  $3.44 \text{ m}^3/\text{s}$ . The peak discharge, expressed as a percentage of MQ, exceeds the threshold for all but the last peak on 30 November. Based on the criteria of Pfaundler et al., (2011), the impact of the experimental hydropeaking in the floodplain downstream was therefore both substantial and significant.

The increased discharge downstream caused increased water levels as well as flow velocities. Table 6 shows the water level changes and flow velocities observed in front of the macroinvertebrate sampling nets during the experimental peaks from 8 to 22 November. Average flow velocities increased on average by 7-8 cm/s in both the riffle and the pool habitat, peak velocities increased on average by 20 cm/s in the riffle and by 13 cm/s in the pool habitat. Average water level changes were 5 cm in the riffle and 1-2 cm in the pool. However, it should be noted, that these sampling sites were located inside channels, and the changes in water levels were smaller than in the main channel (see below).

Table 6: Downstream velocities [m/s] and depths [cm] recorded during baseflow (sample 0) and peak flow (sample 3) for both the riffle and the pool habitats, including average and maximum flow velocity.

Peak	Average velocity [m/s]				Maximum velocity [m/s]				Depth [cm]			
	DS riffle		DS pool		DS riffle		DS pool		DS riffle		DS pool	
	base	peak	base	peak	base	peak	base	peak	base	peak	base	peak
1	0.33	0.46	0.19	0.22	0.41	0.68	0.29	0.41	12	20	25	24
2	0.36	0.34	0.20	0.34	0.65	0.75	0.30	0.53	10	16	14	18
3	0.31	0.47	0.14	0.28	0.55	0.68	0.21	0.45	9	16	12	17
4	0.27	0.34	0.20	0.27	0.45	0.76	0.34	0.41	9	10	15	14
5	0.30	0.30	0.25	0.25	0.40	0.62	0.40	0.41	9	13	13	13

Figure 53 shows the water levels and the water level change rates recorded with the HOBO loggers in the main channel at the downstream site during the five experimental peaks from 8 to 22 November. The results show a consistent increase in water levels of about 15 cm during the peaks of 15 minutes duration and of about 10 cm during the peaks of 30 minutes duration. Observed water level change rates reached peak values between 4 and 7 cm/min during the rising limb and -1.0 to -1.5 cm/min during the falling limb. The peak water level change rates include a high uncertainty due to the time resolution of 2 minutes of the measurements.

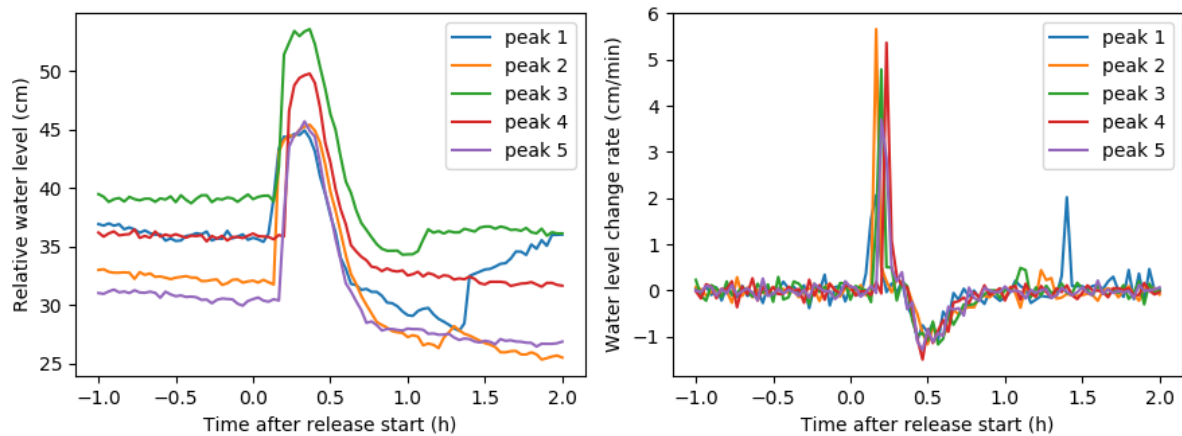


Figure 53: Relative water level and rate of change of water level recorded in the main channel during the five experimental peaks from 8 to 22 November.

Pfaundler et al (2011) describe two indicators that can be used to assess to what extent the hydraulic regime in a river stretch influenced by hydropeaking differs from a natural state. These indicators can be roughly estimated from the results presented above as described in Aksamit et al. (2021b). Based on these indicators, the hydropeaking state of the floodplain downstream of the hydropower plant release during the field study in November 2018 would be classified in class 3 (yellow, significantly modified) for the experimental peaks of 60 or 120 minutes duration that correspond to power peaks of less than 2 MW (see Figure 18) or class 5 (red, far from natural) for the experimental peaks of 15 or 30 minutes duration, i.e., for power peaks larger than 2.5 MW. Furthermore, during these tests, the ratio between the peak flows and the baseflow also clearly exceeded the threshold of 1.5 (around 3 for the power peaks of less than 2 MW) above which a site-specific assessment of the hydropeaking effects is required following article 41e of the Swiss Waters Protection Ordinance. During this period of the year, the baseflow is very low. Between March and October, the baseflow will be higher, and the factor of 1.5 should not be exceeded for production peaks of 1.5 MW.

For a more thorough assessment of the hydraulic changes resulting from the hydropeaking, stream-specific goals for different hydraulic indicators will have to be developed as described by Tonolla et al. (2017). Depending on the outcome of such an analysis, operational and/or structural measures to reduce these effects would need to be implemented according to the hydropeaking rehabilitation guidelines of Tonolla et al. (2017), and their costs need to be considered when assessing the profitability of the implementation.

The grain size distribution (Figure 54) showed a clear coarsening of the substrate in the pool following the first experimental peak in the pool habitat. No relevant changes were observed during the following peaks or in the riffle habitat during the entire experiment.

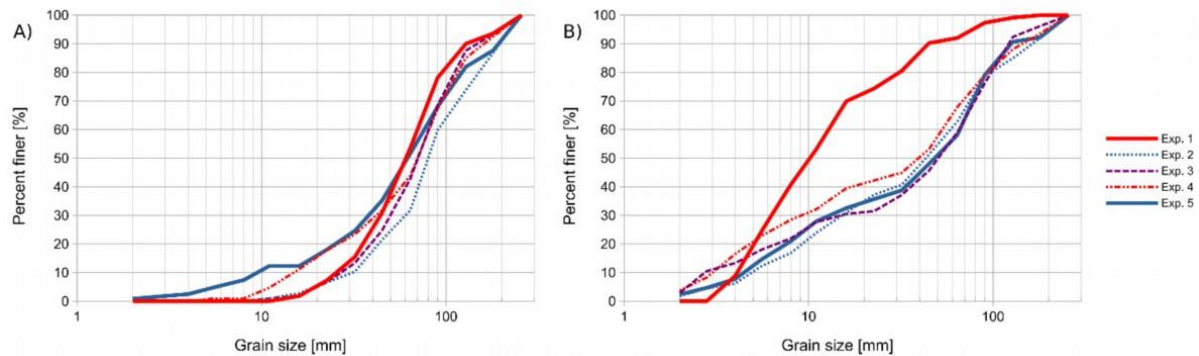


Figure 54: Grain size distribution for the riffle (A) and pool (B) habitats. Continuous lines represent the grain size distribution before the first (red, exp. 1) and last (blue, exp. 5) hydropeak, respectively. Dashed lines indicate observations from intermediate hydropeaks (exp. 2 to 4).

#### *Effects of hydropeaking on water temperature and water quality*

Water temperatures were evaluated for the period from 8 to 28 November. Until the second peak on 16 November, daytime air temperatures still reached maxima of 10 to 13 °C whereas air temperatures were clearly colder afterwards (Figure 55).

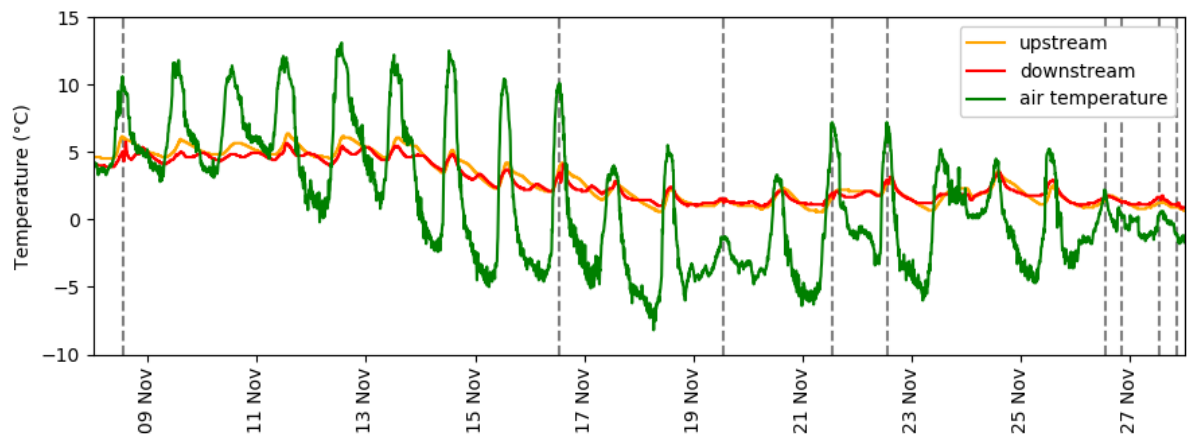


Figure 55: Observed temperature time series at the upstream and downstream sites and air temperature from the MeteoSwiss station in Ulrichen from 8 to 28 November. The dashed vertical lines mark the experimental hydropeaks.

Under warmer and sunnier conditions, the water in the residual flow reach is warmed up during the day as compared to the water transferred through the penstock, and consequently, the upstream temperature exceeds the downstream temperatures in the afternoon by a few degrees. An additional water release during the hydropeak then leads to an additional decrease in temperature, called thermopeak. During the colder conditions, the two temperatures are much more similar and thermopeaking is less relevant. This is exemplified by the observed temperature time series during the first 5 hydropeaks between 9 and 22 November (Figure 56), which show negative thermopeaks of ~1.0 °C on 8 and 16 November. During the following hydropeaks, the temperature decreased only by a few tenths of a degree.

According to Tonolla et al. (2017), the rate of change of temperature caused by the hydropeaking can be used as an indicator for the relevance of thermopeaking. Due to the comparably slow residence time of the temperature loggers, this value cannot be exactly determined based on the available observations. But on the warmer days, the artificial drop in temperature was approximately 1°C within 10 to 20 minutes, corresponding to a temperature decrease rate of -3 to -6 °C / hour, which would be





considered between poor and bad. Conversely, during the cold days, the absolute rate of change in temperature was probably mostly below 1 °C, and the value of the indicator would be considered as very good.

Besides that, the hydropeaking expectedly also caused peaks in turbidity. Observed turbidity ranged between 4.6 and 6.2 NTU during baseline conditions and ranged between 13.4 and 27.8 NTU during hydropeaks. For the other observed water quality parameters (specific conductivity, dissolved oxygen and pH) no relevant effects of the hydropeaking were observed.

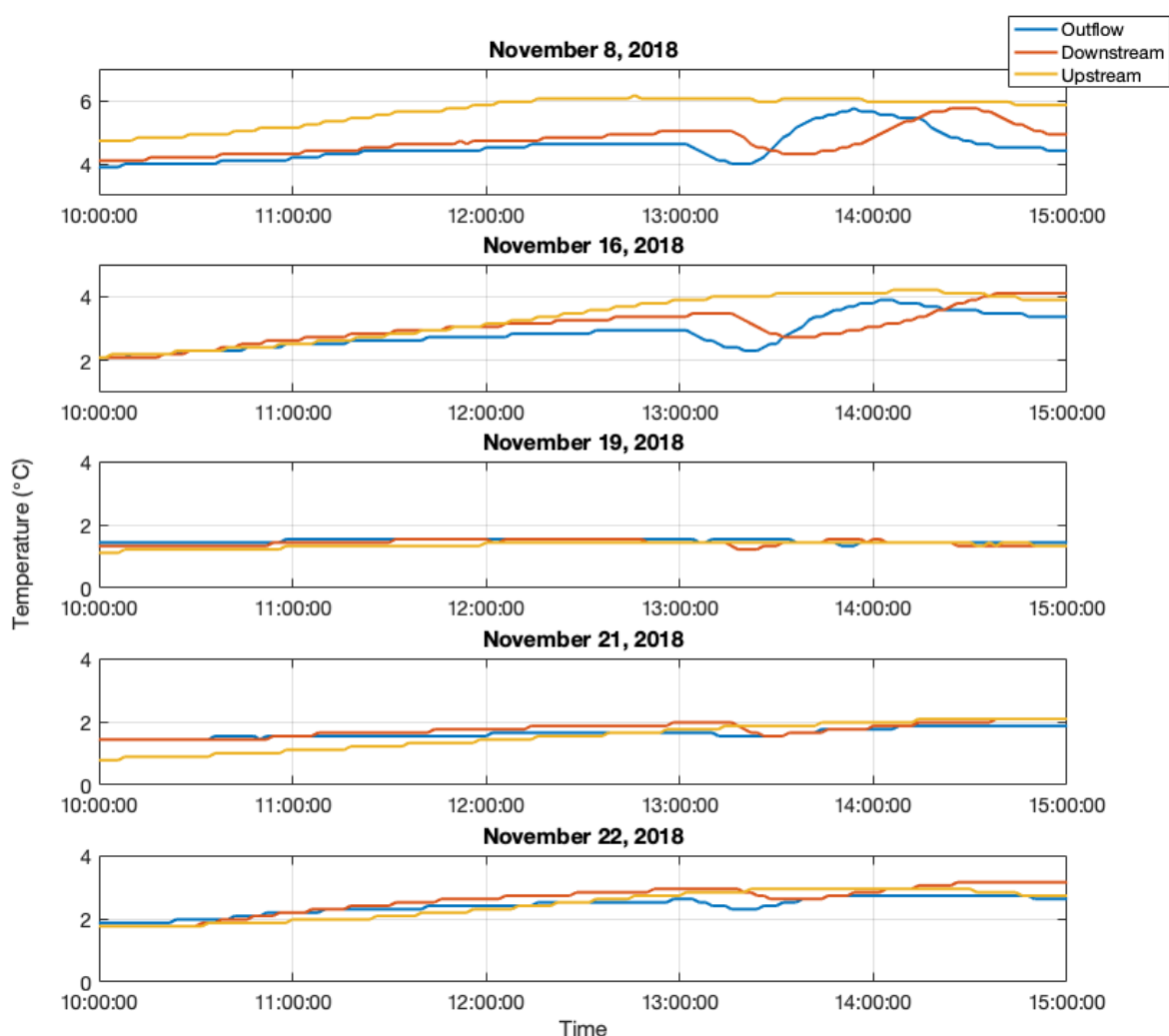


Figure 56: Observed temperature time series upstream and downstream of the for the 5 experimental peaks from 8 to 22 November. Peak water releases started on each at 13:00 and lasted 15 minutes.

#### *Effects on the macroinvertebrate community*

The observed effects of the experimental hydropeaking on macroinvertebrates are shown in detail in Aksamit et al. (2021a) and shortly summarized here. The analysis is based on a total of 192'889 individual macroinvertebrates that were collected and determined to family level.

The hydropeaking caused a strongly increased macroinvertebrate drift, with densities of drifting animals typically increasing by more than an order of magnitude from baseline conditions (Figure 57). The drifting macroinvertebrates were dominated by *Limnephilidae*, a family of caddisflies, followed by *Chironomidae* (informally known as non-biting midges) and *Baetidae*, a family of mayflies (Figure 58). The composition



of the drifting macroinvertebrate community showed consistent patterns throughout the experimental field study, where the composition was significantly different during the hydropeak compared to baseline conditions, but quickly approached that of baseline conditions after each hydropeak. This is exemplified for the observations in the pool habitat in Figure 59, but similar observations were also made in the riffle habitat (Aksamit et al., 2021a).

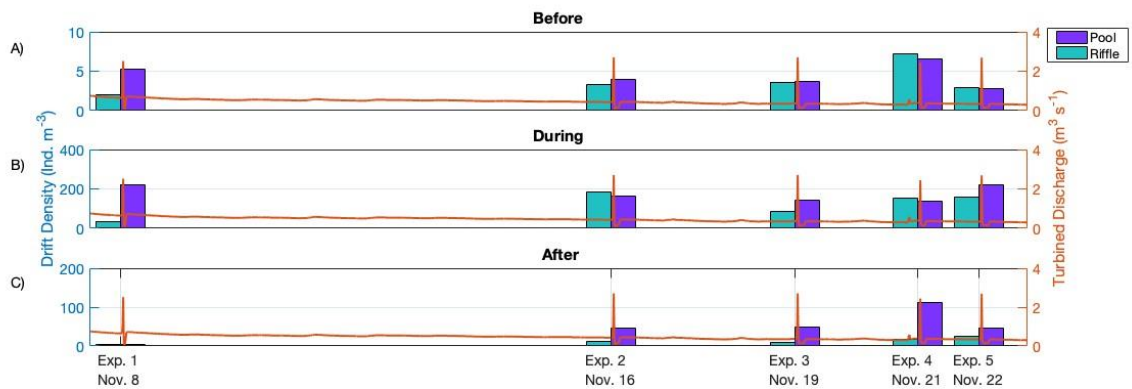


Figure 57: Drift density [ind. m<sup>-3</sup>] measured at the central net for the downstream riffle and pool habitats A) before (sample 0), B) during (samples 1-3) and C) after (samples 4-5) hydropeaking. Note the different scales on the y-axis (Figure from Aksamit et al., 2021a).

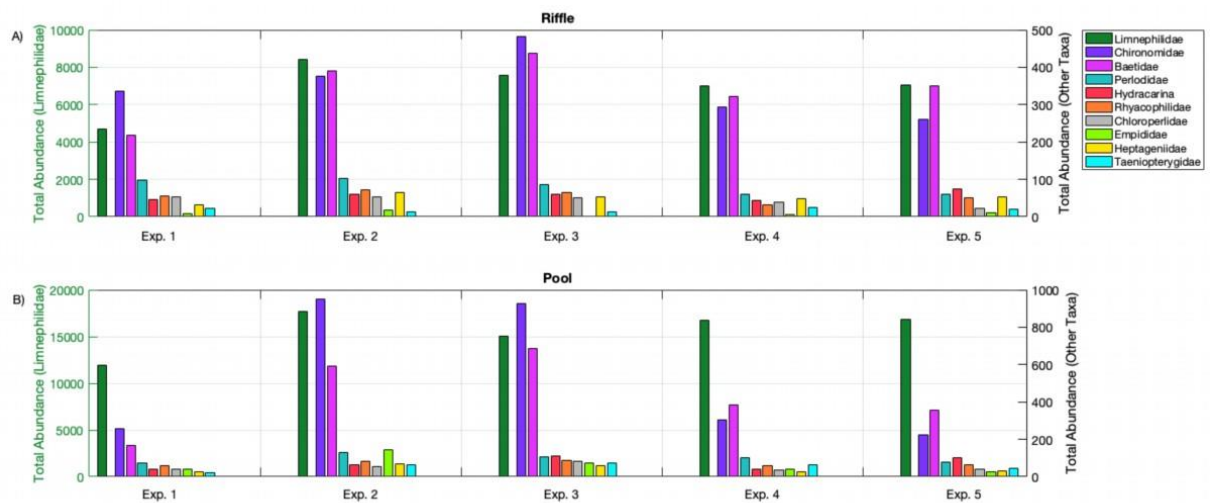


Figure 58: Abundances (sum of all samples and nets for each experimental peak) of drifting macroinvertebrates during the 5 experimental peaks in the downstream riffle (A) and pool (B). The left y-axis is total abundance of *Limnephilidae* and the right y-axis total abundance for all other taxa.

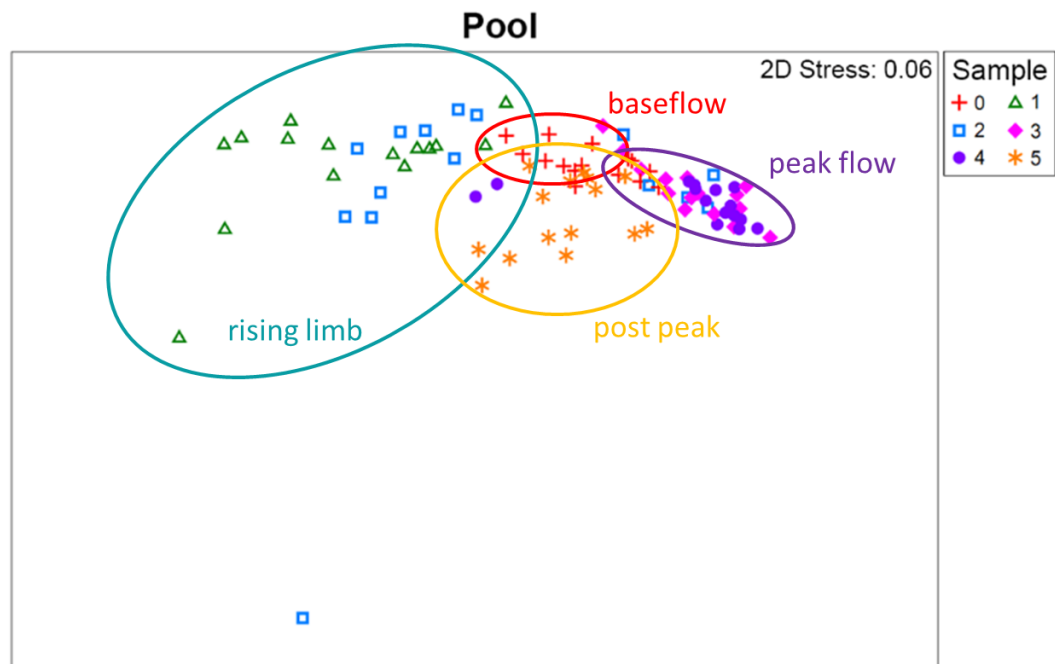


Figure 59: Non-metric multidimensional scaling (NMDS) of macroinvertebrate densities in downstream drift samples (from all hydropeaks and all individual nets) based on the Bray Curtis Similarity Index for the pool habitat. The sample numbers follow the description in Figure 12: 0 - baseflow, 1 – first stage of the rising limb, 2 – second stage of the rising limb, 3 – peak, 4 - peak transition to falling limb, 5 - post-peak. The ellipses are drawn for illustrative purposes only and have no statistical meaning.

No significant decrease in abundance (Table 7) or composition of the drifting macroinvertebrates was observed during the field study, with recovery time between hydropeaks progressively decreasing from 8 days to 1 day. This indicates efficient recolonization by macroinvertebrates between the hydropeaks, which is likely supported by the near-natural condition of the upstream river.

Table 7: Abundance and drift density observed at the five experimental peaks in the two habitats at the downstream and upstream measurements site. The given abundance corresponds to the sum of all individuals across all nets and sample stages (0-5), the density is the abundance divided by the total filtered volume (Aksamit et al., 2021a)

Habitat	Experimental peak	Downstream [Ind.]		Upstream [Ind.]	
		Abundance [Ind.]	Density [Ind m <sup>-3</sup> ]	Abundance [Ind.]	Density [Ind m <sup>-3</sup> ]
Riffle	1	5'680	13.0	143	0.40
	2	9'654	26.0	196	0.59
	3	8'919	26.8	212	0.86
	4	7'830	25.1	224	1.04
	5	8'047	26.5	74	0.63
Total		40'130	22.9	849	0.67
Pool	1	12'616	32.0	155	0.42
	2	19'846	52.7	280	1.27
	3	17'406	55.1	178	0.55
	4	17'751	47.2	280	1.25
	5	17'845	50.4	170	1.06
Total		85'464	47.0	1'063	0.82



However, the abundance of some families in the drifting community showed a consistent pattern, with low abundances during the first peak, highest abundances during the second and third peak, and clearly decreasing abundance with shorter recovery time during the following peaks. A possible hypothesis to explain this pattern is decreased abundance at the first peak due to increased discharge caused by a precipitation event on the days before the start of the experiment, subsequent recovery during the 8 days between the first and the second experiment, and then preferential removal of these macroinvertebrate families due to the hydropeaking. This hypothesis would need to be supported by observations over longer time scales during operational hydropeaking. However, if it is indeed correct, it would indicate a risk of eliminating certain families of macroinvertebrates by frequent operational hydropeaking.

## 4.5 Task 5: On-site tests

For the first on-site tests, in November 2018, the Pelton turbines were still under warranty, which prevents dewatering the head race tunnel since the turbines are not designed for these operating conditions. Therefore, only the forebay tank has been dewatering and the campaign allows the validation of:

- the procedure developed for the program generation,
- the accuracy of the sensors,
- the feasibility of the measurements,
- the investigation of the impact of hydropeaking on the alluvial area (see task 4).

An example of the validation of the accuracy of the measurements is shown in Figure 60 that compares the water level in the forebay tank provided by the SCADA system of the power plant, by HydroClone and extracted by postprocessing the images taken by the IR camera.

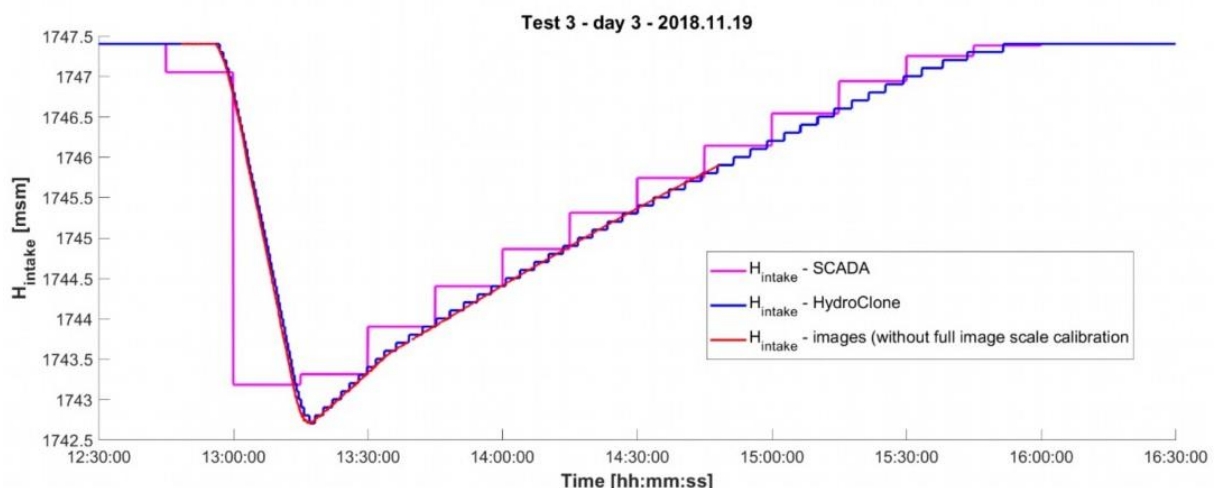


Figure 60: Comparison of the measurement of the water level in the forebay tank based on the images taken by the IR camera (red line).

The second campaign carried out in May 2020 has been designed to perform hydropeaking by dewatering 25% of the head race tunnel. Three peaks over two days have been performed.

The two Pelton units have been run in parallel (the unit 1 was only used to adjust the total power at the desired value). Figure 61 shows the head variation and the power of the two units during the two days of tests. The time duration of the hydropeaking and the energy produced are added on the graph. The



first peak lasted 3h35 for a production of 12.8 MWh whereas the third one lasted 1h15 for a production of 5.8 MWh.

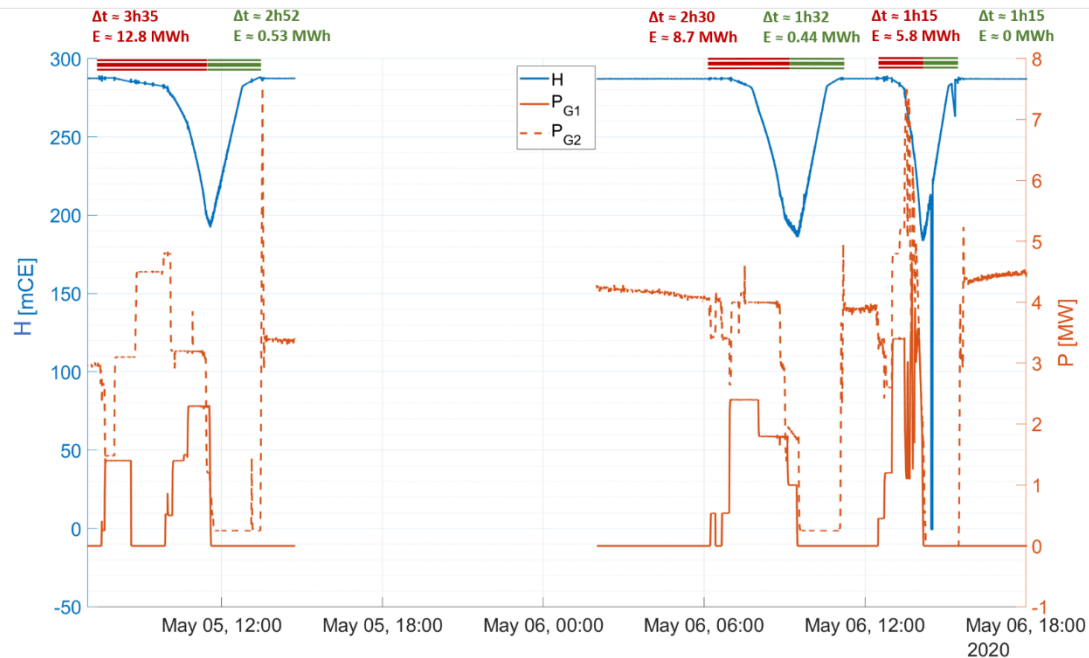


Figure 61: Variation of the head and the power of each group during the two days of the second campaign (May 2020). The duration of the peaks of production and the corresponding energy produced are added at the top of the chart.

During the third peak, the number of needles opened has been changed several times. Therefore, a large range of operating points have been explored allowing the construction of the turbine performance maps. Figure 62 shows two maps giving the flow rate and the efficiency as a function of the power set and the available head. The efficiency map (Figure 62 right) put in evidence the “falaise” effect with an abruptly drop of the efficiency for low heads. The head at which the “falaise” effect occurs dependant on the power demand. It occurs at a head of 240 m for a power demand of 6 MW and at a head of 220 m for a power demand lower than 3 MW. Such maps are useful to prepare the programs of production and to assess the business model.

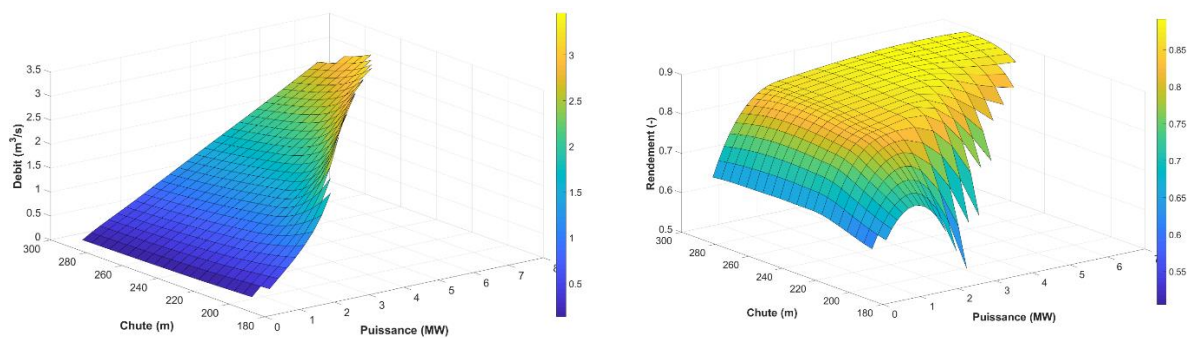


Figure 62: Performance maps of the Pelton turbines. Flow discharge (left) and efficiency (right) as a function of the power and the head.



Figure 63 shows the accelerometer signal along its x-axis as a function of the head. The fluctuations increase by a factor of 4 for a head lower than 210 m, which increases the risk of fatigue. Such an information is valuable to define a minimum level for the dewatering of the head race tunnel.

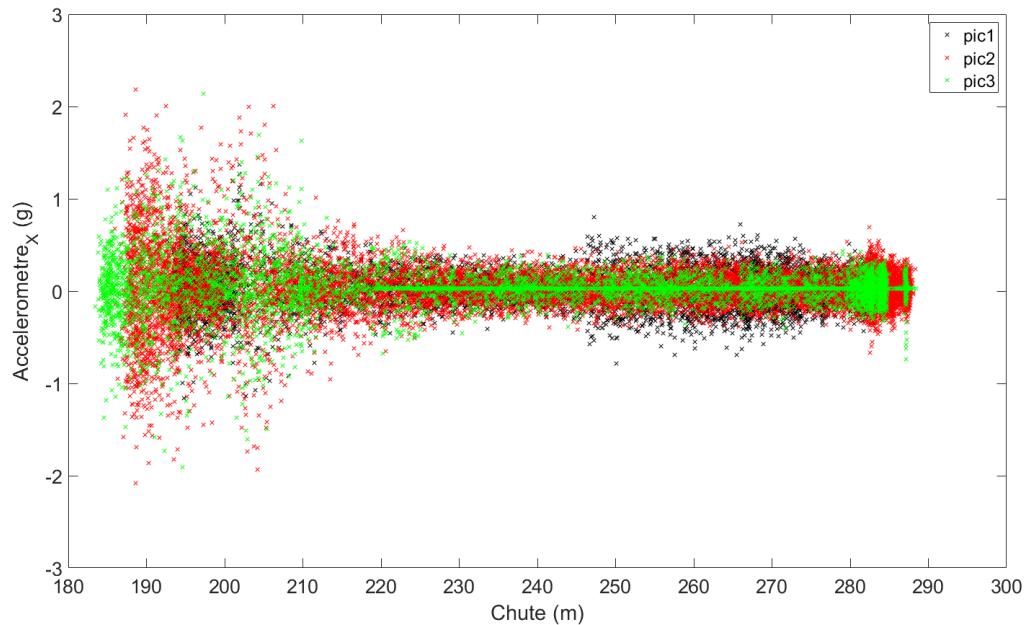


Figure 63: Variation of the accelerometer signal as a function of the head for the three peaks of the second campaign.

Furthermore, no waves have been observed on the free surface in the forebay tank neither during the emptying nor the filling (Figure 64). Few vortices have been noticed but with a weak intensity, which is not a problem.

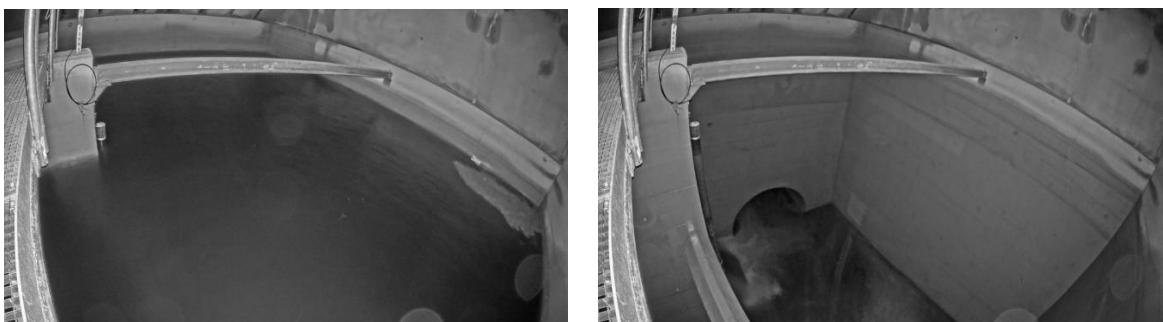


Figure 64: Instantaneous view of the free surface in the forebay tank. Filled tank (left) and last stages of the emptying (right).

#### 4.6 Task 6: Business model of a flexible small hydropower plant

The optimization of the revenue as a function of the electricity market price has been carried out for the years 2018 and 2019 for which the incoming flow and the SPOT price are known. The TSE software is not able to correctly adjust the efficiency of the turbine as a function of the storage volume available. It always chooses the highest efficiency. For this reason, the results are arbitrarily decreased by 10%.



Over the two years, the use of the storage volumes allows increasing the production by 0.6% with a benefit growth of 1%. The increase is not very high, but an analysis of the results per seasons gives interesting insights:

- From December to March, the production of the power plant can be increased by 130% since the storage volume allows operating the power plant even if the incoming flow rate is lower than the minimal value of 345 l/s (see Figure 65). In addition, the number of start and stop decreases and should tends to zero by a fine tune of the production.
- In April and May and in October and November, the power is between 2 MW and 10 MW, which allows some peak of production. However, the benefits are not significant. The production can even be lower due to the low efficiency of the turbines at head below 287 Wcm.
- From June to September, the power is above 10 MW i.e., above the maximum power set for the peak of production (2x5 MW).

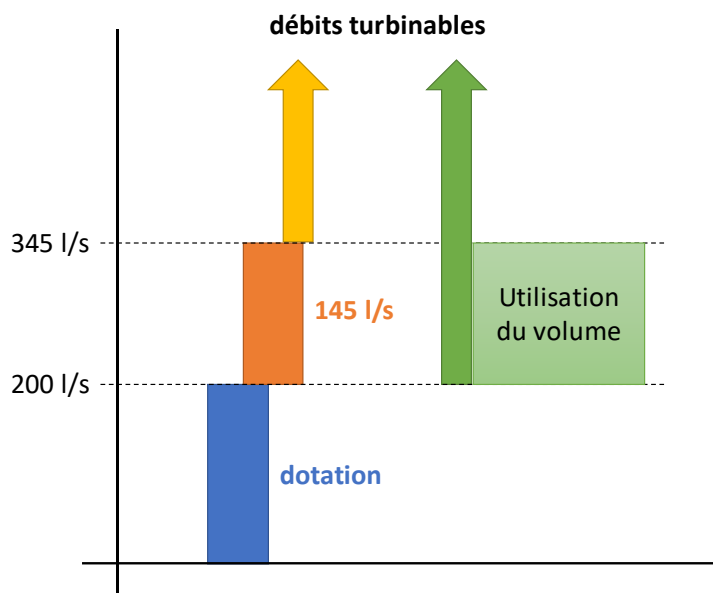


Figure 65: Possible flow discharge usable without (yellow arrow) or with (green arrow) the use of the storage volumes.

The optimization of the revenue depending on power used for PFC ancillary services are given in Table 8. In parenthesis, the percentage of the power and the revenue over the period from the 15<sup>th</sup> of May to the 15<sup>th</sup> of October shows that approximately 60% of the service occurs during the operation of the power plant in the summer mode. The amount of revenue during the winter period (December to March) represents approximately 1% of the total revenue. It is therefore noticeable that the period suitable for PFC ancillary service is not in conflict with the period for optimizing the production depending on the electricity market prices. Consequently, the two sources of additional revenues can be coupled.

Table 8: Amount of power used for primary frequency control and associated revenues. In parentheses, the percentages over the period from the 15<sup>th</sup> of May to the 15<sup>th</sup> of October.

	PFC sold [MW]	Revenue [€]
<b>2018</b>	610 (59%)	13'933 (59%)
<b>2019</b>	541 (60%)	12'348 (60%)
<b>Average</b>	576 (59%)	13'141 (59%)





Furthermore, keeping in mind that the PFC ancillary service is provided through a pool off four SHPs, the use of additional storage provides not only additional local flexibility but also opens new business model by coupling several power plants together.

Interestingly, the outputs of the economic analysis should not negatively impact the environment in the alluvial area. Indeed:

- during the winter period, by decreasing the number of start and stop, it is expected that the flow discharge fluctuations will be smoothed, and no hydropeaking is expected.
- The power peaks for providing PFC services mainly during the summer period are limited to a maximum power of 1.5 MW for which the flow discharge peaks will be below 150% of the baseflow.

## 5 Conclusions

Description of the findings that were generated through the project, plus their relevance for the study areas concerned and subsequent evaluation of the activities that were carried out.

### 5.1 Task 1: Investigation of the storage potential

The investigation of the additional storage volumes that could be used at the KWGO powerplant for increasing the flexibility of the powerplant has been carried out in two stages. First, five storage volumes have been selected: the head race tunnel, the forebay tank, the settling basin, the access gallery and a reservoir at the intake. The last one to be built. For each volume, the economic value versus the storage volume provided has been assessed. This assessment shows the interest to bore two gates between the settling basin and the forebay tank to allow the use of the settling basin as an additional storage volume during the winter period, when the sediment transport is low. Furthermore, this task allows providing an accurate curve of the volume available as a function of the water level. Such a curve is necessary for the assessment of the business model carried out in the task 5.

### 5.2 Task 2: Hydraulic machines flexibility

The estimation of the available power/energy for ancillary services has been assessed by carrying out simulations with a SIMSEN numerical model of the SHP KWGO. The parameters of the complete 1D-model have been calibrated based on the commissioning test, including an emergency shutdown of the 2 Pelton turbines. The model proved to be very accurate, with the ability to replicate almost perfectly the transient behavior of the power plant, such as discharge, pressure and power evolution. After implementing a turbine governor model integrating a power and speed setpoint, simulations of primary control scenarios have been performed with the numerical model of the power plant in order to find best compromise between reactivity and system stability. The simulation results revealed that the primary control capability correspond to a reserve power comprised between  $\Delta P = (2x) \pm 0.5$  MW to  $(2x) \pm 0.75$  MW, which represents a permanent droop between BS-4-6%. The estimations of the pressure fluctuations in the tunnel suggest that no penstock fatigue is to be expected and that the impact of the primary control on the service life of the penstock is insignificant.

The follow-up of the test campaigns has been successfully performed with the deployment of the Hydro-Clone® real-time monitoring system at the SHP KWGO. The benefits of this digital twin have also been used during the plant's commissioning tests in the summer of 2018, allowing detailed follow-up of the tests and a close monitoring the turbines operation. Furthermore, the recording of all the test results in a dedicated database permitted the fine post-processing and analysis of the test campaign outcomes to assess the consequences of the new operating conditions. The digital twin of the power plant was also used to carry out some predictive analysis prior to the second test campaign, to anticipate the water



level variations at the inlet and outlet of the power plant for a given water inflow, as well as the turbine governor behaviour. Finally, the numerical model was used to estimate the occurrence of the so-called «falaise effect» which is characterized by an abrupt drop of the machine efficiency when the turbine net head is lowered. It was estimated that this effect occurs as soon as the net head falls below 215 m, which corresponds to 75% of the nominal head.

The investigation of the hydraulic machine flexibility has been carried out by CFD. Since the flow in a Pelton turbine is complex and requires dealing with various physics, two software have been used. The OpenFOAM toolbox better suited for flow with fixed boundaries of the computational domain is used to compute the flow in the distributor and the development of the jet downstream the nozzle. The GPU SPHEROS better suited for flow with moving boundaries is used to compute the interaction between the jets and the runner buckets using inlet data provided by the OpenFOAM simulations. For these simulations, two consecutive jets and three runner buckets are considered allowing the investigation of the influence of the first jet on the second one.

Simulations for six different heads and three needle strokes have been run. For each simulation, the quality of the jet, the torque and the efficiency have been analysed. The quality of the jet is not modified by lowering the head whereas the velocity of the jet decreases as expected from the theory. The jet is more influenced by the stroke of the needle than by the head variation. For a small stroke (20% of the maximum stroke), the jet is a mix of air and water whereas for a larger opening, the jet is fully filled by water. Whatever the head, the second jet is always influenced by the first jet. The influence is small for the nominal head and increases by lowering the head. For a head of approximately 215 m, the simulations predict a drop of the efficiency below 60% due the occurrence of the so-called “falaise” effect. The predicted torque and efficiency are in accordance with the available data excepted for a small flow discharge for which the torque is underestimated.

The CFD results help the team to define a lowest head for the tests around 190 m, for which the “falaise” effect would be observed without a high risk of failure and for which the quantification of the vibration level and the measurement of the efficiency would be performed.

### 5.3 Task 3: Real-time hydrological forecasts

The main outcomes regarding the real-time hydrological forecasts listed hereafter.

- An operational (fully automated) runoff forecast system for the Rhone river at the SHP intake in Gletsch was successfully set up and run for the entire project period (May 2018 - January 2021). It consists of an advanced model chain making use of most recent MeteoSwiss forecast products (INCA-CH, extended-range forecasts) and a state-of-the art hydrological model (PREVAH). The forecast system showed to be robust and user-friendly for the purpose of the project, i.e., for the planning and performance of a flexible operation of HP Gletsch-Oberwald. The accuracy of the runoff forecasts decreases from very short-term forecast, where the error is negligible, to monthly forecasts, where only tendencies can be determined. For the spring season, where snowmelt generates a highly dynamic change in runoff (between “winter flow” of 0.5 m<sup>3</sup>/sec and “peak flow” of 10 to 15 m<sup>3</sup>/sec), a forecast with a lead time of 24 hours has an accuracy of ~0.7 m<sup>3</sup>/sec and with a lead time of 48 hours an accuracy of ~0.9 m<sup>3</sup>/sec.
- Using a state-of-the-art sediment transport formula for alpine rivers we were also able to set up a sediment transport forecast for the Rhone river at the intake of HP Gletsch-Oberwald that agreed reasonably well with bedload estimations of EPFL carried out in 2018. The sensitivity of the sediment forecast model to (predicted) runoff is substantial, and the validation of the model was associated with great uncertainty. Therefore, this sediment forecast system must be considered as a preliminary result and would need much further data and analyses before using it for operational purposes.
- The developed and implemented forecast methods (including web platform) can easily be transferred to other SHP plants and their catchments of similar size in Switzerland where a flexible



operation could be an option. The meteorological and hydrological forecast models are already today available for the entire country. Specific efforts (and costs) would be needed for the tailoring of the model domain to the corresponding catchment and for the long-term operation of the system (which is not the strategic business of WSL).

- For a further improvement of a runoff and sediment forecast system, as implemented in this project, the following critical shortcomings would have to be tackled in the first place: a) the availability of sediment data should be improved either by a more in-depth quantification of sediments in the sand trap or by performing sediment transport measurements in the stream; b) the simulation of snow and glacier melt in steep, complex alpine terrain is still a challenge and needs further improvement, which is currently ongoing at WSL and SLF Davos.

## 5.4 Task 4: Short term hydropeaking effects on ecosystems

To our knowledge, we performed the first real world study of a novel small hydropower plant with the objective to measure and compare the response and recovery of drifting and benthic invertebrates to short hydropeaking events. We did not detect a statistically significant change in the benthos or in the drift community in either the upstream or downstream riffle or pool between experimental peaks. An ecologically intact upstream reach, as well as an abundance of organic matter, resulted in no significant changes in the drift community for recovery times between 8 days and 24 hours. Considerable differences between riffle and pool habitats highlight the complexity of impacts on natural streams, and the hazards of direct application of results from channel or flume studies. Furthermore, our results cannot exclude potential long-term effects of flexible small-scale hydropower production at this site. Specifically, decreasing numbers of drifting macroinvertebrates from selected families with decreasing recovery times during the field study indicate a potential risk of eliminating or reducing certain taxa in case of frequent operational hydropeaking. For this reason, a long-term monitoring of the macroinvertebrate community is required in case flexible production will be effectively implemented.

Furthermore, the results of the hydrograph analysis indicated that, despite the small reservoir volume, hydropeaking resulting from flexible operation of the small hydropower plant Gletsch-Oberwald can have a significant impact on the hydrology and the water temperature of the river stretch downstream the hydropower release, including the floodplain of national importance. Before implementation of such a flexible operation more detailed analyses of the expected effects should be performed for the entire range of boundary conditions (meteorological conditions, discharge, duration and frequency of hydropeaks), and depending on the outcome of such an analysis, operational and/or structural measures should be considered to reduce these effects.

## 5.5 Task 5: On-site tests

Two on-site tests have been carried out in November 2018 and May 2020. The first campaign was dedicated to the validation of the instrumentation and the methodologies used to prepare and to analyse the tests. Only a part of the forebay tank was dewatering during this first campaign. For the second campaign, three peaks of production have been carried out by dewatering 25% of the head race tunnel.

To achieve the on-site tests:

- A methodology has been developed to define a production program for the day of the tests including a protocol to send the program in due time. In parallel, detailed maps of the powerplant characteristics have been drawn to allow the definition of various peaks of production during the days of the tests without losing any water.
- A risk assessment due to the dewatering of the head race tunnel has been done. Two main risks have been identified: the risk of damaging the gallery and the risk of air entrainment. Both can cause strong damages and make the turbines out of operation during several months. Specific actions have been undertaken. For the risk of damaging the head race tunnel, a design



brief has been written and a contract with a third party has been signed. The study does not put in evidence a high risk of failure during the planned tests. For the risk of air entrainment, a model test has been built at the HES-SO laboratory that shows no risk of air entrainment even at the maximum flow discharge. Moreover, numerical studies have been performed to investigate the possibility to do an emergency shutdown without overtaking the limits of the powerplant whatever the water level in the head race tunnel.

- A dedicated instrumentation has been set up allowing the monitoring of the Pelton unit during the tests and the acquisition of data for further analysis.

The two campaigns were a success. No risk of air entrainment has been observed. The efficiency and flow rate maps of the units as a function of the available head and power demand are now available for defining an accurate program of production and to perform economic studies. The occurrence of the “falaise” effect (i.e., an abrupt drop of the efficiency) as a function of the head has been determined for the entire range of power. Based on the performance maps and the vibration level of the Pelton unit, a minimal head of 230 m has been set if the dewatering of the head race tunnel is used in the future.

## 5.6 Task 6: Business model of a flexible small hydropower plant

The storage volumes identified and considered as usable by the experimental campaigns carried out are interesting for FMV, the owner of the power plant. The additional volumes improve the flexibility of the power plant by allowing:

- an optimization of the production depending on the electricity market prices,
- the possibility to provide a PFC ancillary service over all the year.

Compared to the today situation, the storage volumes are useful:

- during the winter period while the flow discharge is sometimes lower than the 345 l/s necessary to operate the power plant and above the residual flow discharge for environmental purpose set to 200 l/s,
- during the summer period, by giving the possibility to use part of the head race tunnel to get the necessary volume of 540 m<sup>3</sup> ensuring a full capacity for the PFC ancillary service.

Over the years 2018 and 2019, the increase in the range of flow discharge usable allows increasing the winter production by 130%. A total gain combining the optimization of production and the PFC ancillary service is estimated to approximately 30 k€ per year. By combining several SHP in pool, the gain can be increased and new services can be provided.

Furthermore, the economic benefits should not have an environmental impact since the flow discharge fluctuations during the winter period would be smoothed due to a decrease in the number of start and stop and during the summer period, the flow discharge peaks should be lower than 150% of the baseflow.



## 6 Outlook and next steps

The main result of the SmallFLEX project developed a methodology to:

- identify the potential of flexibility of a hydropower plant.
- identify the possibility to provide ancillary services using numerical simulations.
- determine the limits of the powerplant flexible operation using numerical simulations and field tests with an adapted monitoring system.
- improve the inflow forecast using numerical modelling.
- determine the influence of hydropeaking on the environment.
- assess the increase of the production and the revenue.

The next step will be to apply this methodology to other run-of-river hydropower plants, first with similar characteristics i.e., with a headrace tunnel without compensating basin and Pelton turbines. Then run-of-river power plants equipped with different types of machine could be also considered.

FMV already plans to extend this study to power plants in Valais to enlarge their pool of small power plants, which can provide ancillary services. Regarding the KWGO SHP, the implementation of the extending operating range and new services will be pushed one step forward, keeping in mind both the infrastructure and environmental limits. Other power plant owners will be also contacted to identify potential powerplants which can be considered for such flexible operation.

To promote the project at national and international levels, the research partners will present the results in scientific conferences and journals.

## 7 National and international cooperation

The multi-disciplinary SmallFLEX project already gathered several Swiss academic and industrial partners. All the participants are members of the Swiss Competence Center for Energy Research for the Supply of Electricity (SCCER-SoE). Throughout the duration of the project, the highlights have been regularly presented at the annual conference of the SCCER-SoE which gave a good visibility in Switzerland.

The hydrometeorological forecast system (Task 3) was developed and operated in close collaboration with MeteoSwiss. In particular, the implementation of the nowcasting system INCA (for lead times of 0 to 6 hours) and the operational use of extended (monthly) meteorological forecasts was only possible thanks to the valuable support by MeteoSwiss.

At the international level, this study has been presented as an example of Hidden Hydro activities in the Annex XVI of International Energy Agency (IEA) in 2019 and the results will be in 2021 presented in several conferences such as HydroES in France. The study on macroinvertebrate recovery was presented at the Symposium for European Freshwater Sciences in 2019.



## 8 Publications

- [1] J. Zordan, P. Manso, A. Gaspoz, C. Münch, S. Crettenand, “Introducing flexibility in alpine small hydropower plants using smart storage”, Hydro2019, Porto, Portugal.
- [2] A. Gaspoz, V. Hasmatuchi, J. Decaix, C. Nicolet, M. Dreyer, J. Zordan, P. Manso, S. Crettenand, C. Münch-Alligné. “First insights on the production flexibility at the KWGO Power Plant”, SCCER-SoE Annual Conference 2019, Lausanne, Switzerland
- [3] M. Dreyer, C. Nicolet, A. Gaspoz, S. Crettenand, C. Münch-Alligné, “Monitoring of small hydropower plants with a digital clone”, SCCER-SoE Annual Conference 2019, Lausanne, Switzerland
- [4] M. Ponce, J. Zordan, P. Manso, C. Münch-Alligné “Added value of smart storage operations on an alpine run-off-river HPP obtain from hydrological-hydraulic modelling”, SCCER-SoE Annual Conference 2019, Lausanne, Switzerland
- [5] R. Casimiro de Figueiredo; J. Zordan, P. Manso, C. Münch-Alligné, “Control of sediment transport on an alpine catchment basin for the safe application of smart storage operations on a run-off-river HPP”, SCCER-SoE Annual Conference 2019, Lausanne, Switzerland
- [6] K. Bogner, M. Buzzi, M. Zappa, “Analysis of the Nowcasting System INCA-CH at Gletsch (VS)”, SCCER-SoE Annual Conference 2019, Lausanne, Switzerland
- [7] C. Aksamit, D. Vanzo, M. Carolli, N. Friese, K. Mathers, C. Weber, M. Schmid, “Ecological Impacts of Small-Flexible Hydropower: Macroinvertebrate Resilience to Varying Frequency Hydropeaking”, SCCER-SoE Annual Conference 2019, Lausanne, Switzerland
- [8] C. Münch et al., “WP5 Pilot & Demonstration Projects SMALL FLEX”, SCCER-SoE Annual Conference 2019, Lausanne, Switzerland.
- [9] C. Münch et al., “SMALL FLEX Increase Flexibility in Small Hydropower Plants”, SCCER-SoE Annual Conference 2020, Switzerland.
- [10] G. Morand et al., “Augmentation de la flexibilité d’exploitation d’aménagements hydroélectriques de haute chute au fil de l’eau en Valais », SCCER-SoE Annual Conference 2017, Birmensdorf, Switzerland
- [11] C. Münch et al., “Production flexibility of small run-of-river power plants: KWGO case study”, Hydro 2020, Strasbourg, France.
- Accepted publication, not yet published.*
- [12] C. K. Aksamit, M. Carolli, D. Vanzo, C. Weber, M Schmid, “Macroinvertebrate recovery to varying hydropeaking frequency: a small hydropower plant experiment”, *Frontiers in Environmental Science*, 8, 602374, doi: 10.3389/fenvs.2020.602374.
- [13] C. Münch et al., “Production flexibility of small run-of-river power plants: KWGO case study”, IAHR 2020, Lausanne, Switzerland.
- [14] J. Decaix et al., “Numerical simulation of the interaction between the jet and the Pelton runner under low head conditions”, SimHydro 2021, Nice, France.
- [15] J. Decaix et al., “Emptying a penstock to improve the power plant flexibility”, HydroES 2021, Lyon, France.
- [16] S. Alimirzazadeh, J. Decaix, F. Avellan, S. Crettenand, C. Münch-Alligné, 2021, “Numerical simulations of Pelton turbine flow to predict large head variation influence”, IOP Conference Series: Earth and Environmental Science, accepted for publication.





## 9 References

- Aksamit, C.K., Carolli, M., Vanzo, D., Weber, C., Schmid, M., (2021a) Macroinvertebrate recovery to varying hydropeaking frequency: a small hydropower plant experiment. *Frontiers in Environmental Science*, 8, 602374, doi: 10.3389/fenvs.2020.602374.
- Aksamit, C.K., Friese, N., Vanzo, D., Weber, C., Schmid, M., (2021b) Analysis of hydro- and thermopeaking in the Upper Rhone River during the SmallFlex experiment in November 2018. Report, Eawag, Kastanienbaum.
- Badoux, A.; Rickenmann, D., (2008). Berechnungen zum Geschiebetransport während der Hochwasser 1993 und 2000 im Wallis. *Wasser, Energie, Luft*, 100 (3), 217-226.
- BFE (2019), Potentiel hydroélectrique de la Suisse - Évaluation du potentiel de développement de la force hydraulique dans le cadre de la Stratégie énergétique 2050. (2019). Office fédéral de l'énergie OFEN - Section Force hydraulique.
- EN, BS. "13445-3: 2009.", (2009) BSI British Standards. Unfired pressure vessels-Part 3
- Nerini, D., Foresti, L., Leuenberger, D., Robert, S. and Germann, U. (2018) A reduced-space ensemble Kalman filter approach for flow-dependent integration of radar extrapolation nowcasts and NWP precipitation ensembles. *Monthly Weather Review*, 147(3), 987– 1006.
- Nicolet, C., Bollaert E., (2017) "Hydroelectric power plant real-time monitoring system and method", European patent EP 2 801 879 B1, 27.9.2017.
- Nicolet, C., Bollaert E., (2020) "Hydroelectric power plant real-time monitoring system and method", European patent EP 3 285 128 B1, 18.11.2020.
- Mbenza, B., (2020), Small Flex : Modèle d'exploitation flexible d'aménagements hydroélectriques de haute chute au fil de l'eau en Valais, 2020, <http://infoscience.epfl.ch/record/274021>
- Pfaundler, M et al. (2011). Methoden zur Untersuchung und Beurteilung der Fliessgewässer. *Hydrologie – Abflussregime Stufe F (flächendeckend)*. Bundesamt für Umwelt, Bern. Umwelt-Vollzug Nr. 1107, 113 S.
- Rickenmann, D. (2012). Alluvial Steep Channels: Flow Resistance, Bedload Transport Prediction, and Transition to Debris Flows. In *Gravel-Bed Rivers* (eds M. Church, P.M. Biron and A.G. Roy). <https://doi.org/10.1002/9781119952497.ch28>
- Tonolla, D., Chaix, O., Meile, T., Zurwerra, A., Büsser, P., Oppliger, S., Essyad, K., (2017). Schwall-Sunk – Massnahmen. Ein Modul der Vollzugshilfe Renaturierung der Gewässer. Bundesamt für Umwelt, Bern. Umwelt-Vollzug Nr. 1701, 133 S.
- Viviroli, D.; Zappa, M.; Gurtz, J.; Weingartner, R., (2009). An introduction to the hydrological modelling system PREVAH and its pre- and post-processing-tools. *Environmental Modelling and Software*, 24 (10), 1209-1222. doi: 10.1016/j.envsoft.2009.04.001